Oral Drug Pharmacokinetics and Treatment Effects in Populations Affected by Diarrheal Diseases

Cindy Xinyi Zhang

A dissertation

submitted in partial fulfillment of the

requirements for the degree of

Doctor of Philosophy

University of Washington

2024

Reading Committee:

Samuel L.M. Arnold, Chair

Kenneth Thummel

Jeannine McCune

Program Authorized to Offer Degree:

Department of Pharmaceutics

University of Washington

Abstract

Oral Drug Pharmacokinetics and Treatment Effects in Populations Affected by Diarrheal Diseases

Cindy Xinyi Zhang

Chair of the Supervisory Committee:

Samuel L.M. Arnold

Department of Pharmaceutics

Diarrheal diseases are a major global health concern. Globally, over 4.5 billion episodes of diarrhea occur among all ages every year. Diarrhea disproportionally affects young children and those living in low- and middle-income countries. In 2019 alone, diarrhea was responsible for approximately 1.5 million deaths among people of all ages, including over 500,000 deaths in children under 5 years of age (Dadonaite *et al.*, 2024). Moreover, around 90% of diarrheal mortalities occur in sub-Saharan Africa and South Asia, where undernutrition, poor sanitation,

and limited access to medical care are common (GBD 2016 Diarrhoeal Disease Collaborators, 2018). The high prevalence of diarrheal diseases creates a challenge for oral drug administration, as physiological changes associated with diarrhea can impact key processes involved in oral drug absorption, thus leading to alterations in oral drug pharmacokinetics (PK). As a result, the safety and effectiveness of oral drugs may be altered when taken during episodes of diarrhea. The understanding of how diarrheal diseases affect the oral drug PK, whether this impact influences treatment outcomes, and if dosage adjustments are necessary is essential for making accurate dosing decisions and optimizing the likelihood of treatment success. To this end, we leveraged PK modeling approaches to characterize and simulate oral drug PK and make predictions about treatment efficacy for populations affected by diarrheal diseases.

In Chapter 2, to estimate the magnitude of diarrhea-associated impact on oral clofazimine PK, we developed a population PK model using clofazimine PK data collected from a phase 2a clinical trial of HIV-infected adults with/without cryptosporidiosis and diarrhea. Among potential covariates of cryptosporidiosis-associated diarrhea severity, HIV infection burden, baseline demographics, and study assignment, maximum diarrhea grade over the study duration was significantly associated with clofazimine bioavailability. Our model quantified a 6- and 22-fold reduction in clofazimine bioavailability associated with mild and severe diarrhea, respectively. Moreover, the model also estimated clofazimine PK parameters apparent clofazimine clearance (3.71 L/h), intercompartmental clearance (18.2 L/h; inter-individual variability [IIV] 45.0%), central volume of distribution (473 L; IIV 3.46%), peripheral volume of distribution (3434 L), absorption rate constant (0.625 h^{-1}; IIV 149%), and absorption lag time (1.83 h), all of which were aligned with literature values.

To determine whether cryptosporidiosis-associated diarrhea reduced clofazimine levels below levels associated with efficacy against *Cryptosporidium* infection, a pharmacokinetic/pharmacodynamic (PK/PD) modeling approach was undertaken in Chapter 3. Exposure-response relationships were determined using data collected in a preclinical mouse model of *Cryptosporidium* infection. E_{max} and logistic models were constructed, supporting predictions of efficacious clofazimine concentrations. By comparing the observed clofazimine concentrations from an unsuccessful phase 2a clinical trial to our predicted efficacious target, it was shown that the observed concentrations were well below concentrations associated with anti-*Cryptosporidium* efficacy. Thus, the prescribed doses were inadequate, even without any impact of diarrhea.

Since the effect of diarrhea on oral drug absorption is likely disease- and drug-specific, tebipenem for shigellosis treatment in Bangladeshi pediatric patients was studied in Chapter 4. By validating an existing tebipenem pediatric population PK model with observed tebipenem PK data collected from the pilot study of an ongoing clinical trial, we first demonstrated that the existing model adequately predicted tebipenem PK in a population with diarrhea. Then, we performed population PK simulations using the validated model, incorporating demographic characteristics of the target Bangladeshi pediatric population. The simulated tebipenem PK profiles were used to predict the probability of achieving maximum treatment effect in the target population and the main trial's chance of success, comparing two different dosing regimens. The findings of Chapter 4 showed that the effect of shigellosis-associated diarrhea on tebipenem PK was minimal. Moreover, Chapter 4 demonstrated an effective modeling workflow that can be adapted to support dose evaluation and efficacy predictions for other drugs and disease areas.

TABLE OF CONTENTS

LIST OF FIGURES

LIST OF TABLES

ACKNOWLEDGEMENTS

I would like to express my deepest gratitude to everyone who has inspired, supported, mentored, and cheered me throughout this journey. I could not have become the budding scientist I am today without you.

First, I want to express my sincere gratitude to my advisor, Dr. Sam Arnold, for his mentorship. I was granted the independence I desired while having access to help when needed. My research interests and career goals were well respected and supported. I am proud to be a member of the Arnold Lab.

I am also extremely grateful to the remaining members of my advisory committee and my CAB mentor, Dr. Kenneth Thummel, Dr. Shiu-Lok Hu, Dr. Jeannine McCune, Dr. Brian Werth, and Dr. Anita Mathias: thank you for the inspiring discussions and your unwavering support. I would like to extend a heartfelt thank you to Dr. Jeannine McCune and Dr. Kenneth Thummel for their invaluable advice, not only in science but also in career paths and life in general.

Special thanks to my collaborators Dr. Wesley Van Voorhis, Dr. Pui-Ying Iroh Tam, Dr. David Hermann, and Dr. Sharika Nuzhat for allowing me to work on these exciting projects.

Many thanks to my current and former lab members, my cohort, and my peers for your friendship. Thank you for listening to my complaints and sharing my joy. I have never been lonely throughout my journey because I could always count on your support.

To my friends and family, thank you for your unconditional love. I couldn't have succeeded in this endeavor without knowing that you'd always be there for me, even if I failed.

DEDICATION

This work is dedicated to my family, who love me not for what I have accomplished, but for who I am.

Chapter 1. INTRODUCTION

Intestinal drug absorption is a key area of interest for pharmaceutical sciences and drug development, as oral administration is the most common and preferred route of drug administration due to its convenience, accessibility, and availability. An important consideration for oral drug administration is that drug absorption along the gastrointestinal (GI) tract can be highly variable, and the absorption process is prone to changes induced by disease states. For instance, diarrheal diseases are associated with physiological changes impacting gut motility, luminal pH, absorptive surface area, fluid volume, and permeability, all of which can impact oral drug dissolution and permeation through the GI epithelial barrier and into the perfusing capillary blood.[1–5] Consequently, it is both challenging and crucial to understand how the multifold disease-associated physiological changes impact oral drug absorption and to be able to estimate and predict oral drug pharmacokinetics (PK) in a population with diarrheal disease.

1.1 Diarrheal Disease Impacts on Systems Regulating Oral Drug Absorption

Diarrheal disease is a major global health concern, and it is a leading cause of death in children. It was estimated that approximately 1.5 million people of all ages, including about 500,000 children under 5 years, died from diarrheal disease in 2019.[6] An analysis for the Global Burden of Diseases, Injuries, and Risk Factors Study 2017 also found that diarrhea was responsible for over 530,000 deaths among children younger than 5 years globally in 2017.[7] It was estimated that over 1 billion episodes of diarrhea occurred among children younger than 5 years in 2016 alone.[8] Furthermore, diarrhea was estimated as the third leading cause of disability-adjusted life-years (DALYs) in 2016, responsible for 74.4 million DALYs among all ages, of which 40.1

million occurred among children younger than 5 years.[8] Hence, given the high prevalence of diarrheal diseases, it is crucial to study how diarrhea-associated changes can impact the biophysical and physiological factors involved in oral drug absorption.

Although diarrhea is a common symptom of many GI disorders, its etiology, severity, duration, and pathophysiology can vary greatly. For instance, diarrhea can be categorized as inflammatory, fatty, or watery.[9] Inflammatory diarrhea is marked by the presence of leukocytes or leukocyte proteins in the stool and is associated with inflamed mucosa, such as that caused by ischemic colitis. Fatty diarrhea is due to malabsorption and maldigestion, such as that caused by celiac disease, cirrhosis, or as a side effect of gall bladder removal. Watery diarrhea can be further classified as either osmotic or secretory.[9,10] Osmotic diarrhea is caused by the presence of poorly absorbable yet osmotically active solutes in the GI lumen, resulting in fluid movement into the GI lumen in response to the osmotic gradient. Secretory diarrhea, on the other hand, involves increased secretion and/or impaired absorption of water and electrolytes. The region of the GI tract impacted by diarrheal diseases can be limited or diffused. For example, while Crohn's disease (CD) and ulcerative colitis (UC) are both types of inflammatory bowel disease, CD can affect any region along the GI tract and result in inflammation that penetrates all intestinal layers whereas UC is localized to the colon (including the rectum and anus) and affects only the mucosal layer of the colon.[11] The diversity and complexity of diarrhea precludes extrapolating a known diarrheal disease impact on a specific oral drug to all other diarrheal diseases and additional drugs.

Oral bioavailability (F), a parameter describing the fraction of orally administered dose reaching the systemic blood circulation, is a function of three separate terms reflective of drug penetration through the GI epithelium, GI elimination, and hepatic elimination (**Equation 1.1**).

$$F = F_a * F_g * F_h$$

Equation 1.1

F_a is the net fraction of the drug dose penetrating the gut wall from the gut lumen, F_g is the fraction that escapes intracellular gut metabolism, and F_h is the fraction that escapes first pass hepatic elimination via metabolism or biliary excretion. While the processes summarized by these three terms can all be affected by diseases, this thesis introduction mainly focuses on pathophysiological changes that appreciably impact the dissolution and membrane permeation of drugs in the GI tract (F_a) and discusses the potential application of PK modeling approaches to capture, estimate, and predict the resulting changes in the PK of an oral drug.

Many key factors have been identified to estimate drug dissolution, including the undissolved drug mass, luminal drug concentration, drug solubility, diffusion coefficient for the dissolved drug in a given solvent, effective diffusion layer thickness, particle size, surface area, density, and shape.[12–15] These parameters may differ at different regions of the GI tract for various reasons. For instance, there may be site-specific changes in local solubility due to differences in bile salt concentration/pH. Hence, the dissolution rate varies along the GI tract, depending on the local environment.

Once drug molecules have dissolved in the fluid within the GI lumen, the drug can penetrate the epithelial barrier by paracellular and/or transcellular diffusion.[16] With paracellular diffusion, the drug travels through the intercellular space between intestinal epithelial cells and generally enters the lymphatic system for delivery to systemic venous blood. However, for many small molecules, the predominant route to the blood is transcellular diffusion, which includes drug entry into and out of the gut epithelium, before penetration through capillary endothelium and entry into blood.[17] Both paracellular and transcellular diffusion processes depend on time-

varying drug levels in the GI lumen, paracellular space/gut wall, and lymph/blood. In addition to diffusion, the drug's permeation into and transit through enterocytes can also be affected by carrier-mediated transport (apical and basolateral) and gut metabolism. Similar to passive diffusion, active transport and metabolic activities depend on unbound drug concentration in the GI lumen, enterocytes, and/or blood, based on where the transporters and/or metabolic enzymes involved are located.[18] Moreover, the expression and distribution of relevant transporters and metabolic enzymes along the GI tract, their availability (absence/presence of inducers/inhibitors), as well as their clearance efficiency, also impact the absorption rate of oral drugs.[18] Because the GI environment is dynamic, the net permeation of drug particles into the body, accounting for diffusion, carrier-mediated transport, and drug metabolism, varies throughout the GI tract. Consequently, the diarrheal disease impacts on oral drug absorption can be highly variable across different causative organisms and drugs, depending on the GI regions affected by the diseases, physiological changes associated with the diseases, and the unique properties of the drugs.

1.1.1 *pH*

GI pH is an important factor for oral drug PK because it can directly impact oral drug solubility which may change dissolution rates. The drug permeation rate is also impacted because the luminal drug concentration, which depends on solubility and dissolution, determines the concentration gradient driving membrane permeation. Drugs in class II of the biopharmaceutics classification system (BCS) have low solubility and high membrane permeability, and their oral bioavailability can be significantly altered by GI pH. For weakly acidic or basic drugs with solubility-limited absorption and a pKa close to the physiologic pH of the part(s) of the GI tract, even slight shifts in GI pH may affect the ionization state of a drug, which in turn impacts the drug's solubility, protein binding, permeability, and dissolution rate, potentially leading to

changes in drug absorption [19–21]. For example, elevated gastric pH can reduce the ionization and solubility of weakly basic drugs, thus decreasing their bioavailability. Reduced absorption of weakly basic drugs ketoconazole, itraconazole, dipyridamole, indinavir, enoxacin, dasatinib, cinnarizine, and cefpodoxime proxetil have been reported in association with elevated gastric pH.[5] Similarly, GI pH changes can also impair the dissolution and subsequent supersaturation of drugs in supersaturating drug delivery systems, which is a drug delivery approach to enhance the oral bioavailability of poorly water-soluble drugs.[22] Furthermore, drug release from formulations can be impacted by GI pH since the disintegration of some coating polymers is pH-dependent. This may result in unforeseen changes in the maximum concentration (C_{max}) and the time C_{max} is achieved (T_{max}) of impacted drugs. Unpredicted shifts in the release profile of extended or controlled release formulations may occur, potentially leading to suboptimal treatment effects, reduction in duration of therapeutic response, and/or undesired side effects.

The luminal pH differs among different sections of the GI tract. Moreover, there is high between- and within-subject variability in GI pH due to factors such as fed/fasted state, meal caloric content, circadian rhythms, drug intake, and diseases.[23–26] Therefore, it is important to consider changes in GI pH relevant to the study population. Acid-reducing agents, such as proton pump inhibitors and H2-receptor antagonists, are well known to elevate gastric pH and alter the bioavailability of oral drugs that have pH-dependent solubility.[27–29] Although the interference of antacids with the absorption of concurrently administered oral drugs is a common example of clinically relevant drug-drug interaction, it is beyond the scope of this thesis. Instead, the focus of my work is on pH changes induced by diseases and their impact on oral drug pharmacokinetics. For example, hypochlorohydria, a state of low stomach acid with fasting gastric pH greater than 4.0, was significantly associated with human immunodeficiency virus

(HIV) infection[30] or *Helicobacter pylori* and HIV co-infection (**Table 1.1**).[31] Hence, when oral drugs studied in a different population are administered to HIV-infected patients, the impact of hypochlorohydria may need to be taken into consideration.

Another common cause of GI pH change associated with GI diseases is changes in bile acid production or reabsorption. Bile acid diarrhea (BAD), a common cause of chronic diarrhea, is estimated to impact 1% of the population and up to 50% of patients with functional or diarrhea-predominant irritable bowel syndrome.[32–34] BAD can be caused by either overproduction of bile acids due to defective feedback inhibition during synthesis or ileal malabsorption due to diseases or resection. Not only can BAD impact oral drug absorption by directly changing GI luminal pH, but it is also associated with modified colonic motility through alterations in colonic neuromuscular activity.[35–37]

1.1.2 *Absorptive Surface Area/Epithelial Integrity*

GI disorders often cause changes to the available absorptive surface area, which may lead to impaired drug absorption, further complicating the prediction of oral drug PK for impacted populations. For example, celiac disease is commonly associated with villous atrophy, leading to a reduction in absorptive surface area (**Table 1.1**).[4] Villous blunting has also been reported for Common Variable Immunodeficiency,[38,39] HIV infection,[40,41] and CD (**Table 1.1**).[42]

In addition to absorptive surface area changes, altered intestinal permeability has been reported for various GI disorders. The symptoms of celiac disease, an autoimmune disorder where an immune response in the small intestine is triggered upon the ingestion of gluten, often include diarrhea, abdominal pain, nausea, bloating, and nutrient/drug malabsorption. Studies suggest that the barrier function of the small intestine is compromised in celiac disease due to modifications to tight junctions, resulting in increased ionic permeability (**Table 1.1**).[43–46] CD, a

form of inflammatory bowel disease that causes chronic inflammation of the GI tract, is associated with increased paracellular permeability due to a reduction in tight junction integrity in the GI tract.[4]

1.1.3 *Transit Times*

The transit time of a drug within the GI tract is an important system parameter affecting oral absorption. Alterations in the transit time of a drug through any section of the GI tract would result in changes in the amount of time that the GI section is exposed to the drug of interest, consequently impacting absorption in the respective section and contributing to changes in overall drug absorption and the drug's PK profile. The transit time of a drug through the GI tract may depend on a variety of factors including drug formulation (liquid vs. solid), fed/fasted state of the recipient, composition of food taken with the drug if applicable, and the recipient's age, sex, and disease status.[47,48]

UC is a form of inflammatory bowel disease that is associated with inflammation of the mucosa and submucosa of the colon and rectum. Common symptoms of active UC include diarrhea, rectal bleeding, abdominal pain, rectal pain, weight loss, and fever.[49] GI transit time is reported to be prolonged and more variable in UC patients compared with healthy adults (**Table 1.1**).[4,50–56] Therefore, oral drugs administered to UC patients may require more time to travel through the GI tract, potentially driving changes in oral drug PK profiles in UC patients compared to those in a healthy population.

Altered GI pathology is commonly observed in HIV-infected patients because the GI tract is a major site of HIV replication. Moreover, co-infections in HIV-infected patients can lead to diarrhea as well as other GI disorders. Previous studies on GI transit times in HIV-infected subjects revealed delayed gastric emptying and accelerated small bowel transit, especially in

patients with protozoal diarrhea (**Table 1.1**).[57] Similar GI transit time changes have been reported in children with severely symptomatic acquired immunodeficiency syndrome (AIDS).[58] Accelerated whole-GI transit time in HIV-infected children was found to be significantly associated with malnutrition. The prevalence of GI transit time changes in various disease populations highlights the importance of quantitatively evaluating the impact of these changes on oral drug PK.

1.1.4 *Luminal Fluid Volume*

Not only does luminal fluid volume have a direct role in drug dissolution and permeation predictions, but it also impacts many of the previously discussed physiological parameters, including drug motility and luminal pH. Fluctuations in luminal pH due to changes in fluid volume can impact the ionization states of weakly acidic or weakly basic drugs, leading to changes in their solubility and, ultimately, their absorption. Altered bile acid concentrations in the luminal content may have a direct impact on the dissolution of lipophilic drugs. Furthermore, digestive enzyme concentrations depend on fluid volume as well, adding another layer of complexity to understanding the stability and dissolution of drugs in an altered GI environment. In addition, fluid volume affects the luminal drug concentration, thus impacting the drug concentration gradient driving diffusion between the luminal content and the enterocytes/blood. Lastly, changes in fluid secretion (e.g., by mucosal goblet cells) can affect the thickness and composition of the mucus layer lining the luminal membrane surface, potentially compromising the barrier function of the mucus layer which may impact drug permeability.[59]

Changes in intestinal fluid secretion or absorption are common for diarrheal diseases. For instance, cholera is characterized by extensive fluid loss due to decreased absorption and increased secretion of fluid in the GI tract (**Table 1.1**).[60,61] Therefore, given the impact of

luminal fluid volume on oral drug absorption, it is likely that oral drug PK is altered in association with diarrheal diseases.

1.1.5 *Transport and Metabolism*

In addition to compromising the epithelial integrity, as discussed earlier, diarrheal diseases are associated with alterations in the expression or activity of proteins involved in active transport and/or metabolism by gut epithelial cells (enterocytes). For example, decreased epithelial P-glycoprotein (P-gp) and Breast Cancer Resistance Protein (BCRP) expression were observed for the colon and the rectum in patients with active UC.[4,62,63] Altered intestinal expression of P-gp and cytochrome P450 (CYP) 3A4 have been reported for CD patients.[63–67] A reduction in intestinal CYP3A4 activity has also been observed in celiac disease patients.[68] While the importance of active transport and metabolism on oral drug PK cannot be overlooked or dismissed, the breadth of their respective research areas warrants separate discussions of their own that is outside the scope of this introduction.

1.2 Examples of Clinically Significant Diarrheal Disease Impact on Oral Drug Pharmacokinetics

The section above summarized the numerous ways diarrheal diseases can impact oral drug PK. With that background now summarized, the question becomes: Can the impact of diarrheal diseases on oral drug PK be clinically significant? Are PK changes associated with diarrheal diseases sufficient to warrant special dosing considerations for populations affected by diarrhea, or are the impacts too minuscule to influence clinical practice? Several studies suggest diarrhea can lead to significant PK changes and demonstrate the pressing need for better characterization and understanding of oral drug PK changes in populations affected by diarrhea.

1.2.1 *Subtherapeutic Antiretroviral Plasma Levels Associated with Diarrhea in AIDS Patients*

HIV infection is often complicated by diarrhea and a compromised GI tract, and there is clinical evidence that these complications can impact plasma levels of antiretrovirals used to control HIV infection and prevent comorbidities. A clinical study in northeast Brazil compared stavudine and didanosine plasma concentrations between AIDS patients with (n=12) or without (n=7) diarrhea.[69] Between the six subjects with diarrhea and three controls without diarrhea, all of whom had received stavudine at doses prescribed by their physicians, plasma stavudine levels were significantly lower for the group presenting with diarrhea. Alarmingly, subtherapeutic (<0.3 μg/mL) stavudine plasma levels were observed in five out of the six subjects with diarrhea, whereas all three control subjects without diarrhea had stavudine plasma levels of ~0.8 μg/mL. Similarly, plasma didanosine levels were lower in subjects with diarrhea. Three out of the four subjects with diarrhea who took didanosine had plasma levels below the limit of detection (<0.1 μg/mL). Although the only control subject who took didanosine also had a subtherapeutic plasma level of 0.5 μg/mL, it was substantially higher than those of the subjects with diarrhea.

Although this study had limitations, including the varying antiretroviral regimens assigned to study participants and significant BMI differences between patient groups, the findings strongly suggest reduced oral antiretroviral exposure in association with diarrhea. The observation that antiretroviral plasma levels could fall below therapeutic levels in patients with diarrhea possibly contributed to the significant difference observed in HIV viral load between the diarrhea group and the non-diarrhea group, where the median viral load was 230 x 10^3 copies/mL for the diarrhea group and 81 x 10^3 copies/mL for the non-diarrhea group. Based on these opportunistic observational findings, a randomized, double-blinded, placebo-controlled trial was

conducted by the same group to evaluate the effect of glutamine and alanyl-glutamine for treating diarrhea and improving antiretroviral drug PK in patients with AIDS.[70] It was found that glutamine and alanyl-glutamine treatment significantly improved diarrheal symptoms and antiretroviral drug levels, supporting a link between diarrhea and compromised antiretroviral drug absorption in HIV patients. Another study of antiretroviral zidovudine bioavailability in HIV-infected patients also reported a significant correlation between mild diarrhea and reduced zidovudine bioavailability.[71] However, conflicting evidence exists where a lack of significant association was found between zidovudine PK and the presence of diarrhea such that the story remains inconclusive.[72,73]

Since diarrhea is commonly observed in HIV-infected individuals,[74–77] antiretroviral medications are often administered in the presence of diarrhea. Failure in achieving therapeutic antiretroviral levels due to the influence of diarrhea may result in worsening HIV infection status, further aggravating the GI complications and forming a vicious cycle propagating treatment failure.

1.2.2 *iOWH032 PK in Cholera Patients Experiencing Severe Diarrhea*

iOWH032 is an inhibitor of the cystic fibrosis transmembrane conductance regulator (CFTR) chloride channel and was developed to treat cholera toxin-induced secretory diarrhea. A study compared the PK of iOWH032 following a single oral 300 mg dose in Bangladeshi cholera patients (n=14) and healthy Bangladeshi volunteers (n=8).[78] When the study populations were compared, the investigators observed that the mean area under the plasma concentration-time curves from time 0 to infinity (AUC_{inf}) was only 6,250 ng*h/mL for cholera patients, compared with 22,700 ng*h/mL for healthy Bangladeshi volunteers. The mean C_{max} was also markedly lower for cholera patients at 482 ng/mL, in contrast to 1,280 ng/mL for healthy Bangladeshi

volunteers. Moreover, T_{max} was earlier at 3.8 h in Bangladeshi cholera patients in comparison to 4.8 h in healthy Bangladeshi volunteers. While this study did not directly test the relationship between cholera or cholera-induced diarrhea and the observed variability in iOWH032 PK, the observation of a pronounced 3.6-fold reduction in iOWH032 AUC_{inf} and a 2.7-fold reduction in iOWH032 C_{max} among Bangladeshi cholera patients with severe diarrhea, compared to healthy Bangladeshi volunteers that were comparable in baseline demographic variables, supported a suspected diarrheal disease impact on iOWH032 absorption.

1.2.3 *Reduced Clofazimine Plasma Concentrations in HIV-Infected Adults with Cryptosporidiosis*

A randomized, double-blind, placebo-controlled Phase 2a clinical trial was conducted in adults infected with HIV and with or without cryptosporidiosis.[79] Cryptosporidiosis, a parasitic disease resulting from *Cryptosporidium* infection, causes watery diarrhea, abdominal pain, nausea, and fever.[80] The symptoms can persist and more severe consequences, such as malnutrition, severe weight loss, growth stunting, and mortality, may also manifest in immunocompromised persons and malnourished children.[80–82] The goal of the Phase 2a clinical trial was to study the safety, efficacy, and PK of clofazimine in patients living with HIV, for the treatment of cryptosporidiosis.

This clinical trial consisted of two parts, Parts A and B. Part A participants were HIV-positive, aged between 18 and 65 years, weighed at least 35.4 kg, tested positive for *Cryptosporidium* infection, and experienced at least 14 days of diarrhea at the time of study enrollment. Part A participants were randomized at approximately 1:1 to receive either clofazimine (n=12) or placebo (n=10). Part B participants were matched to the first 10 Part A participants based on age, sex, and weight, but differed from Part A participants by

Cryptosporidium infection status. All Part B participants were HIV-positive but *Cryptosporidium*-negative at enrollment. All Part B participants received clofazimine. The clofazimine dosing regimen was the same for all Part A and B participants assigned to receive clofazimine treatment; clofazimine was administered orally three times daily for 5 days. Participants who weighed over 50 kg at enrollment received 100 mg clofazimine per dose, whereas those who weighed less than 50 kg received 50 mg clofazimine per dose.

Despite being similar in baseline demographic characteristics and receiving the same clofazimine dose, Part A participants living with HIV, *Cryptosporidium* infection, and diarrhea had approximately 2-fold less plasma clofazimine exposure than Part B participants that had only HIV infection but not *Cryptosporidium* infection or diarrhea. The mean area under the curves for the initial 24 h following study initiation ($AUC_{0\text{-}24H}$) was 1364.0 ng*h/mL for Part A participants, compared to 2851.0 ng*h/mL for Part B participants. On study Day 5, the last day of clofazimine dosing, $AUC_{0\text{-}24H}$ ($AUC_{96\text{-}120H}$ of the entire study) was 6,863.0 for Part A and 11,298.0 for Part B participants. This observation suggests that *Cryptosporidium* infection or cryptosporidiosis-associated diarrhea might have impacted oral clofazimine PK in this clinical trial, resulting in reduced drug AUC. This echoed the findings of the studies described in Sections 1.3.1 and 1.3.2, highlighting the importance of studying the potential impact of diarrheal disease on oral drug PK, as the resulting decrease in drug exposure may necessitate dose adjustments.

1.3 Application of Population Pharmacokinetic Modeling for Estimating Diarrheal Disease Impact on Oral Clofazimine Pharmacokinetics

Population pharmacokinetic (popPK) modeling is a mathematical modeling approach; it estimates drug PK parameters and evaluates sources of variability in target patient populations. PopPK modeling allows the simultaneous evaluation of concentration-time data from multiple individuals using a nonlinear mixed-effects (NLME) model. Not only can popPK modeling describe a typical drug disposition profile, using parameters that do not change across individuals ("fixed effects"), but it also accounts for unexplained "random" variability within the population (such as interindividual variability, interoccasion variability, and residual variability) and evaluates PK variability associated with subject characteristics (covariate effect).[83] Therefore, it differs from the individual PK modeling approach in its ability to identify and quantify variability in drug PK and to retain individual-level information from population studies. Moreover, the identification of sources of PK variability is key to making correct dosing decisions; knowledge of important covariates for drug PK would enable the identification of special populations that require dose adjustments to produce adequate treatment effects.

As discussed previously, there are various mechanisms through which diarrheal diseases can potentially impact oral drug PK. However, the extent of diarrheal disease impact on oral drug PK has not been quantitatively described to date. To bridge this knowledge gap, popPK modeling techniques can be applied to oral drug PK data collected from a population affected by a diarrheal disease to investigate whether the disposition of a drug of interest is impacted by the diarrheal disease. The Phase 2a clinical trial of clofazimine, described in Section 1.3.3, provides a unique opportunity for applying a popPK modeling approach to study the impact of

cryptosporidiosis-associated diarrhea on oral clofazimine PK. In this clinical trial, Part B participants who were HIV-positive but did not have *Cryptosporidium* infection received the same doses of clofazimine as Part A participants who were HIV- and *Cryptosporidium*-positive.[79] Moreover, Part B and Part A participants were comparable in baseline demographic characteristics because Part B participants were matched to Part A participants.[79] This ruled out potential confounders, such as an imbalanced distribution of baseline characteristics between the two study arms, and allowed better estimation of any cryptosporidiosis disease effect. In addition, although Part A participants had all been experiencing at least 14 days of diarrhea at enrollment, some diarrhea cases were resolved by study initiation.[84] This further enabled the delineation between a cryptosporidiosis-associated diarrhea effect (i.e. participants experiencing diarrhea during clofazimine treatment) and a *Cryptosporidiosis* infection effect (i.e. participants testing positive for *Cryptosporidiosis* infection by qPCR).

1.4 Pharmacokinetic/Pharmacodynamic Modeling for Efficacious Dose Prediction

Pharmacokinetic/Pharmacodynamic (PK/PD) modeling utilizes mathematical expressions to describe the relationship between drug concentration or exposure and pharmacodynamic (PD) responses, thus allowing the prediction of drug levels/doses associated with desired outcomes. Examples of PD models commonly used in PK/PD modeling include the linear model, the Emax model, the sigmoidal Emax model, the log-linear model, etc..[85–87] Drug concentration can drive PD effect directly or indirectly, the latter requiring more complex PK/PD models such as the effect compartment model, turnover model, transit compartment model, or tolerance compartment model.[85–87] The selection of a model depends on many factors, such as data availability, the type of data, trends revealed by exploratory analyses, questions to address, and

physiological relevance. PK/PD modeling is a valuable tool in all stages of drug development to provide crucial information for decisions on compound selection, dose optimization, and study design, augmenting the chance for study success.[88]

For studying diarrheal disease impact on oral drug PK, it is not sufficient to only quantitatively evaluate the magnitude of such impact, if it exists. Rather, the diarrheal disease impact on an oral drug of interest should also be evaluated for its clinical significance – whether it can potentially lead to treatment failure. To evaluate whether cryptosporidiosis-associated diarrhea led to treatment failures in the Phase 2a clinical trial of clofazimine for the treatment of cryptosporidiosis, PK/PD modeling techniques can be employed to predict a clofazimine level associated with treatment success and subsequently compare the predicted target level to the observed clofazimine levels in the clinical trial.[89] Through utilizing preclinical data, PK/PD relationships between clofazimine levels and desired treatment outcomes can be correlated. This information can guide the establishment of a dose target for the clinical trial.

1.5 Extending the Population Pharmacokinetic Modeling Approach to Predict Clinical Trial Outcomes for Investigational Shigellosis Treatment

Shigellosis is a diarrheal disease caused by an infection with the bacterium *Shigella*.[90] Patients with shigellosis usually experience bloody diarrhea, high fever, and abdominal pain.[91] Tebipenem is an oral carbapenem that is currently being studied as a potential alternative treatment for shigellosis. To evaluate whether shigellosis-induced diarrhea could impact the PK of tebipenem-pivoxil, the prodrug form for tebipenem, a popPK modeling approach can be used. Furthermore, popPK models are powerful predictive tools; they can simulate variability in drug disposition associated with unique characteristics of the target population. Therefore, by estimating

important covariates to accurately represent the target population and including this piece of information in a popPK model, predictions can be made specific to the dosing regimens of interest in the target population for the clinical trial. Subsequently, the PK predictions can be used to estimate the probability of trial success.

1.6 Hypothesis and Specific Aims

The overarching hypothesis of this thesis was that pharmacokinetic modeling approaches can be utilized to characterize and simulate oral drug pharmacokinetics in a population with diarrheal disease and make predictions about treatment efficacy. To test this hypothesis, the pharmacokinetics of clofazimine and tebipenem, for the treatment of cryptosporidiosis and shigellosis, respectively, was studied using popPK and PK/PD modeling approaches. With my work, I would like to establish a popPK model workflow that can be adapted to evaluate the impact of various diarrheal diseases on different oral drug PK and demonstrate the power of popPK modeling in conjunction with PK/PD modeling for making efficacy predictions and informing dosing decisions. Namely, the specific aims of my dissertation are:

Aim 1: To quantitatively evaluate cryptosporidiosis-associated diarrhea impact on oral clofazimine pharmacokinetics using a population pharmacokinetic modeling approach.

Aim 2: To determine whether cryptosporidiosis-associated diarrhea reduced clofazimine levels below levels associated with efficacy against *Cryptosporidium* infection.

Aim 3: To predict the population pharmacokinetics of oral tebipenem in a target Bangladeshi pediatric population with shigellosis and estimate the probability of target attainment and non-inferiority trial success, compared with intravenous ceftriaxone.

Table 1.1. Summary of physiological changes associated with ulcerative colitis, Crohn's disease, celiac disease, HIV infection, and cholera.

Disease	Parameter	Region	Study Population	Physiological Change	References
Ulcerative Colitis (UC)	pH	Stomach, small intestine, colon	UC patients (n=11), healthy controls (n=12)	Median gastric pH for UC patients (1.95) was significantly higher than that of the healthy controls (1.55). UC patients had significantly higher pH values in the terminal ileum, the caecum and the right colon.	[23]
	pH	Stomach, small intestine, colon	Active UC (n=6)	Normal pH values in the stomach and small intestine. Three patients had very low pH levels (2.3, 2.9, 3.4) in the proximal colon.	[92]
	pH	Rectum	Moderate UC patient (n=1), severe UC patients (n=4), healthy subjects (n=15)	Median pH in UC patients was 7.8, compared to 7.2 in healthy controls.	[93]
	pH	Small intestine, colon	Active UC patients (n=8), normal controls (n=4)	Mean colonic pH was not different. Small intestinal pH was similar between UC patients and controls.	[51]
	Permeability	Small and large intestine	Healthy controls (n=11), UC patients (n=21)	Intestinal permeability was increased for UC patients.	[94]
	Permeability	GI	Crohn's disease patients (n=86), UC patients (n=32), healthy controls (n=23)	Serum zonulin concentration, reflective of paracellular permeability, was higher in UC patients (40.3 ng/mL) compared to healthy controls (8.6 ng/mL).	[95]
	Transit time	Total GI	Severe UC patients (n=20), healthy subjects (n=20)	Significantly longer total GI transit time in severe UC patients (median 44.5 h) compared with healthy subjects (median 27.6h).	[50]
	Transit time	Small intestine, colon	Active UC patients (n=8), normal controls (n=4)	Mean transit time in small intestine was similar for UC patients (7 h) and for normal controls (6 h). Transit time through the distal colon was longer for UC patients (12 h) compared to the controls (7 h). Transit time in the proximal colon were comparable for UC patients (7h) and for controls (8h).	[51]

	Transit time	Mouth to caecum, gastric	UC patients (n=62), healthy controls (n=20)	Orocaecal transit was significantly slower in UC patients. Gastric emptying was similar between UC patients and healthy controls, except for a slight increase in those with quiescent distal colitis. Total GI transit time was not significantly different among UC patient groups and the healthy controls.	52
	Transit time	Orocaecal transit time (OCTT)	UC patients (n=95), healthy controls (n=115)	Mean OCTT in UC patients (2.0h) was longer than in the controls (1.5h).	53
	Transit time	Small intestine	UC patients (n=23), non-IBD patients (n=125)	Median small intestinal transit time in UC patients (4.4h) was significantly longer than in non-IBD patients (3.6h).	54
	Transit time	Stomach, small intestine	Active UC patients (n=2), quiescent UC patients (n=4)	Mean gastric emptying time of 1.6 h and mean small intestinal transit time of 3.4h were similar to previously reported values for healthy subjects.	55
	Transit time	Stomach, small intestine	Familial adenomatous polyposis, intestinal lymphoma, and ulcerative colitis patients (n=116), healthy volunteers (n=87)	Mean gastric transit time for the combined pathology patient group (48 min) and that for healthy volunteers (39 min) were not significantly different. Mean small intestinal transit time in the patient group was 4 h 27 min, whereas that for healthy volunteers was 3 h 56 min.	56
Crohn's Disease (CD)	pH	Terminal ileum	CD patients (n=15), healthy subjects (n=15)	Median pH in CD patients was 7.5, compared to 7.2 in healthy controls.	93
	pH	Stomach, small intestine, colon	CD patients (n=12), healthy controls (n=12)	Median gastric pH for CD patients (2.4) was significantly higher than that of healthy controls (1.55). Small intestinal and colonic pH were similar between CD patients and healthy controls.	23
	pH	Small intestine, right colon	Ileocecal-resected CD patients (n=9), healthy volunteers (n=13)	Small intestinal pH was not significantly different in CD patients vs. controls. Median right colon pH was 0.9 pH units higher in resected CD patients (6.7) compared to controls (5.8).	96
	Absorptive surface area	Duodenum and terminal ileum	Biopsies from children 1-19 years with/out CD (n=107)	Villous length was reduced by 2-fold in inflamed duodena and ilia.	42

Permeability	Small and large intestine	CD of the small intestine (n=15) and CD/UC of the colon (n=19)	CD patients had increased intestinal permeability, particularly in the colon.	97
Permeability	Small and large intestine	Healthy controls (n=11), CD patients (n=35)	Intestinal permeability was increased in CD patients.	94
Permeability	Stomach, small and large intestine	CD patients (n=50), healthy controls (n=30)	CD patients showed higher gastric and intestinal permeability.	98
Permeability	GI	CD patients (n=86), UC patients (n=32), healthy controls (n=23)	Serum zonulin concentration, reflective of paracellular permeability, was significantly higher in CD patients (33.5 ng/mL) compared to healthy controls (8.6 ng/mL).	95
Transit time	Stomach	CD patients (n=12), controls (n=13)	Mean gastric emptying $t_{1/2}$ was significantly increased in CD subjects (38.5 min) compared with controls (23.6 min)	99
Transit time	Orocaecal transit time (OCTT)	CD patients (n=45), healthy subjects (n=20)	OCTT was delayed in 67% CD patients (120 min) compared to the control (88.2 min). OCTT was more prolonged in ileal localization CD (182.2 min), and less in patients with ileocolonic (122 min) or colonic (106 min) localization.	100
Transit time	Orocaecal transit time (OCTT)	CD patients (n=57), healthy controls (n=4)	Longer OCTT was observed in patients (154 min) compared to controls (136 min) but the difference was not significant. OCTT was significantly longer in 14 CD patients with ileocolic resection (180 min) compared to controls.	101
Transit time	Orocaecal transit time (OCTT)	CD patients (n=42), healthy controls (n=115)	Mean OCTT in UC patients (2.3h) was higher than that in the controls (1.5h).	53
Transit time	Small intestine	Active CD patients (n=33), inactive CD patients (n=22), non-IBD patients (n=125)	Median small intestinal transit time was significantly longer in active CD patients (4.2h) than in non-IBD patients (3.6h) and inactive CD patients (3.1h).	54

	Transit time	Stomach, small intestine, colon	CD patients (n=6), healthy controls (n=8)	Mean gastric emptying was significantly longer for CD patients (4.0 h) compared to healthy controls (2.7h). Small intestinal transit time was not significantly different between CD patients (2.4h) and controls (3.0 h). Transit through the ascending colon tended to be shorter in CD patients (8.1h) than in healthy controls (15.5h), but the difference was not significant.	[102]
	Transit time	Stomach, small intestine	CD patients (n=19), non-CD patient controls (n=178)	Mean gastric emptying time was comparable between CD patients (36.4 min) and the controls (34.9 min). Small intestinal transit time was significantly longer for the CD patients (337 min) than for the controls (243.6 min).	[103]
	Transit time	Stomach	Inactive CD patients (n=26), age- and sex-matched healthy controls (n=19)	CD patients had significantly delayed and prolonged gastric emptying compared to the controls.	[104]
	Transit time	Small intestine	Ileocecal-resected CD patients (n=9), healthy volunteers (n=13)	Median small intestinal transit time was significantly shorter in ileocecal-resected patients (5.2 h) compared to controls (8.0 h).	[96]
	Transit time	Stomach, small intestine	Suspected CD patients (n=96), healthy volunteers (n=87)	Mean gastric transit time for CD patients (42 min) and that for healthy volunteers (39 min) were not significantly different. Mean small intestinal transit time was 3 h 58 min in CD patients and 3 h 56 min in healthy volunteers.	[56]
Celiac Disease	pH	Jejunum	Treated and untreated celiac disease patients (n=19), healthy controls (n=10)	Jejunal surface pH was significantly higher in celiac disease patients compared with healthy controls.	[105]
	Absorptive surface area	Duodenum	Celiac disease patients who underwent follow-up biopsy (n=7648)	Persistent villous atrophy was found in 43% of patients.	[106]
	Permeability	Jejunum	Biopsy specimens from celiac patients and healthy controls	Epithelial barrier function was reduced in acute celiac disease, compared with the controls.	[45]

	Permeability	Jejunum	Children with treated and untreated celiac disease	Epithelial barrier function was reduced by structural modifications of the tight junction in acute celiac disease. Children with a gluten-free diet had partially recovered barrier function.	[43]
	Permeability	Duodenum	Healthy controls and celiac disease patients receiving a gluten-containing diet	Celiac disease patients had increased paracellular leakage associated with alteration to tight junction protein expression and assembly.	[44]
	Transit time	Stomach	Treated (n=9) and untreated (n=7) celiac disease subjects, controls (n=13)	Mean gastric emptying $t_{1/2}$ was significantly increased in untreated celiac disease patients (35.1 min) and treated celiac disease patients (45.2 min) compared with controls (23.6 min).	[99]
	Transit time	Stomach, small intestine	Untreated celiac disease patients (n=30), age-, sex-, and BMI-matched healthy controls (n=30)	No statistically significant differences in gastric emptying and small intestinal transit times were found between the two groups.	[107]
	Transit time	Orocaecal transit time (OCTT)	Celiac disease patients (n=16), healthy volunteers (n=20)	Before gluten-free diet, mean OCTT was significantly prolonged in celiac disease patients (243 min) compared to controls (117 min). After a gluten-free diet, OCTT in celiac patients (134 min) was not significantly different from that of the controls.	[108]
	Transit time	Stomach, small intestine	Celiac disease patients (n=65), healthy volunteers (n=87)	Mean gastric transit time for celiac disease patients (33 min) and that for healthy volunteers (39 min) were not significantly different. Mean small intestinal transit time in celiac disease patients was 4 h 43 min, whereas that for healthy volunteers was 3 h 56 min.	[56]
Cholera	pH	Vomitus	Patients with acute, severe cholera (n=18 samples)	Median pH in vomit samples was ~7.6	[109]
	pH	Stool	Patients with acute, severe cholera (n=18 samples)	Median pH in stool samples was ~8.5	[109]

	Permeability	Ileum	Female Sprague-Dawley rats treated with cholera toxin perorally via a gastric tube (n=2) or locally (n=4), control animals (n=4)	Cholera toxin significantly increased permeability to large molecules. The increase was the greater for local administration of cholera toxin compared to peroral treatment.	[110]
	Transit time	Whole gut	Children ≤ 5 years (n=68; including 29 cholera, 17 rotavirus, 13 enterotoxigenic Escherichia coli, and 9 Shigella cases) during acute stages of diarrhea	Mean whole gut transit time ranges from 5.5 to 7.3 h.	[111]
	Luminal fluid volume	Jejunum	Dog jejunal mucosa exposed to cholera toxin	In vitro fluid absorption rate was reduced by ~50% of the control value. Fluid secretion rate was increased.	[61]
	Luminal fluid volume	Fluid output	Adults with cholera	1 L/h fluid output	[112,113]
HIV Infection	pH	Stomach	Fasting adults with/out HIV infection (n=203)	HIV infection was significantly associated with hypochlorhydria. Digitized median gastric pH was ~1.5 for HIV-negative subjects, ~4.9 for HIV+ subjects with CD4 cell count >200 cells/μL, ~3.5 for HIV+ subjects with CD4 <200 cells/μL, and ~1.5 for HIV+ subjects on highly active antiretroviral therapy.	[30]
	pH	Stomach	HIV-positive (n=17), HIV-negative (n=78) outpatients symptomatic for hypochlorhydria and referred for gastroscopy	Mean gastric pH was 4.6 for HIV-negative patients and 5.6 for HIV+ patients. HIV infections was not independently associated with hypochlorhydria. Co-infection with HIV and *Helicobacter pylori* was significantly associated with hypochlorhydria.	[31]
	pH	Stomach	HIV-infected subjects (n=19)	60% of HIV+ patients and 67% of AIDS patients had persistently elevated gastric pH during the baseline period.	[114]

Absorptive surface area	Jejunum	HIV-infected subjects with chronic diarrhea (n=21), controls (n=14)	Significant difference was found in mean surface area/volume ratio: 41.6 in HIV+ subjects and 56.5 in controls. Mean crypt length was significantly different: 45.9 in HIV+ subjects and 31.4 in controls.	[41]
Absorptive surface area	Duodenum	HIV-infected patients (n=24), controls (n=21)	Villous atrophy was found in 54% of HIV-infected patients, compared to 0% in control subjects.	[40]
Absorptive surface area	Duodenum	HIV-positive patients (n=63), HIV-negative controls (n=36)	Based on duodenal biopsies, HIV+ patients had more inflamed duodenum than the controls. Those with chronic diarrhea and parasitic infection had more blunting than those with diarrhea but not parasitic infection.	[115]
Permeability	Small intestine	HIV-positive subjects (n=60), HIV-negative controls (n=20)	Intestinal permeability was significantly increased with AIDS.	[57]
Permeability	Small intestine	Black (n=39) and white (n=39) HIV-infected patients, black (n=40) and white (n=57) healthy controls	Both black and white HIV-infected patients with diarrhea had increased intestinal permeability and malabsorption compared to their respective healthy controls. Only white HIV-positive patients without diarrhea had increased intestinal permeability as compared with white healthy controls.	[116]
Transit time	Stomach, jejunum to caecum	HIV-positive subjects (n=60), HIV-negative controls (n=20)	Gastric emptying was significantly delayed in AIDS patients. Mean jejunal to caecal transit time was not significantly different between controls (246 min) and patients without diarrhea or patients with diarrhea of causes other than cryptosporidiosis, although a trend of reduced transit time was seen for patients with pathogen-negative diarrhea or microsporidiosis. Patients with cryptosporidiosis and diarrhea had significantly reduced jejunal to caecal transit time (135 min) compared to the controls.	[57]
Transit time	Whole GI	HIV-positive children (n=40) between 1 month and 3 years old, HIV-negative age-matched controls (n=30)	Whole GI transit time was most rapid in severely symptomatic AIDS patients.	[58]

	Transit time	Stomach	HIV-positive patients (n=20), healthy volunteers (n=20 for liquid emptying rate, n=54 for sold emptying rate)	Mean gastric emptying was significantly faster in HIV patients (18 min) than in healthy controls (28 min). Mean solid emptying rate was significantly delayed in HIV patients ($t_{1/2}$ = 88 min) compared to in healthy volunteers ($t_{1/2}$ = 47 min).	117

Chapter 2. CLOFAZIMINE PHARMACOKINETICS IN HIV-INFECTED ADULTS WITH DIARRHEA: IMPLICATIONS OF DIARRHEAL DISEASE ON ABSORPTION OF ORALLY ADMINISTERED THERAPEUTICS

The work presented in this chapter was published in *CPT: Pharmacometrics & Systems Pharmacology* 2024 Jan (doi: 10.1002/psp4.13092).

Authors: C. X. Zhang, T. M. Conrad, D. Hermann, M. A. Gordon, E. Houpt, P.Y. Iroh Tam, K. C. Jere, W. Nedi, D. J. Operario, J. Phulusa, G. V. Quinnan Jr, L. A. Sawyer, L. K. Barrett, H. Thole, N. Toto, W. C. Van Voorhis, and S. L. M. Arnold

Author contributions: C.X.Z., T.M.C., D.H., M.A.G., E.H., P.-Y.I.T., K.C.J., W.N., D.J.O., J.P., G.V.Q., L.A.S., L.K.B., H.T., N.T., W.C.V.V., and S.L.M.A. wrote the manuscript. C.X.Z., T.M.C., D.H., M.A.G., E.H., P.-Y.I.T., K.C.J., W.N., D.J.O., J.P., G.V.Q., L.A.S., L.K.B., H.T., N.T., W.C.V.V., and S.L.M.A. designed the research. C.X.Z., T.M.C., D.H., M.A.G., E.H., P.-Y.I.T., K.C.J., W.N., D.J.O., J.P., G.V.Q., L.A.S., L.K.B., H.T., N.T., W.C.V.V., and S.L.M.A. performed the research. C.X.Z., T.M.C., and S.L.M.A. analyzed the data.

2.1 ABSTRACT

Oral drug absorption kinetics are usually established in populations with a properly functioning gastrointestinal tract. However, many diseases and therapeutics can alter gastrointestinal physiology and cause diarrhea. The extent of diarrhea-associated impact on drug pharmacokinetics has not been quantitatively described. To address this knowledge gap, we used a population pharmacokinetic modeling approach with data collected in a phase 2a study of matched HIV-infected adults with/without cryptosporidiosis and diarrhea to examine diarrhea-associated impact on oral clofazimine pharmacokinetics. A population pharmacokinetic model was developed with 428 plasma samples from 23 HIV-infected adults with/without *Cryptosporidium* infection using nonlinear mixed-effects modeling. Covariates describing cryptosporidiosis-associated diarrhea severity (e.g., number of diarrhea episodes, diarrhea grade, etc.) or HIV infection (e.g., viral load, CD4+ T cell count) were evaluated. A two-compartment model with lag time and first-order absorption and elimination best fitted the data. Maximum diarrhea grade over the study duration was found to be associated with over 6-fold reduction in clofazimine bioavailability. Apparent clofazimine clearance, intercompartmental clearance, central volume of distribution, and peripheral volume of distribution were 3.71 L/h, 18.2 L/h (inter-individual variability [IIV] 45.0%), 473 L (IIV 3.46%), and 3434 L, respectively. The absorption rate constant was 0.625 h^{-1} (IIV 149%) and the absorption lag time was 1.83 h. In conclusion, the maximum diarrhea grade observed for the duration of oral clofazimine administration was associated with a significant reduction in clofazimine bioavailability. Our results highlight the importance of studying disease impacts on oral therapeutic pharmacokinetics to inform dose optimization and maximize the chance of treatment success.

2.2 INTRODUCTION

Oral drug delivery is the most common and preferred route of drug administration due to its ease of delivery, non-invasiveness, high compliance, and cost-effectiveness. Conditions in the gastrointestinal (GI) tract, such as motility, transit time, luminal pH, fluid composition, absorptive surface area, and permeability may have a profound impact on oral drug release, dissolution, and permeation, reflected by changes in oral drug bioavailability.[1–3,5,118,119] While not studied in detail, it is plausible that dosing recommendations based on data collected from populations with typical, healthy GI physiology may result in unexpected changes in drug exposure and subtherapeutic responses in populations presenting with diarrhea.

Observations of potential diarrhea-associated changes in drug exposure have indeed been reported in the literature. A study in Brazil found that antiretroviral stavudine and didanosine plasma levels were substantially lower in human immunodeficiency virus (HIV)-infected patients with diarrhea or wasting compared to HIV-infected patients without diarrhea.[69] However, limitations to this study such as variable antiretroviral regimens, doses, and durations, significant body mass index (BMI) differences between patient groups, and the lack of in-depth statistical analyses precluded the study from conclusively proving that diarrhea had a significant role in influencing antiretroviral absorption in the study population. Other studies of diarrhea and oral drug pharmacokinetics (PK) yielded mixed results; while some observed potential relationships between diarrhea and reduced plasma drug levels,[70,71] others did not find any significant diarrhea effect.[72,73,120]

The potential impact of cryptosporidiosis, a diarrheal disease caused by *Cryptosporidium* infection, on drug disposition has not been previously studied.[80,121,122] Clinical symptoms of cryptosporidiosis range from watery diarrhea, abdominal pain, dehydration, nausea, vomiting, and

fever in immunocompetent subjects to persistent diarrhea, severe weight loss, malnutrition, and mortality in malnourished children and immunocompromised persons.[80–82,123] It was estimated that *Cryptosporidium* infection resulted in over 48,000 deaths and more than 4.2 million disability-adjusted life-years lost in 2016 alone.[124] Clofazimine, an orally administered antimicrobial approved by the FDA to treat leprosy and a "Group B" drug recommended by the World Health Organization (WHO) to treat multidrug-resistant (MDR) tuberculosis (TB), was shown to be effective in controlling *Cryptosporidium* infection in preclinical in vitro and in vivo models.[89,125,126] While clofazimine's PK and safety profiles had been studied in healthy volunteers and patients with leprosy or MDR-TB, no study had been conducted for patients with cryptosporidiosis until a phase 2a trial was conducted in Malawi in HIV-infected adults.[79,127–130] The trial enrolled HIV-infected adults, with or without Cryptosporidium infection, matched based on weight, sex, and age, utilizing a unique two-part design.[79,127] Using PK data from this trial, our study applied population PK modeling to quantify the impact of cryptosporidiosis-associated diarrhea on oral clofazimine PK. Our findings highlight the importance of studying the potential impact of diarrhea on oral drug PK for optimizing dosages and improving treatment outcomes.

2.3 METHODS

2.3.1 *Study Design*

Detailed descriptions of the protocol and clinical outcomes of the study have been published previously.[79,127] This single-center, randomized, double-blind, placebo-controlled phase 2a clinical trial was conducted in Blantyre, Malawi (NCT#: 03341767). Written informed consent was received from all study participants, and the study protocol was approved by relevant regulatory and ethics committees.[127] The study consisted of two parts, Part A and B (**Figure 2.1A**). Eligible participants for Part A were infected with HIV, aged between 18 and 65 years,

weighed over 35.4 kg, received antiretrovirals for at least 1 month, had ≥ 14 days of diarrhea, and tested positive for *Cryptosporidium* infection by qPCR. Part A participants were randomized to receive either clofazimine (n=12) or placebo (n=10). Part B participants (n=11) were HIV-infected but did not have *Cryptosporidium* infection or diarrhea. Part B participants were matched to the first 10 Part A participants based on demographic criteria age, sex, and weight to minimize confounding as the result of an imbalanced distribution of potential confounders between the two groups.[127] All Part B participants received clofazimine.

Clofazimine (a Lamprene® product from Novartis Pharmaceuticals Corporation) was administered orally with food three times daily at approximately 5 a.m., 11 a.m., and 6 p.m. for five days (**Figure 2.1B**). Every study participant received peanut based Plumpy'Nut (Nutriset) supplement 30 minutes before each dose, which was administered at least 1.5 hours before the next anticipated meal.[127] Participants who weighed ≥50 kg received 100 mg clofazimine and those <50 kg received 50 mg clofazimine per dose. After the 5-day drug dosing period, patients were followed up by a visit at 19-24 days post-last dose and a final visit at 41-55 days post-last dose.

2.3.2 *Data Collection and Analysis*

Blood samples were collected at screening for CD4+ T cell count and HIV viral load quantification. Additional blood samples were taken for PK measurements on Day 1 before the first dose; 2, 3, 4 h after the first dose; and immediately before the second and third doses (**Figure 2.1B**). On Days 2 and 3, predose blood samples were collected for every dose. On Day 5, predose samples for every dose and 2, 3, and 4 h post-first dose samples were taken. Clofazimine concentrations were measured using a liquid chromatography-tandem mass spectrometry assay developed by Q2 Solutions. The assay methods were validated for

clofazimine quantification in human plasma within the range of 1.0 ng/mL–1000 ng/mL according to US FDA guidelines.

Stool samples were assessed to determine the presence and severity of diarrhea three times a day before each dose from Days 1 to 5, and once on Day 6 before discharge. Diarrhea, if present at an assessment, would result in a severity grade greater than 0, with Grade 1 representing mild diarrhea and Grade 2 representing severe diarrhea. Daily maximum diarrhea grade was the highest grade observed in three assessments (second and third assessments of the specified study day and the first assessment of the next day), whereas overall maximum diarrhea grade was the highest grade observed among all assessments for each participant. Each assessment with diarrhea counted as one episode of diarrhea. Therefore, up to three episodes of diarrhea could be reported in a day during which stool sample data were collected.

2.3.3 *Modeling Software*

Exploratory statistical and graphical analyses were conducted in R (version 4.1.1, R project, http://www.r-project.org/). Population PK model development and analysis were performed with Phoenix NLME (version 8.3.5, Pharsight, Certara Inc.) using the first-order conditional estimation-extended least squares method.

2.3.4 *Population Pharmacokinetic Structural Model Development*

Selection of the structural model was based on the following factors: minus two log likelihood (-2LL), Akaike's information criterion (AIC), theta correlation matrix, relative standard error (RSE) of parameter estimates, and goodness-of-fit (GOF) diagnostic plots. One-, two- and three-compartment models with first-order absorption and linear elimination were first compared to identify the simplest structural model that best captured the observed data (Table S1[84]).

Absorption lag time (T_{lag}) was then introduced to the most parsimonious model to determine whether significant improvement to the model was made based on changes in the objective function value (OFV) as determined by Δ-2LL. Lastly, the inclusion of a relative bioavailability (F_{rel}) function, where the typical value of bioavailability (F) was fixed at 1, was assessed.

Additive, proportional, combined proportional and additive, and power residual error models were tested. A combined proportional and additive residual error model was selected as it best fitted the distribution of the residual errors (**Equation 2.1**).

$$C_{obs,ij} = C_{pred,ij} + C_{pred,ij} \times \varepsilon_{1,ij} + \varepsilon_{2,ij}$$

Equation 2.1

ε_i is the unexplained residual variability for the plasma concentration at the jth time point in participant *i*.

Interindividual variability (IIV) in PK parameters was evaluated using an exponential model with a mean of zero and a variance of ω^2, in line with the PK parameters' log-normal distributions (**Equation 2.2**).

$$Par_i = \theta_{pop} \times e^{\eta_i}$$

Equation 2.2

In **Equation 2.2**, Par_i is the estimated PK parameter for the i^{th} participant and θ_{pop} is the typical value of that parameter in a population. The random effect η_i describes the amount by which the i^{th} participant's parameter value deviates from the population mean.

Interoccasion variability (IOV) was evaluated for F, apparent systemic clearance (CL/F), apparent central compartment volume of distribution (V/F), apparent intercompartmental clearance (Q/F), and apparent peripheral compartment volume of distribution (V2/F). The occasions were defined by the visits during which PK samples were collected. For each

participant, there were 8 visits in total. Visits 1 to 6 correspond to Days 1 to 6 of the study. Visit 7 corresponds to the first follow-up visit at approximately 19-24 days post-last dose. Visit 8 represents the final follow-up visit at 41-55 days post-last dose.

2.3.5 *Covariate Selection*

Study participant demographic and disease-related characteristics were selected as potential covariates based on clinical interest, mechanistic plausibility, and any possible correlation with PK parameters suggested by trends in eta scatter plots (**Table 2.1**). The candidate covariates were classified into categorical and continuous covariates. Age and body weight were continuous demographic covariates tested. Disease (HIV or *Cryptosporidium* infection)-related continuous covariates assessed included CD4+ T cell count at screening, HIV viral load at screening, the daily number of diarrhea episodes, and the total number of diarrhea episodes. Disease-related categorical covariates tested included study part assignment (A or B), number of diarrhea episodes across all assessments (no diarrhea, $\leq$7 episodes of diarrhea, and $>$7 episodes of diarrhea), presence of diarrhea on Day 1 (yes or no), daily maximum diarrhea grade (0, 1, or 2), and overall maximum diarrhea grade (0, 1, or 2). The effects of these covariates on PK parameters absorption constant (k_a), F, CL/F, V/F, and Q/F were tested. Continuous covariates were normalized by the mean or median of observed values when appropriate and incorporated into the base model by either the linear or the power model based on the level of improvement in model fit (**Equation 2.3, Equation 2.4**). Categorical covariates were incorporated in a proportional shift model (**Equation 2.5**). An exception to this rule was the evaluation of

covariates on F. Categorical covariates were included on F using an exponential form (**Equation 2.6**).

$$Par_i = \theta_0 + \theta_1 \times Cov_i$$

Equation 2.3

$$Par_i = \theta_0 \times Cov_i^{\theta_1}$$

Equation 2.4

$$Par_i = \theta_0 \times (1 + \theta_1|(Cov_i = 1) + \theta_2|(Cov_i = 2) + \cdots + \theta_k|(Cov_i = k))$$

Equation 2.5

$$F_i = 1 \times exp(\eta F_i + \theta_1|(Cov_i = 1) + \theta_2|(Cov_i = 2) + \cdots + \theta_k|(Cov_i = k))$$

Equation 2.6

θ_0 in **Equation 2.3**-**Equation 2.5** represents the typical parameter estimate for the reference group or the baseline. θ_1 to θ_k estimate the covariate effect, describing how a parameter changes with the covariate tested. The subscript *i* represents the ith participant. For categorical covariates (**Equation 2.5, Equation 2.6**), all possible categories for the covariate of interest are denoted by numbers 1 to k. For example, if participant *i* falls under category 2 for the categorical covariate of interest, **Equation 2.5** would reduce to $Par_i = \theta_0 \times (1 + \theta_2)$ because the condition ($Cov_i = 2$) holds true.

Candidate covariates were evaluated one at a time using forward addition followed by backward elimination. The threshold for inclusion of a covariate during the forward addition process was set at $p<0.01$. When multiple covariates satisfied this criterion, the most significant covariate was chosen. Only data from 22 participants (388 PK samples) were used in the first round of forward addition because HIV viral load information was missing for 1 participant in Part B. After having determined that HIV viral load was not the most significant covariate to

introduce to the structural model and that no appreciable covariate effect by HIV viral load remained after the first selected covariate had been added to the model, subsequent covariate selection steps were performed with the full dataset (n=23; 428 PK samples). $p<0.001$ was set as the threshold for backward elimination. The final inclusion of a covariate was further confirmed by at least a 20% decrease in IIV in the PK parameter of interest.

2.3.6 *Model Evaluation*

The final population PK model was evaluated with GOF diagnostic plots, bootstrap resampling analysis, prediction-corrected visual predictive checks (pcVPC), and case deletion diagnostics. The GOF plots examined included observed concentrations (DV) versus population-predicted concentrations (PRED), DV versus individual-predicted concentrations (IPRED), individual weighted residuals (IWRES) versus IPRED, conditional weighted residuals (CWRES) versus time, and quantile-quantile plot of IWRES (**Figure 2.2**). Final model stability was assessed using the nonparametric bootstrap method with 1,000 replicates. The final model's ability to reproduce the central tendency and the variability of the observed data was inspected by pcVPC where 1,000 replicates were simulated using the fixed- and random-effect estimates from the final model (**Figure 2.3**). Furthermore, pcVPC stratified by the covariate overall maximum diarrhea grade was performed to confirm final model performance for these subsets of the population (Figure S1[84]). Lastly, case deletion diagnostics were performed to assess the presence and impact of influential participants on model parameter estimation (Figure S2[84]).

2.4 RESULTS

2.4.1 *Patient Demographics and Characteristics*

Part B participants were matched to Part A participants based on age, sex, and weight; demographic characteristics were similar between the two groups (**Table 2.2**). Although Part A participants were selected based on prolonged diarrhea at screening, only 9 of 12 participants had diarrhea during the 5-day study period during which clofazimine was administered. No one in Part B had diarrhea during the study. Clofazimine PK data, grouped by the overall maximum diarrhea grade, are plotted in **Figure 2.4**. Compared to Part B participants, Part A participants generally displayed more pronounced signs of immunosuppression with a lower median CD4 count and a higher median HIV viral load (**Table 2.2**).

2.4.2 *Structural Pharmacokinetic Model*

A two-compartment model with lag time, first-order absorption, and linear elimination was selected based on the law of parsimony (**Table 2.3**). One- and three-compartment models with first-order absorption and elimination were examined in addition to a two-compartment model. Whereas the one-compartment model fell short of describing the bi-exponentiality in clofazimine PK profile, the three-compartment did not significantly improve the model fit (ΔOFV = 0.2) over the two-compartment model (Table S1[84]).

Subsequently, T_{lag} and F_{rel} were added to the model as the inclusion of both significantly improved the model fit. IIV was included on k_a, V/F, Q/F, and F (**Table 2.3**). IOV was included on F. The residual error was best captured by a combined proportional and additive residual error model.

2.4.3 *Covariate Model*

Of all the covariates tested, the covariate "overall maximum diarrhea grade" was most significantly associated with F and produced the greatest improvement in model performance (**Table 2.1**). Therefore, it was chosen as the first covariate to be added to the base structural model.

Although many covariates, when added to the base model in the first round of forward search, produced *p*-values less than 0.01, they were no longer significant in the second round of forward addition after the overall maximum diarrhea grade on F had been added to the model. Not surprisingly, most of these covariates were alternative measures of diarrhea severity, such as Day 1 diarrhea presence and total number of diarrhea episodes (**Table 2.1**). The other covariates that were significant in Round 1 but no longer significant in Round 2 were HIV viral load, study part assignment, and CD4 count. Although they were not direct measures of diarrhea severity, all three covariates were correlated with diarrhea status (Figure S3[84]). Therefore, the variability attributed to these covariates in round 1 of the forward search was possibly accounted for with the addition of overall maximum diarrhea grade as a covariate on F.

For backward elimination, the covariate overall maximum diarrhea grade on F was removed and this resulted in a significant increase in the OFV (**Table 2.1**). The inclusion of the overall maximum diarrhea grade on F remarkably reduced the IIV of F from 137% to 37.5%, demonstrating that this covariate was able to account for a substantial portion of the observed variability. Whereas a typical individual without diarrhea during the study has a reference F set to 1, an individual that experienced Grade 1 diarrhea would instead have an F_{rel} of only 0.165 (i.e., a sixfold decrease in F), and an individual that experienced Grade 2 diarrhea would have an F_{rel} of 0.0460 (i.e., a 22-fold decrease in F). This extent of F reduction is further supported by

comparing maximum clofazimine concentration and area under the clofazimine concentration-time curve for study participants with different overall maximum diarrhea grades, whereby remarkable differences were observed among the groups (Table S2[84]).

2.4.4 *Population Pharmacokinetic Model Evaluation*

The final population PK model estimated all fixed-effect parameters with high confidence, as shown by the reduction in RSE (**Table 2.3**). GOF plots for the final population PK model demonstrate reasonable homoscedasticity and normality for the distribution of residual errors (**Figure 2.2**). All weighted residuals, when plotted against time or individual predicted concentrations, suggest the model is stable. The pcVPC plots support agreement between the simulated and the observed data for all groups of participants (**Figure 2.3,** Figure S1[84]). The final population model estimates were closely aligned with the mean bootstrap parameter estimates, and all the final model estimates fell within the bootstrap 95% CI (**Table 2.3**). Case deletion diagnostics show that while a few individuals had more influence on certain parameter estimates than others, the resulting changes in parameter estimates were not pronounced (less than 17%) (Figure S2[84]).

2.5 DISCUSSION

Although oral therapeutics are routinely administered to patients experiencing diarrhea, knowledge about the impact of diarrhea on therapeutic disposition is still limited. To the best of our knowledge, this manuscript is the first to report a significant diarrhea impact on an oral therapeutic's PK and to describe the magnitude of such impact using a quantitative modeling approach. Our findings not only have important implications for oral clofazimine dosing but also highlight the importance of understanding potential diarrhea impact on oral drug PK in general.

The final model predicted slow oral clearance (CL/F = 3.71 L/h), large apparent volume of distribution (V/F = 473 L and V2/F of 3434 L), and a prolonged half-life (35.3 days) for clofazimine, in line with current knowledge of clofazimine PK.[131–133] Our estimated k_a of 0.625 hr^{-1} also falls within the k_a range of ~0.2 to 1.3 hr^{-1} reported by existing literature.[131,132] Significant yet highly variable lag time was previously noted for clofazimine.[132] In line with this notion, the inclusion of T_{lag} into the structural model significantly improved the model (Table S1[84]). Moreover, model evaluation by pcVPC and bootstrap confirmed the stability, precision, and performance of the final model (**Table 2.3, Figure 2.3,** Figure S1[84]). The pcVPC plots show that not only was the trend of the observed data captured by the final model, but the observed variability was also accurately depicted (**Figure 2.3**). Furthermore, the final model parameter estimates closely matched the mean parameter estimates of the bootstrap analysis and were all within 95% CI, supporting that the final model estimates were stable and unlikely to be biased due to the inclusion of highly influential points (**Table 2.3**).

The application of nonlinear mixed-effects modeling allowed the estimation of population heterogeneity and assessment of potential demographic and disease-associated covariate effects. Previous studies suggested sex was a significant covariate on the peripheral volume of clofazimine distribution with women having a larger peripheral volume.[131] However, neither sex nor body weight was a significant covariate in our final model, and this may be due to the very narrow range of body weight in our study. Another potential source of variability examined was the dose of clofazimine. The distribution of IWRES for the final model, stratified by clofazimine dose, is comparable between participants who received 50 mg and those who received 100 mg of clofazimine per dose (Figure S4[84]). Although Part B participants were matched to Part A participants based on weight, age, and sex, Part A participants had lower CD4

cell counts and higher HIV viral load compared to their Part B counterparts (**Table 2.2**). To examine whether the degree of immunosuppression, HIV-infection status, or other unidentified underlying differences between Part A and Part B participants impacted clofazimine PK, baseline CD4 count, baseline HIV viral load, and study group assignment were assessed in the covariate selection process. None of these variables remained in the final covariate model as they could not further explain the observed variability (**Table 2.1**). The inclusion of the covariate overall maximum diarrhea grade alone accounted for a remarkable level of variability of the observed clofazimine PK. This is evident by comparing the IIV and the RSE of parameter estimates between the base model and the final model, whereby an approximately 100% reduction in IIV on F and up to a fivefold reduction in RSE was achieved for the final model parameters once the overall maximum diarrhea grade covariate had been included (**Table 2.3**).

A limitation of this study is the sample size. With a total of 23 participants in the clofazimine PK study, it is possible that there was insufficient data to allow identification of other covariates with higher variability or less pronounced effect on clofazimine PK. Moreover, only one study participant had an overall maximum diarrhea grade of 2; additional data from more participants experiencing Grade 2 diarrhea are necessary to confidently quantify the magnitude of F reduction associated with an overall maximum diarrhea grade of 2. Furthermore, due to the limited sample size, certain participants can influence PK parameter estimates while the impact is limited (Figure S2[84]). Nevertheless, this study is explorative and the first of its kind for clofazimine.

As a Biopharmaceutics Classification System (BCS) class II drug, clofazimine is expected to have solubility rate-limited absorption. Therefore, pathophysiological changes that impact the solubility of the drug may lead to changes in clofazimine bioavailability. Examples of

such pathophysiological changes include altered composition of GI fluids, luminal fluid volume, and gut pH.[57,118,119,134] Accelerated small bowel transit has been reported for HIV-infected subjects with cryptosporidiosis-associated diarrhea.[57] While a reduction in GI transit time does not directly impact the dissolution process, it leads to less available time for drug dissolution and absorption to take place, potentially resulting in decreased clofazimine bioavailability. Another factor that might have been responsible for the estimated diarrhea impact on clofazimine bioavailability is a change in luminal fluid volume, which can affect both drug dissolution and drug permeation by impacting the drug concentration gradient between the GI lumen and the enterocytes and affecting the thickness and composition of the mucus layer lining the luminal surface. The exact mechanism of how clofazimine bioavailability is impacted, whether a single factor is responsible or if a concerted effort is at play, remains to be elucidated. Mechanistic modeling approaches such as implementing physiologically-based pharmacokinetic (PBPK) modeling may help address this question.[119] A thorough understanding of cryptosporidiosis disease physiology is also critical for future investigations of the mechanisms behind the impact of diarrhea discovered by our current study. Furthermore, mechanistic knowledge is key to making correct dosing decisions across different populations, particularly for drugs like clofazimine which may have nonlinear PK at doses higher than what is currently administered clinically, as suggested by a dose-ranging mouse study.[89] For these drugs, simply increasing the dose by the same extent by which bioavailability is impacted by disease-associated covariate(s) may not produce the same targeted drug exposure, since bioavailability depends on both the physicochemical properties of the drugs as well as physiological parameters of the target population. The solubility limitation for BCS class II drugs may lead to incomplete dissolution and decreased F at high doses, resulting in a less-than-proportional increase in exposure with

increasing doses. Therefore, additional modeling approaches that can account for the interaction between drug-specific parameters and system parameters, such as PBPK modeling, should be utilized to inform dose predictions.

In conclusion, maximum diarrhea grade over the duration of clofazimine administration was significantly associated with an over sixfold reduction in clofazimine oral bioavailability in HIV-infected adults. This quantitative knowledge is crucial for making correct dosing decisions and may contribute to shaping clinical practices. For instance, alternative treatment options to oral clofazimine may need to be considered for HIV-infected adults experiencing diarrhea. Our finding also draws attention to studying how diarrhea impacts the PK of other oral therapeutics in other disease areas. Since drug properties and physiological parameters may both be involved in causing a diarrhea impact on oral drug PK, the magnitude of the impact is likely disease-specific and drug-specific. Therefore, additional studies are needed to identify diseases and drugs that are particularly prone to variability associated with diarrhea. We hope that our findings will inspire future studies of diarrhea impact on oral drug PK and pave the way to informing drug dosing considerations that would expand to benefit additional patient populations.

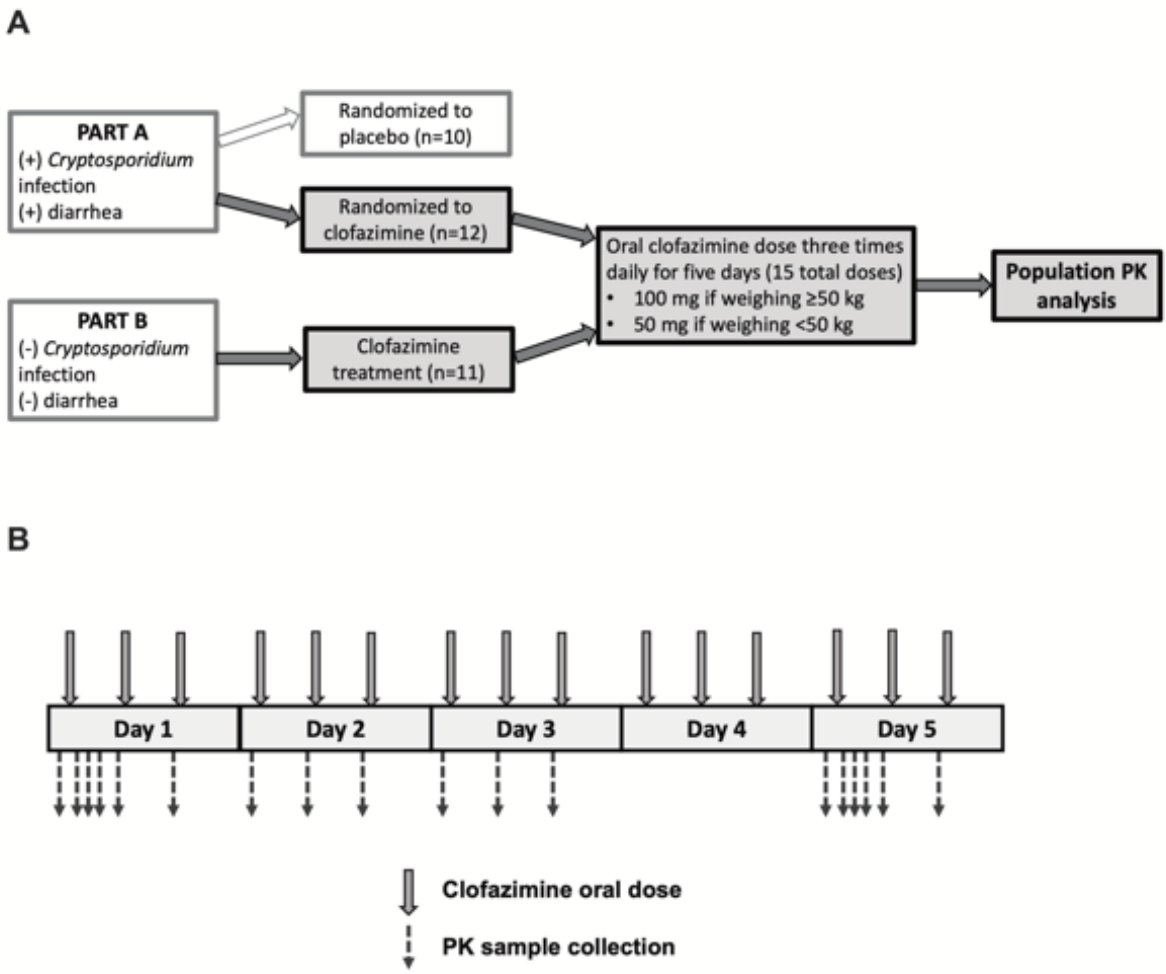

Figure 2.1. Overview of clofazimine phase 2a clinical trial pharmacokinetic sub study.

(**A**) The trial consisted of two parts, Part A and B. Part A participants were HIV-infected, tested positive for *Cryptosporidium* infection by qPCR, and had persistent diarrhea at enrollment. Part A participants were randomized at approximately 1:1 to receive either clofazimine (n=12) or placebo (n=10) orally three times daily (TID) for five consecutive days. Part B participants were *Cryptosporidium*-negative and diarrhea-free at enrollment. All Part B participants (n=11) received clofazimine orally TID for five days. The dose of clofazimine was determined by each participant's body weight at enrollment. Participants who weighed greater than or equal to 50 kg received 100 mg clofazimine each dose, whereas those who weighed less than 50 kg received 50

mg clofazimine each dose. Only data from Part A and Part B participants who received clofazimine treatment (n=23) were included in the population pharmacokinetic analysis. (**B**) Dosing and sampling scheme for Part A and B participants who received clofazimine treatment. Oral clofazimine was administered at approximately 5 a.m., 11 a.m., and 6 p.m. on study Days 1 to 5. Blood samples were collected for pharmacokinetic measurements on Day 1 pre-first dose, 2, 3, 4 hours post-first dose, and immediately before the second and third doses. On Days 2 and 3, predose blood samples were collected for every dose. On Day 5, predose samples for every dose and 2, 3, and 4 hours post-first dose samples were taken.

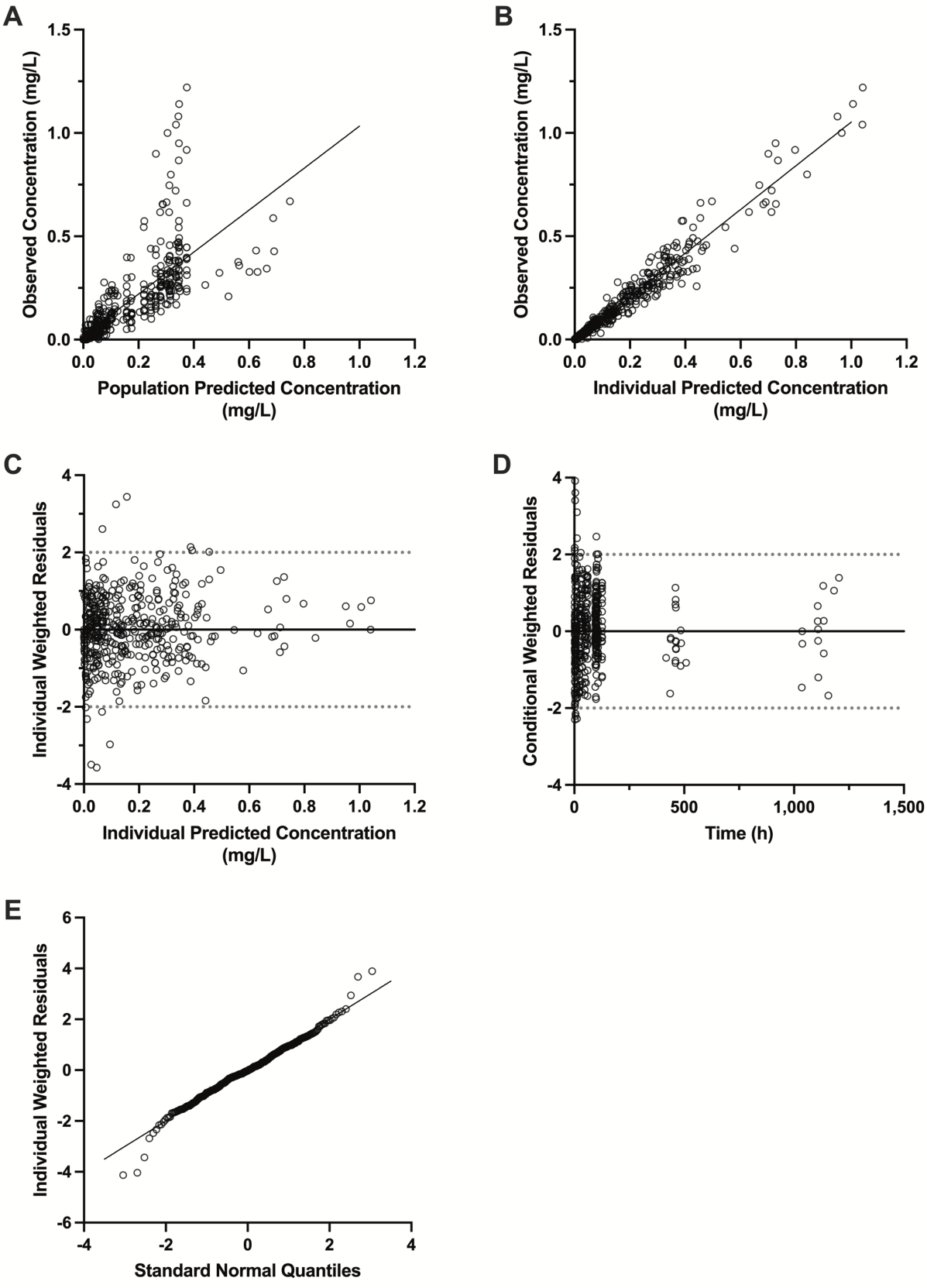
A
Observed Concentration (mg/L)
Population Predicted Concentration (mg/L)
B
Observed Concentration (mg/L)
Individual Predicted Concentration (mg/L)
C
Individual Weighted Residuals
Individual Predicted Concentration (mg/L)
D
Conditional Weighted Residuals
Time (h)
E
Individual Weighted Residuals
Standard Normal Quantiles

Figure 2.2. Goodness-of-fit plots of the final population pharmacokinetic model for clofazimine.

(**A**) Observed plasma concentration against population predicted concentration, (**B**) observed plasma concentration against individual predicted concentration, (**C**) individual weighted residuals against individual predicted concentrations, (**D**) conditional weighted residuals against time, and (**E**) quantile-quantile plot of individual weighted residuals.

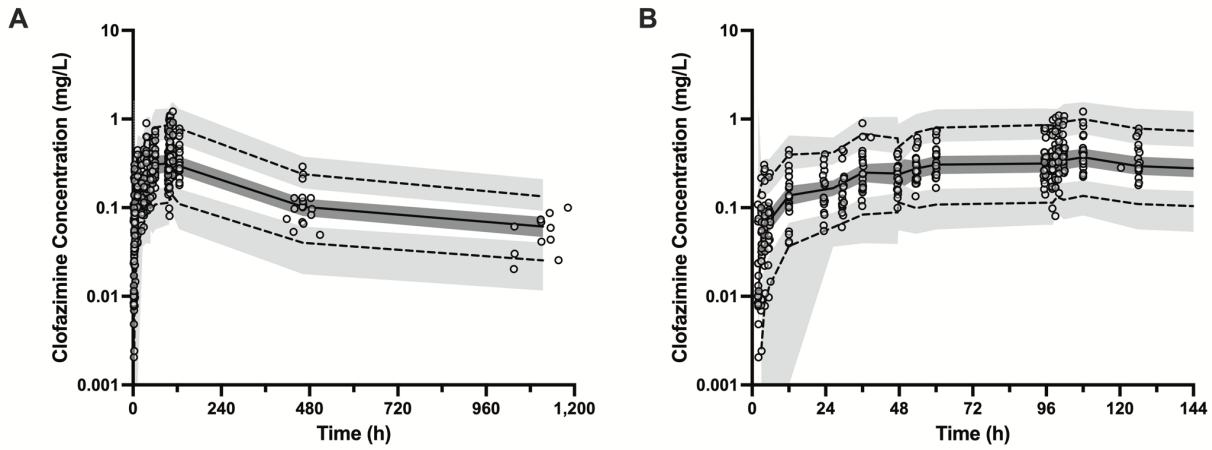

Figure 2.3. Prediction-corrected visual predictive check for clofazimine concentration versus time spanning (A) the total duration of the study including the follow-up visits, and (B) the initial 6 days of the study.

Open circles represent prediction-corrected observed plasma concentrations. The observed 5th and 95th percentiles are depicted by dashed lines, and the observed median is represented by the solid line. The shaded regions represent the corresponding model predicted 90% confidence intervals around the predicted 5th and 95th percentiles and the median, based on 1,000 simulations.

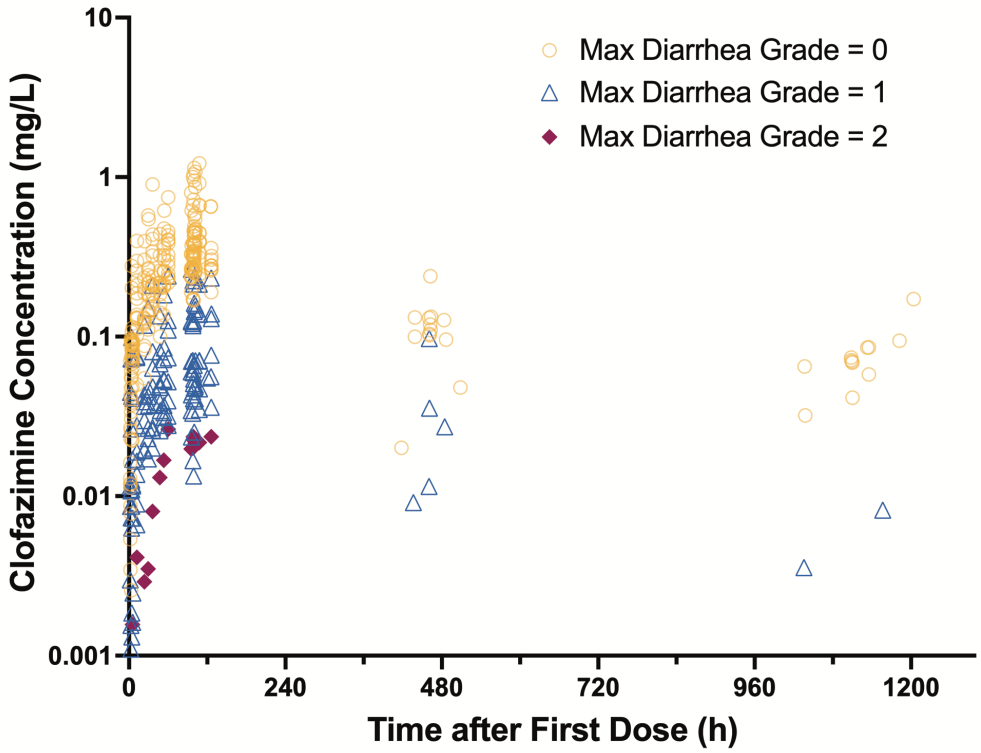

Figure 2.4. Clofazimine plasma concentrations categorized by overall maximum diarrhea grade.

Gold open circles represent pharmacokinetic samples collected from participants who did not have diarrhea for the duration of the study. Dark blue triangles represent samples from participants who only had Grade 1 (mild) diarrhea during the study. Maroon diamonds represent samples from participants who had at least one episode of Grade 2 (severe) diarrhea during the study.

Table 2.1. Stepwise covariate search summary. The final model, which included the overall maximum grade of diarrhea upon F, is shaded gray.

Model	Covariate Added/Removed	-2(LL)	Δ-2(LL)	#Parms	P-value	Compare with
1[a]		-1660.7		13		
2	HIV viral load on Q	-1666.1	-5.4	14	0.020	1
3	HIV viral load on F	-1668.8	-8.1	14	0.004	1
4	HIV viral load on CL	-1661.8	-1.1	14	0.291	1
5	Presence of diarrhea on Day 1 on F	-1695.3	-34.6	14	4.09×10^{-9}	1
6	Presence of diarrhea on Day 1 on CL	-1667.4	-6.7	14	0.010	1
7	Presence of diarrhea on Day 1 on k_a	-1662.2	-1.6	14	0.210	1
8	Categorical variable of diarrhea episode[b] on CL	-1667.6	-7.0	15	0.031	1
9	Categorical variable of diarrhea episode[b] on F	-1695.6	-34.9	15	2.58×10^{-8}	1
10	Daily max diarrhea grade on F	-1667.7	-7.1	15	0.029	1
11	Daily max diarrhea grade on CL	-1661.3	-0.6	15	0.746	1
12	Daily max diarrhea grade on k_a	-1663.2	-2.6	15	0.278	1
13[c]	Overall max diarrhea grade on F	-1700.4	-39.8	15	2.31×10^{-9}	1
14	Study part on CL	-1662.4	-1.8	14	0.185	1
15	Study part on F	-1670.9	-10.2	14	0.001	1
16	Age on V	-1663.3	-2.6	14	0.104	1
17	CD4 count on F	-1667.4	-6.7	14	0.009	1
18	Daily number of diarrhea episode on F	-1666.5	-5.8	14	0.016	1
19	Daily number of diarrhea episode on CL	-1660.5	0.17	14	-	1
20	Daily number of diarrhea episode on k_a	-1660.7	-0.1	14	0.794	1
21	Total number of diarrhea episode on F	-1675.5	-14.8	14	1.16×10^{-4}	1
22	Weight on V	-1663.4	-2.7	14	0.099	1
23[d]	Overall max diarrhea grade on F	-1767.1		15		
24	Presence of diarrhea on Day 1 on F	-1767.1	0.0	16	0.970	23
25	Presence of diarrhea on Day 1 on k_a	-1768.1	-1.0	16	0.306	23
26	Daily max diarrhea grade on k_a	-1769.5	-2.4	17	0.295	23

27	Overall max diarrhea grade on k_a	-1771.5	-4.4	17	0.111	23
28	Age on V	-1769.2	-2.1	16	0.145	23
29	Age on k_a	-1767.3	-0.2	16	0.633	23
30	Daily number of diarrhea episode on k_a	-1767.3	-0.2	16	0.692	23
31	Categorical variable of diarrhea episode[b] on F	-1767.1	0.0	17	0.978	23
32	Weight on V	-1769.0	-1.9	16	0.164	23
33	Weight on CL	-1767.1	0.0	16	0.860	23
34	Remove overall max diarrhea grade on F	-1724.73	42.3671	13	6.31×10^{-10}	23

Abbreviation: #Parms, number of parameters in the model; -2(LL), $-2 \times log\ (likelihood)$ for each model; Δ-2(LL), -2(LL) of current model minus -2(LL) of the reference model; CD4, CD4+ T cell; CL, systemic clearance; F, bioavailability; k_a, absorption rate constant; Q, intercompartmental clearance; V, central compartment volume of distribution.

[a] *Base model.*

[b] *The categorical variable of diarrhea episodes classifies the total number of diarrhea episodes across all assessments into three categories: no diarrhea, $\leq$7 episodes of diarrhea, and $>$7 episodes of diarrhea.*

[c] *Selected after the first round of forward addition.*

[d] *Models 1-22 were run with 22 study participants with all covariate information available. Model 23, which is the final model, is Model 13 rerun with all n=23 to include the participant without HIV viral load data (see Section 2.3.5 for more details).*

Table 2.2. Patient characteristics at baseline for Part A and Part B participants who received clofazimine (CFZ).

	Part A: HIV+/Cryptosporidiosis+ (n=12)		**Part B: HIV+/Cryptosporidiosis- (n=11)**	
	Median (Range)	**Mean ± SD**	**Median (Range)**	**Mean ± SD**
Age (year)	40.5 (30, 51)	39.75 ± 7.79	43 (31, 64)	44.09 ± 9.65
Weight (kg)	45.45 (36.6, 52)	45.11 ± 4.70	47 (41, 53)	46.96 ± 3.24
No. (%) of study participants who were:				
Male	8 (66.7)		7 (63.6)	
Female	4 (33.3)		4 (36.4)	
HIV viral load (copies/mL)[a]	139819 (26366, 889360)	241981.50 ± 262806	0 (0, 2683)	275.80 ± 846.13
CD4 (cells/μL)	23 (3, 93)	25.33 ± 24.44	419 (125, 816)	454.18 ± 227.38
No. (%) of study participants with overall max diarrhea grade of:				
0	3 (25)		11 (100)	
1	8 (66.7)		0 (0)	
2	1 (8.3)		0 (0)	
No. of study participants who received 100 mg/50 mg CFZ	2/10		1/10	

Abbreviation: CD4, CD4+ T cell; HIV, human immunodeficiency virus; SD, standard deviation.

[a] HIV viral load data was missing for 1 Part B participant. Therefore, HIV viral load information at baseline was summarized for n=10 Part B participants.

Table 2.3. Base and final population PK model parameter estimates for clofazimine and bootstrap validation (n=1000).

	BASE MODEL			FINAL MODEL			BOOTSTRAP	
Parameter	**Estimate**	**RSE (%)**	**Shrinkage**	**Estimate**	**RSE (%)**	**Shrinkage**	**Mean**	**95% CI**
k_a (1/h)	0.601	38.8		0.625	21.0		0.671	0.330 - 1.25
T_{lag} (h)	1.83	3.02		1.83	2.82		1.83	1.72 - 1.91
F	1 (fixed)			1 (fixed)			1 (fixed)	
CL/F (L/h)	7.85	31.9		3.71	10.0		3.72	2.89 - 4.59
V/F (L)	993	30.5		473	10.7		477	350 - 639
Q/F (L/h)	39.5	27.3		18.2	13.2		18.4	13.1 - 24.6
V2/F (L)	7416	23.4		3434	8.07		3424	2685 - 4354
Between-Subject Variability								
IIV on V/F (%)	15.2	82.3	0.661	3.46	15.1	0.915	3.48	3.05 - 3.90
IIV on Q/F (%)	45.0	80.8	0.228	45.0	32.4	0.214	42.7	19.1 - 74.4
IIV on k_a (%)	161	42.7	0.103	149	28.4	0.105	143	73.8 - 303
IIV on F (%)	137	26.0	0.0308	37.5	35.1	0.151	33.7	9.21 - 49.2
Inter-Occasion Variability								
IOV on F (%)	35.7	38.4	0.502	36.8	32.8	0.478	37.0	21.9 - 54.3
Covariate Effect								
Overall max diarrhea grade = 1				-1.80	11.2		-1.80	-2.25 - -1.35
Overall max diarrhea grade = 2				-3.08	3.55		-3.08	-3.38 - -2.75
Residual Unexplained Variability (Additive + Multiplicative Model)								
σ	0.00273	47.9	0.129	0.00268	42.0	0.125	0.00269	0.00100 - 0.00532

Abbreviation: CI, confidence interval; CL, systemic clearance; IIV, interindividual variability; k_a, absorption rate constant; Q, intercompartment clearance; RSE, residual standard error; T_{lag}, lag time; V, central compartment volume of distribution; V2, peripheral compartment volume of distribution; σ, an estimate of residual unexplained variability in the plasma concentrations.

Chapter 3. PHARMACOKINETICS AND PHARMACODYNAMICS OF CLOFAZIMINE FOR TREATMENT OF CRYPTOSPORIDIOSIS

The work presented in this chapter was published in *Antimicrobial Agents and Chemotherapy* 2022 Jan; 66(1): e0156021 (doi: 10.1128/AAC.01560-21).[89]

Authors: Cindy X. Zhang, Melissa S. Love, Case W. McNamara, Victor Chi, Ashley K. Woods, Sean Joseph, Deborah A. Schaefer, Dana P. Betzer, Michael W. Riggs, Pui-Ying Iroh Tam, Samuel L.M. Arnold

Author contributions: C.X.Z., M.S.L., C.W.M., S.J., A.K.W., D.A.S., M.W.R., P.-Y.I.T., and S.L.M.A. participated in study design. M.S.L., A.K.W., V.C., D.P.B., and D.A.S. were involved in specimen processing and laboratory testing. C.X.Z., M.S.L., C.W.M., S.J., A.K.W., D.A.S., M.W.R., D.P.B., and S.L.M.A. were involved in data analysis and interpretation. C.X.Z. did the statistical analysis and prepared the figures and tables. C.X.Z. wrote the first draft of the manuscript. All authors contributed to the writing of the manuscript and approved the final version for submission.

3.1 ABSTRACT

Infection with *Cryptosporidium* spp. can cause severe diarrhea leading to long-term adverse impacts and even death in malnourished children and immunocompromised patients. The only FDA-approved drug for treating cryptosporidiosis, nitazoxanide, has limited efficacy in the populations impacted the most by the diarrheal disease. Safe, effective treatment options are urgently needed. Initially identified by a large-scale phenotypic screening campaign, the antimycobacterial therapeutic clofazimine demonstrated great promise in both in vitro and in vivo preclinical models of *Cryptosporidium* infection. Unfortunately, a Phase 2a clinical trial in HIV-infected adults with cryptosporidiosis did not identify any clofazimine treatment effect on *Cryptosporidium* infection burden or clinical outcomes. To explore whether clofazimine's lack of efficacy in the Phase 2a trial may have been due to subtherapeutic clofazimine concentrations, a pharmacokinetic/pharmacodynamic modeling approach was undertaken to determine the relationship between clofazimine in vivo concentrations and treatment effects in multiple preclinical infection models. Exposure-response relationships were characterized using E_{max} and logistic models which allowed predictions of efficacious clofazimine concentrations for the control and reduction of disease burden. After establishing exposure-response relationships for clofazimine treatment of *Cryptosporidium* infection in our preclinical model studies, it was unmistakable that the clofazimine levels observed in the Phase 2a study participants were well below concentrations associated with anti-*Cryptosporidium* efficacy. Thus, despite a dosing regimen above the highest doses recommended for mycobacterial therapy, it is very likely the lack of treatment effect in the Phase 2a trial was at least partially due to clofazimine concentrations below those required for efficacy against cryptosporidiosis. It is unlikely that clofazimine will provide a remedy for the large number of cryptosporidiosis patients currently without a viable

treatment option unless alternative, safe clofazimine formulations with improved oral absorption are developed. (This study has been registered in ClinicalTrials.gov under identifier NCT03341767.)

3.2 INTRODUCTION

The symptoms of cryptosporidiosis, the disease caused by parasitic infections with *Cryptosporidium* spp., include prolonged episodes of watery diarrhea along with other symptoms, such as stomach pain, dehydration, nausea, vomiting, and fever. While cryptosporidiosis is most commonly self-limiting in healthy adults, the disease can cause recurrent or chronic diarrhea in children and immunocompromised individuals and can lead to death in severe cases.[135,136] Cryptosporidiosis is also highly associated with long-term adverse impacts, including growth stunting, poor physical fitness, and poor cognitive development when infections occur at a young age, even when the infections are asymptomatic.[137–141] A reanalysis of the Global Enteric Multicenter Study (GEMS) revealed that *Cryptosporidium* was one of the top six pathogens responsible for moderate to severe diarrhea in children younger than 5 years in Africa and Asia.[142] For children under the age of 1 year, *Cryptosporidium* was the third most common cause of moderate to severe diarrhea, ranking higher than *Shigella*, norovirus, and *Salmonella*. Due to underdiagnosis and underappreciation of the disease, the true global burden of cryptosporidiosis is not known. The pervasive impact of cryptosporidiosis was illustrated by The Global Burden of Disease 2016 study, which estimated that over 44.8 million episodes of diarrhea and 48,000 deaths globally can be attributed to cryptosporidiosis annually.[143] *Cryptosporidium* infections, while exerting the most detrimental effects in under-resourced countries, are also common to high-income countries. Due to the parasite's highly infectious nature and its resistance to water chlorination, it is a leading cause of waterborne disease in the United States.[144–149]

As a historically neglected disease, cryptosporidiosis has only one drug, nitazoxanide, approved for treatment by the U.S. Food and Drug Administration (FDA). While nitazoxanide is effective in treating otherwise healthy adults, with parasite clearance reported in up to 93% of

treated subjects (compared to 37% with placebo treatment),[150] its efficacy is greatly compromised in malnourished children, in whom the response rate dropped to only 56% following nitazoxanide treatment, compared to 23% with placebo control.[151] No significant treatment benefit was observed when nitazoxanide was compared to placebo in Zambian children living with HIV,[151,152] supporting the belief that the efficacy of nitazoxanide is heavily dependent on the competency of infected individuals' immune systems. Unfortunately, immunocompromised individuals and malnourished children, who may not benefit from nitazoxanide treatment, are those who are most vulnerable and suffer the most severe consequences of *Cryptosporidium* infection. Therefore, there is an urgent need for an effective and safe treatment that can be used to treat malnourished children and the immunocompromised. A traditional approach for drug discovery in cryptosporidiosis would require screening against large collections of small molecules, and any hits would most likely need extensive optimization to improve safety, pharmacokinetics, and/or potency. While there are many promising, novel treatments in development, it is not clear if/when any of these new therapeutic candidates will be available in the clinic. Drug repurposing provides an alternative approach to cryptosporidiosis drug development, and repurposing candidates will often already have established safety, toxicity, and pharmacokinetic data.[153,154] Thus, drug repurposing can facilitate the delivery of new therapeutic interventions to the clinic by reducing the time and resources required for development.

Through a phenotypic screening campaign by the California Institute for Biomedical Research (Calibr), ~80,000 compounds were screened in vitro against *Cryptosporidium*, and it was observed that the antimycobacterial clofazimine was active against both *C. parvum* and *C. hominis*.[155] Clofazimine is an FDA-approved antimicrobial agent for the treatment of lepromatous leprosy[156,157], and the therapeutic demonstrated in vivo efficacy in a preclinical mouse model of

Cryptosporidium infection.[155] Nevertheless, when a Phase 2a clinical trial conducted in HIV-infected adults investigated clofazimine as a potential treatment of cryptosporidiosis, clofazimine treatment did not improve microbiological or clinical outcomes compared to placebo.[158] The lack of treatment effect was observed with a clofazimine dosing regimen exceeding the daily recommended dosage and was the maximum given in clinical practice. To determine whether higher clofazimine concentrations in the Phase 2a trial may have led to a favorable therapeutic response, we undertook a pharmacokinetic/pharmacodynamic (PK/PD) modeling approach informed by previously unpublished preclinical in vivo studies to develop exposure-response relationships for clofazimine treatment of *Cryptosporidium* infection.

3.3 METHODS

3.3.1 *Ethics Statement*

All in vivo animal studies were carried out in strict accordance with the recommendations in the *Guide for the Care and Use of Laboratory Animals* of the National Institutes of Health.[159] For the mouse model studies, the protocol (S13013) was approved by the Institutional Animal Care and Use Committee of the University of California, San Diego, CA (Animal Welfare Assurance Number: A3033-01). For the calf model study, the protocol (09-120) was approved by the Institutional Animal Care and Use Committee of the University of Arizona, Tucson, AZ (Animal Welfare Assurance Number: A-3248-01). Calf studies complied with guidelines in the Animal Welfare Act and *Guide for the Care and Use of Agricultural Animals in Research and Teaching*.[160] The animal biosafety level 2 (ABSL-2) facilities used were fully accredited by the American Association for Laboratory Animal Care. All efforts were made to minimize the suffering of animals employed in these studies.

3.3.2 *Clofazimine LC-MS/MS analysis*

Melissa S. Love, Ashley K. Woods, and Victor Chi from the Scripps Research Institue (La Jolla, California, USA), and Dana P. Betzer and Deborah A. Schaefer from the University of Arizona (Tucson, Arizona, USA) performed the specimen processing and laboratory testing. Clofazimine levels in mouse and calf plasma were determined by liquid chromatography with tandem mass spectrometry (LC-MS/MS) using an Agilent 1100 (Agilent, Santa Clara, CA) coupled with an AB Sciex API4000 (AB Sciex, Foster City, California). A calibration curve was generated in plasma of the study species. Calibration curves were generated with concentrations ranging from 0.3 to 5,000 ng/mL. Two hundred fifty microliters of ice-cold acetonitrile was added to 20 µL of calibration curve sample or pharmacokinetic sample. Samples were shaken for 10 min, followed by centrifugation at 4,000 rpm for 20 min. Two hundred microliters of supernatant was removed from each sample into a new plate, and 50 µL 0.1% formic acid in high-performance liquid chromatography (HLPC)-grade water was added and mixed. Ten microliters of sample was injected for LC-MS/MS analysis. A 50- by 2.0-mm Kinetex RP 5.0-µm C_{18} column (Phenomenex, Torrance, CA) was used for analyte separation with mobile phases A (water with 0.1% formic acid) and B (acetonitrile with 0.1% formic acid) at a flow rate of 500 µL/min. The binary gradient was as follows: 10% B for 2 minutes, 10% B to 95% B for 2.0 to 3.5 minutes, 95% B for 3.5 to 5.5 minutes, 95% B to 10% B for 5.0 to 5.5 minutes, and 95% B for 5.50 to 7.0 minutes. Clofazimine was quantified using electrospray ionization in positive ion mode with the 473.2-to-431.0 m/z transition. The source temperature was set at 450°C, curtain gas at 25, ion spray voltage at 3,000, CAD gas at medium, entrance potential at 10, declustering potential at 121, and collision energy at 51. For each species, samples were analyzed over the course of a single day, and the coefficient of variation for calibration curve samples were all <15% with the

exception of one concentration (5,000 ng/mL in mouse plasma had a 23% coefficient of variation). For both the mouse and calf calibration curves, the R^2 values were >0.95. The limit of detection (LOD) and lower limit of quantification (LLOQ) for clofazimine in mouse plasma were 0.15 and 0.3 ng/mL, respectively. For the calf study, the LOD and LLOQ were 0.3 and 1.2 ng/mL, respectively. The human clinical trial samples were analyzed by Q2 solutions, as previously described using an LC-MS/MS assay developed and validated according to FDA guidelines.[158]

3.3.3 *Mouse Pharmacokinetic Study*

Drs. Melissa S. Love, Ashley K. Woods, and Victor Chi from Calibr at the Scripps Research Institute (La Jolla, California, USA) conducted the mouse pharmacokinetic study. Eight-week-old male C57BL/6 mice were used to characterize the pharmacokinetics of clofazimine after a single oral dose. Clofazimine (USP reference standard, Sigma-Aldrich) dose cohorts of 0.03, 0.1, 0.3, 1, 3, 10, 30 ,100, and 300 mg/kg were formulated in 0.5% methylcellulose and 0.5% Tween-80 (MC-Tween) and dosed at 5 mL/kg. Each dose group contained 6 mice randomized to 2 equal cohorts, where blood samples were collected at 0.5, 3, 8, and 120 h postdose for cohort 1 and at 1, 8, 24, and 240 h postdose for cohort 2.

3.3.4 *Mouse Efficacy Study*

The mouse efficacy study was performed by Drs. Melissa S. Love, Ashley K. Woods, and Victor Chi from Calibr at the Scripps Research Institute (La Jolla, California, USA). The mouse model used to characterize clofazimine pharmacodynamics has been described in detail previously.[155] Briefly, four- to five-week-old female C57BL/6 interferon gamma-deficient (INF$\gamma^{-/-}$) mice were inoculated with 10^6 purified *C. parvum* oocysts (Iowa strain) at a density of 5×10^6 oocysts/mL in

sterile water via oral gavage. Four days post infection, clofazimine was administered as a single oral dose to infected mice at 0.03, 0.1, 0.3, 1, 3, 10, 30, 100, and 300 mg/kg (i.e., the same dosing cohorts as the Mouse Pharmacokinetic Study). Each dose group contained four mice. Mice were placed in isolation to allow for collection of feces at 24-hour intervals posttreatment for each mouse. Fecal pellets were weighed immediately after collection, placed in 0.5 mL 2.5% potassium dichromate solution, and stored at 4°C until processing. Oocysts in fecal samples were quantified using a Guava EasyCyte flow cytometer and CytoSoft data acquisition and analysis software (v5.3; Guava Technologies, Inc.).

3.3.5 *Calf Pharmacokinetic and Efficacy Study*

The calf study was conducted at the University of Arizona (Tucson, Arizona, USA), led by Drs. Michael W. Riggs, Dana P. Betzer, and Deborah A. Schaefer. All calves were obtained from the same United States Department of Agriculture (USDA)-licensed closed-herd dairy vendor. Calves were fed a commercial colostrum replacer within 2 h after birth (bovine IgG colostrum replacement; Land O'Lakes, Shoreview, MN) per label instructions. A total of 12 calves were used, with 6 randomly assigned by the Microsoft Excel random number generation tool (Redmond, WA) to the treatment group and 6 to the control group. Experiment personnel were blind to the treatment and control assignments during the study. All calves were housed in an ABSL-2 facility in separate containment rooms. Precautions and disinfection measures were taken for the deliveries and housing of these calves to prevent unintended *Cryptosporidium* or other enteropathogen infections. The calves were fed antibiotic-free milk replacer (Nutrena Snowflakes calf milk II-Utiliz milk replacer; Cargill Animal Nutrition, Minneapolis, MN) twice daily from 12 h of age until termination of the experiment at day 10 post infection. An oral electrolyte solution (Re-Sorb; Pfizer) was supplemented once diarrhea developed in an animal.

At 36 to 48 h of age (study day 0), each calf was infected by oral inoculation of 5 x10^7 purified disinfected *C. parvum* oocysts (Iowa strain).[161] Starting at study day 2 (2 days post-infection), each calf in the treatment group received 30 mg/kg clofazimine twice daily (BID) over 5 days for a total of 10 doses. Clofazimine was dosed in MC-Tween with a total dose volume of 1 mL/kg. Control calves received only MC-Tween. Over the 5-day dosing period, a total of 16 blood samples were collected to characterize clofazimine pharmacokinetics. On study days 2 and 6, pharmacokinetic samples were collected immediately prior to the first dose of the day and 1, 2, 4, 12, 13, and 24 h postdose. In addition, predose pharmacokinetic samples were collected for doses 5 and 7. Stool samples were collected every 24 h starting on study day 3. The total volume of feces excreted for successive 24-h collections was recorded. Total daily oocyst counts for each calf were determined as previously described.[161] Briefly, real-time quantitative polymerase chain reaction (PCR) was used to quantify *C. parvum* oocysts from feces collected over successive 24-h periods which had been well mixed using a commercial blender to ensure sample uniformity. Calves were also assigned numerical scores for the following variables twice daily: clinical symptoms, general health (willingness to rise, stance, rectal temperature, appetite, and food intake, attitude, and hydration status), presence or absence of diarrhea, and fecal consistency.[162] All calves with the exception of one control calf were euthanized on study day 10. The control calf euthanized on study day 9 was withdrawn from the study one day early due to bloating and severe diarrhea.

3.3.6 *Clofazimine Phase 2a Trial for Treatment of Cryptosporidiosis*

The clofazimine clinical trial was a collaborative effort among University of Malawi (Blantyre, Malawi), Bill and Melinda Gates Foundation (Seattle, Washington, USA), Emmes Corporation (Rockville, Maryland, USA), University of Liverpool (Liverpool, UK), Malawi-Liverpool Wellcome Trust Clinical Research Programme (Blantyre, Malawi), University of Virginia

(Charlottesville, Virginia, USA), Calibr (La Jolla, California, USA), and University of Washington (Seattle, Washington, USA), led by Pui-Ying Iroh Tam et al.. The study design and outcomes were described in detail previously.[127,158] Briefly, the trial was a single-center, randomized, double-blind, placebo-controlled Phase 2a trial conducted in Blantyre, Malawi (NCT number: 03341767). HIV-infected adults between 18 and 65 years of age, weighing over 35.4 kg, who had received antiretrovirals for at least 1 month, experienced at least 14 days of diarrhea, and tested positive for *Cryptosporidium* infection by qPCR were eligible to enroll. Subjects were randomized 1:1 to receive oral (PO) clofazimine (n=12) or placebo (n=10). The dosage of clofazimine (Lamprene formulation) was the maximum given in clinical practice, 100 mg PO three times daily (TID) for participants who weighed ≥50 kg or 50 mg PO TID for participants who weighed <50 kg. Participants were dosed with Lamprene or placebo for a total of 5 days. Approximately 30 min before each clofazimine dose administration, subjects received Plumpy'Soy or Plumpy'Nut nutritional supplement.

Blood samples for pharmacokinetic measurements were collected on day 1 predose, at 2, 3, and 4 h after the first dose, and immediately before the second and third doses. On days 2 and 3, blood draws were taken immediately prior to each dose. On day 5, samples were taken immediately prior to each of the three doses and 2, 3, and 4 h after the first dose. Clofazimine concentration assessment was performed by Q2 Solutions (Ithaca, New York, USA) using LC-MS/MS. The assay methods used were validated according to U.S. FDA guidelines for quantification of clofazimine within the range of 1.0 ng/mL to 1,000 ng/mL in human plasma. Stool samples were collected and assessed three times a day prior to each dose administration from day 1 to day 5 and once on day 6 prior to discharge. The presence of diarrhea and severity of diarrhea were recorded. All *Cryptosporidium* shedding was quantified using qPCR.

3.3.7 *Pharmacokinetic-Pharmacodynamic Modeling*

For all in vivo studies, pharmacokinetic parameters were initially estimated through non-compartmental analysis (NCA) using Phoenix WinNonlin version 8.3 (Certara, Princeton, NJ). To determine *Cryptosporidium* oocyst shedding rates for each subject, a linear regression line was fitted to log-transformed daily oocyst shedding counts for the first 3 days beginning on the day of clofazimine treatment initiation. To determine the percent reduction in oocyst shedding, the oocyst count 2 days after initial treatment was divided by the baseline oocyst count on the day of treatment initiation for each study subject, multiplied by 100, and subtracted from 100%.

To quantitatively evaluate the relationship between oocyst reduction rate and clofazimine dose in mice, an E_{max} model was fitted using mean clofazimine concentration for the first 24 h following treatment administration ($Cavg_{0\text{-}24H}$) at each dose determined from the mouse pharmacokinetic study and the individual rate of oocyst reduction following clofazimine administration as calculated from the mouse efficacy study (**Equation 3.1**).

$$RR = E_0 + \frac{E_{max} \times Cavg_{0-24}^{\gamma}}{EC_{50}^{\gamma} + Cavg_{0-24}^{\gamma}}$$

Equation 3.1

where RR is the rate of reduction in daily oocyst shedding, E_0 is the rate of reduction observed in the vehicle control group, γ is the Hill coefficient, E_{max} is the estimated maximum rate of reduction in daily oocyst shedding, and EC_{50} is the average clofazimine concentration at which half the maximum rate of reduction in oocyst shedding can be achieved.

A dichotomous variable was also designed to explore the relationship between treatment success and average clofazimine concentration. A success event was defined as achieving a ≥ 90% reduction in oocyst count by comparing day 6 oocyst shedding numbers to the baseline oocyst count at treatment initiation (day 4 post-infection). A logistic model was developed to describe the

relationship between the probability of success for each individual mouse in the efficacy study and the mean clofazimine concentration $Cavg_{0\text{-}24H}$ for its corresponding dose group in the pharmacokinetic study (**Equation 3.2**).

$$log\left(\frac{P}{1-P}\right) = \beta_0 + \beta_1 \times Cavg_{0-24}$$

Equation 3.2

where P is the probability of achieving a success event (i.e., the probability of achieving a ≥90% reduction in oocyst count), EC_{50} is the average clofazimine concentration at which the probability of success is 0.50 and can by estimated by substituting 0.50 for P in the equation, and β_0 and β_1 are the intercept and slope of the equation, respectively, describing how the logit function of P changes in response to changes in $Cavg_{0\text{-}24H}$.

Lastly, a time-to-event outcome variable was adopted to study the relationship between average clofazimine concentration and the time to achieve treatment success, defined as a ≥90% reduction in oocyst counts compared to day 4 post infection (day of treatment initiation). The number of days following clofazimine administration each mouse took to achieve success was compared to the $Cavg_{0\text{-}24H}$ for its corresponding dose group in the pharmacokinetic study. Since one mouse at the 0.1 mg/kg dose cohort did not achieve success before study termination, it was excluded from this analysis (n = 39). An E_{max} model similar to **Equation 3.1** was fitted to describe the relationship (**Equation 3.3**).

$$TTE = E_0 + \frac{E_{max} \times Cavg_{0-24}^{\gamma}}{EC_{50}^{\gamma} + Cavg_{0-24}^{\gamma}}$$

Equation 3.3

where E_0 is the average number of days after treatment initiation to achieve success for the control group, and this value was fixed at 6.50 days based on the observed data, E_{max} is the largest possible

change in the number of days to achieve success due to a treatment effect and was set to -5.50 days, TTE is the time to event of achieving ≥90% oocyst reduction in days, γ is the Hill coefficient, and EC_{50} is the $Cavg_{0\text{-}24H}$ at which the time to success is reduced by half of the estimated maximum change possible. By fixing E_0 and E_{max}, the lower bound of TTE was designated as 1 day. In other words, when the clofazimine concentration is high enough to produce the maximum treatment effect, the least amount of time required to achieve treatment success would be the sum of E_0 and E_{max}, which is 1 day after clofazimine treatment initiation. This would be the minimum duration possible and plausible given the daily sampling schedule.

Since no baseline oocyst shedding data on study day 2 (day of clofazimine treatment initiation) were collected in the calf study, the rate of reduction in oocyst shedding immediately following treatment initiation and percent reduction comparing daily oocyst counts to the predose baseline cannot be calculated as done for the mouse study. Instead, area under the curves (AUCs) were calculated for oocyst count, fecal volume, fecal consistency, urine volume, and clinical score for the entire duration for which each outcome was assessed. The relationship between the pharmacodynamic (PD) endpoint and clofazimine $Cavg_{0\text{-}24H}$ and $Cavg_{96\text{-}108H}$ was described by a linear regression model (**Equation 3.4**).

$$PD\ endpoint = \beta_0 + \beta_1 \times Cavg$$

Equation 3.4

The outcome variables (PD endpoint) examined include oocyst count $AUC_{24\text{-}192H}$ (from 24 to 192 h after clofazimine initiation), fecal volume $AUC_{24\text{-}192H}$, fecal consistency score $AUC_{0\text{-}192H}$, urine volume $AUC_{24\text{-}192H}$, and clinical evaluation score $AUC_{24\text{-}192H}$. β_0 is the intercept of the equation and estimates the level of the PD endpoint without clofazimine treatment. β_1 is the slope,

describing the direction and magnitude with which a PD endpoint changes with changing clofazimine average concentration. The Cavg examined include $Cavg_{0\text{-}24H}$ and $Cavg_{96\text{-}108H}$.

3.3.8 *Statistical Analysis*

Linear regression, logistic regression, and E_{max} models were used to model the associations between outcome and clofazimine concentration variables. Kaplan-Meier curves and log-rank tests were used for time-to-event comparisons. Bonferroni correction for multiple comparisons was employed for comparing fecal volume, fecal consistency, urine volume, and clinical scores of the treatment and control groups in the calf study. Statistical analyses were all carried out using R version 3.6.1 (2019-07-05).

3.4 RESULTS

3.4.1 *Clofazimine Pharmacokinetics and Efficacy in Mice*

When administered orally to mice as single doses ranging from 0.03 mg/kg to 300 mg/kg, clofazimine was observed to have non-linear kinetics (**Table 3.1**). While the reason for the non-linearity is unclear, the less than proportional increase in exposure with increasing dose may reflect a reduction in gastrointestinal absorption (i.e., lower oral bioavailability) due to the poor aqueous solubility of clofazimine.

The efficacy of clofazimine in the mouse model of *Cryptosporidium* infection was dose dependent. In the mouse efficacy study, a single, oral dose of clofazimine ranging from 0.03 mg/kg to 300 mg/kg was administered 4 days after oral inoculation with 5×10^6 *C. parvum* oocysts/mouse (n= 4/group) and oocyst shedding was measured daily up to 10 days after treatment initiation. It was observed that while oocyst counts declined over time for all treatments, a dose-dependent difference in the rate and onset of decline existed over the first two days post treatment (**Figure**

3.1A). The results, when summarized by dose group, demonstrated that a reduction in oocyst shedding rate between day 4 and day 6 post infection was absent for clofazimine doses lower than 3 mg/kg but started to occur at clofazimine doses ≥ 3 mg/kg (**Figure 3.1B**). The reduction in oocyst shedding rate appeared to increase with increasing clofazimine dose and was the greatest at the highest dose level, 300 mg/kg. When fitted with an E_{max} model (**Figure 3.1C, Equation 3.1**) which describes the relationship between average clofazimine concentration over the 24 h post treatment and the rate of oocyst reduction, it was estimated that E_0 was -0.670 log (oocysts)/mg feces/day, E_{max} was 3.46 log (oocysts)/mg feces/day, Hill coefficient was 1, and EC_{50} was 316 ng/mL with a 95% confidence interval of 205 to 480 ng/mL. These estimates were used to calculate an EC_{90} value of 2,770 ng/mL with a 95% confidence interval of 1,840 to 4,320 ng/mL (i.e., $Cavg_{0\text{-}24H}$ associated with 90% of maximum reduction in oocyst shedding rate).

In addition to changes in oocyst shedding rate in the initial two days post clofazimine administration, a dichotomous variable was designed where "success" was defined as achieving a 90% reduction in oocyst counts by comparing day 6 oocyst shedding numbers to the baseline oocyst count on day 4 post infection. A logistic model was developed to characterize the relationship between success and clofazimine $Cavg_{0\text{-}24H}$ (**Figure 3.1D**, **Equation 3.2**). Based on this logistic model, the EC_{50}, which is the concentration at which there is a 0.50 probability of achieving success, was estimated to be 394 ng/mL and the EC_{90} to be 589 ng/mL.

A time-to-event outcome variable was also used to identify differences in efficacy between clofazimine treatment groups. A success event was designated as a 90% reduction in oocyst infection burden by comparing oocyst shedding counts on each day to the baseline oocyst count at treatment initiation, similar to the dichotomous outcome approach. However, instead of focusing on whether success was achieved by a certain time point, the time-to-event variable evaluated how

quickly success was achieved. At lower doses, 90% reduction in oocyst shedding (i.e., success) was generally achieved around 6 days post treatment (**Figure 3.1E**). However, at higher doses of 30 mg/kg, 100 mg/kg, and 300 mg/kg, success was observed as early as 1 day post treatment. The median number of days mice in these dose groups needed to achieve success was 1 day. An E_{max} model was fitted to the data to describe the relationship between time to success and $Cavg_{0\text{-}24H}$ (**Figure 3.1F**, **Equation 3.3**). The curve illustrates that with increasing clofazimine concentrations, the time needed to achieve a 90% reduction in oocyst shedding was reduced. E_0 was set to 6.50 days post treatment and E_{max} was fixed at -5.50 days post treatment. The Hill coefficient was estimated to be 1, EC_{50} was 227 ng/mL, and EC_{90} was 2,040 ng/mL.

3.4.2 *Clofazimine Pharmacokinetics and Efficacy in Calves*

The microbiological and clinical efficacy of clofazimine treatment was characterized in an established calf model of cryptosporidiosis. Clofazimine concentrations observed with 30 mg/kg clofazimine BID for 5 days treatment for the 6 calves in the treatment group are plotted in **Figure 3.2A**. The mean ± standard deviation (SD) clofazimine concentrations over the initial 24 h ($Cavg_{0\text{-}24H}$,) and from 96 to 108 h post treatment initiation ($Cavg_{96\text{-}108H}$) were 500 ± 248 ng/mL and 1,330 ± 605 ng/mL, respectively. Daily oocyst shedding counts for calves in the treatment and control groups demonstrated that the mean oocyst counts for the treatment group tended to be lower than those of the control group for the duration of the study (**Figure 3.2B**), although the differences were not statistically significant with the single dosing regimen tested and the number of calves involved in this study. Clinical endpoints other than oocyst counts were also collected, including daily fecal volume, fecal consistency score, clinical evaluation score, and daily urine volume. The profiles of these endpoints in the treatment group and the control group animals are summarized in **Figure 3.2C to F**. Daily fecal volume and fecal consistency scores are indicators of the severity

of diarrhea. While the mean daily fecal volume profiles were not different between the control and the treatment groups, the mean fecal consistency score profiles suggested that the treatment group animals had less severe diarrhea than the control group animals (**Figure 3.2C, D**). The mean daily urine volume profile showed that the treatment group calves tended to produce more urine than the control group calves (**Figure 3.2E**), with the difference being significant on days 3 and 4 post infection (within 2 days post treatment initiation). Thus, there were fewer signs of dehydration in the treatment calves compared to control. The clinical evaluation score summarizes clinical symptoms, general health observations, presence or absence of diarrhea, and fecal consistency, where a lower score represents better clinical outcome. The mean clinical evaluation score profile for the two groups suggested that the treatment group had lower clinical scores and thus better clinical outcomes (**Figure 3.2F**). The clinical scores were significantly better for the treatment group than the control group on days 3 and 7 post infection.

To better evaluate the effect of clofazimine in calves quantitatively, additional modeling approaches were undertaken. Linear regression models were employed to examine the relationship between PD outcomes, including oocyst count $AUC_{24\text{-}192H}$, fecal volume $AUC_{24\text{-}192H}$, fecal consistency score $AUC_{0\text{-}192H}$, urine volume $AUC_{24\text{-}192H}$, clinical evaluation scores $AUC_{24\text{-}192H}$, and exposure variables clofazimine $Cavg_{0\text{-}24H}$ and clofazimine $Cavg_{96\text{-}108H}$. The results are summarized in **Table 3.2** and **Figure 3.3A** and **B**. While clofazimine $Cavg_{0\text{-}24H}$ was significantly and inversely associated with oocyst count $AUC_{24\text{-}192H}$ ($P \leq 0.01$), clofazimine $Cavg_{96\text{-}108H}$ was not significantly associated with oocyst count $AUC_{24\text{-}192H}$ ($P = 0.24$). There was a significant, negative correlation between fecal consistency score and clofazimine $Cavg_{0\text{-}24H}$ and $Cavg_{96\text{-}108H}$ ($P \leq 0.05$). The clinical evaluation score $AUC_{24\text{-}192H}$ and clofazimine $Cavg_{96\text{-}108H}$ were also negatively and statistically significantly correlated ($P \leq 0.05$). However, while fecal volume $AUC_{24\text{-}192H}$ and urine volume

$AUC_{24\text{-}192H}$ were negatively and positively correlated with clofazimine average concentrations, respectively, the correlations were not statistically significant. Lastly, for easy visual comparison, boxplots were used to summarize the four additional clinical endpoints by treatment groups (**Figure 3.3C**). Although the clofazimine treatment group appeared to have better outcomes for all four PD endpoints, the difference was not statistically significant after Bonferroni correction, which was a conservative correction method to control the family-wise error rate (**Figure 3.3C**).

3.4.3 *Clofazimine Phase 2a Trial Pharmacokinetics and Efficacy*

As previously reported, a Phase 2a trial demonstrated that clofazimine treatment failed to improve cryptosporidiosis microbiological or clinical outcomes in a population of HIV-infected adults.[158] A high level of variability was observed in clofazimine concentrations among the 12 subjects who were randomized to receive treatment (**Figure 3.4A**). Of the 12 participants, 10 weighed less than 50 kg at study enrollment and thus received 50 mg clofazimine PO TID, whereas only 2 weighed over 50 kg and received 100 mg clofazimine PO TID. Therefore, for this analysis, clofazimine $Cavg_{0\text{-}24H}$ and $Cavg_{96\text{-}108H}$ values were calculated from 10 participants and 2 participants for 50-mg PO TID and 100-mg PO TID doses, respectively (**Table 3.3**). Due to the high level of observed variability in the resulting pharmacokinetic parameters and the limited number of subjects available, especially at the 100-mg PO TID clofazimine dosing regimen, there was considerable uncertainty to the mean estimates. Furthermore, one participant receiving 50 mg PO TID clofazimine treatment had relatively high levels of clofazimine in their plasma (**Figure 3.4A**). The extreme levels of clofazimine observed with the participant further contributed to the uncertainties in mean clofazimine Cavg estimates. The $Cavg_{0\text{-}24H} \pm$ SD for the 10 subjects receiving 50 mg of clofazimine PO TID was 63.0 ± 79.4 ng/mL, and the $Cavg_{0\text{-}24H} \pm$ SD for the 2 subjects receiving 100 mg of clofazimine PO TID was 50.1 ± 45.3 ng/mL (**Table 3.3**). $Cavg_{96\text{-}108H} \pm$ SD was estimated

to be 233 ± 340 ng/mL and 182 ± 60.0 ng/mL for the 50-mg PO TID and 100-mg PO TID clofazimine dose groups, respectively (**Table 3.3**).

To compare daily oocyst shedding between treatment and placebo groups, the mean and SD of daily oocyst shedding counts in the first stool collected in the morning were determined and plotted for the two groups (**Figure 3.4B**). No apparent effect of clofazimine treatment on lowering oocyst shedding counts was observed. Similarly, no correlation was clearly seen when the rate of reduction in oocyst shedding counts was compared to clofazimine $Cavg_{0\text{-}24H}$ (**Figure 3.4C**) or $Cavg_{96\text{-}108H}$ (Supplemental Material[89]). A time-to-event approach was also taken to explore potential clofazimine treatment effects. Defining 90% oocyst shedding count reduction as the success event, the amount of time taken to achieve success was plotted against clofazimine $Cavg_{0\text{-}24H}$ (**Figure 3.4D**) or $Cavg_{96\text{-}108H}$ (Supplemental Material[89]). No significant correlation between the concentration and response variables was detected (**Table 3.4**). Although the trend between clofazimine exposure and time to success appeared to be negative, where increasing clofazimine seemed to be associated with less time to achieve 90% reduction in oocyst shedding counts, it was mostly driven by two subjects with high clofazimine exposure. The lack of a dose-escalation design and the resulting narrow clofazimine exposure range limited these analyses. A Kaplan-Meier curve was used as an alternative approach to detect potential differences in the amount of time taken to achieve 90% oocyst shedding count reduction between treatment and placebo groups (**Figure 3.4E**). However, no significant difference was found, as shown by the log rank test (P = 0.47).

3.5 DISCUSSION

Despite the observed efficacy in preclinical models of cryptosporidiosis, clofazimine administration to patients with cryptosporidiosis in a Phase 2a trial failed to reduce parasitic

excretion.[158] Our PK/PD modeling approach described in this chapter addresses the critical question of whether subtherapeutic clofazimine concentrations during cryptosporidiosis therapy contributed to the lack of clinical and microbiological efficacy against cryptosporidiosis.

Based on oocyst shedding profiles observed in mice after clofazimine treatment, there was a clear dose-dependent decline in oocyst shedding within 2 days of clofazimine oral administration (**Figure 3.1A**). The mouse model of *Cryptosporidium* infection used in our studies does not exhibit clinical signs of cryptosporidiosis (e.g., loose stool), so outcomes were limited to microbiological responses to treatment. Oocyst shedding decreased over time for all dose cohorts and the magnitude and onset of the decrease in infection were dependent on the dose, with doses ≥ 3 mg/kg required for an oocyst reduction rate greater than that of the control (**Figure 3.1B**). This observation supported a dose-response relationship for clofazimine treatment of *Cryptosporidium* infection in mice.

Subsequently, exposure-response analyses were conducted to estimate clofazimine therapeutic concentrations using the mouse study data. Since clofazimine was observed to have non-linear pharmacokinetics at the doses used in the mouse efficacy study, the relationship between oocyst reduction and clofazimine concentrations was explored with several models. The model estimates suggested that a simple E_{max} model was adequate in describing the observed data, as the E_{max} model line captured well the shape of the observed trend (**Equation 3.1**, **Figure 3.1C**). Based on the E_{max} model, the estimated clofazimine concentrations associated with achieving 50% and 90% of the maximum rate of reduction (EC_{50} and EC_{90}) were 316 ng/mL and 2,770 ng/mL, respectively.

In addition to the rate of oocyst reduction model, a second approach used a dichotomous variable to define an outcome as either treatment success or failure for the mouse data (**Equation**

3.2). Here, the success threshold of reaching a parasite reduction by at least 90% of baseline has often been used to define parasitological success in other parasitic infectious disease studies, such as clinical studies investigating malaria treatments.[163,164] The assumption for this definition of success in our study was that a 90% or greater reduction in oocyst shedding 2 days post clofazimine treatment was the threshold for clinically significant treatment success, whereas anything below 90% was insufficient. The logistic model developed to characterize the relationship between the dichotomized outcomes (success/no success) and clofazimine $Cavg_{0\text{-}24H}$ again illustrated that there was a clofazimine concentration-dependent increase in the probability of achieving success (**Figure 3.1D**). Furthermore, the predicted EC_{50} value was 394 ng/mL, which was well aligned with the EC_{50} predicted with the rate of oocyst reduction model (**Equation 3.1**). It should be noted the artificially introduced threshold of 90% and the inflexible nature of using a dichotomous outcome variable are two limitations of this approach. This dichotomous outcome and logistic model approach does not distinguish between varying degrees of "failure"; a case with 89% reduction in oocyst shedding was treated the same as one in which there was an entire absence of reduction, or even a case where there was an increase in oocyst shedding. This also partially explains why the logistic model-predicted EC_{90} of 589 ng/mL was much lower than the E_{max} model-predicted EC_{90} of 2,770 ng/mL (**Figure 3.1C**) for the rate of oocyst reduction model. The black-and-white nature of the outcome variable definition led to a sharp increase in *P*, the probability of achieving success. However, these limitations do not take away the virtue of this approach. Importantly, this approach provided a second layer of easily visualizable and appreciable evidence that increasing clofazimine plasma concentration was correlated with increasing probability of achieving successful reduction in oocyst shedding within 2 days post treatment.

Lastly, a time-to-event outcome variable was employed to examine the mouse data (**Equation 3.3**). This approach recognizes that *Cryptosporidium* infection can be self-limiting and that oocyst numbers may drop over time even without treatment. The clearance of *Cryptosporidium* infection by the natural immune response was addressed by E_0, which specifies that, on average, 6.50 days are needed to achieve 90% oocyst reduction without any clofazimine treatment. The treatment effect of clofazimine evaluated was its ability to induce and accelerate the elimination of oocysts in the feces. The E_{max} model fit to the time-to-event outcome variable and clofazimine $Cavg_{0\text{-}24H}$ describes how increasing clofazimine exposure decreased time to clear the infection by 90% until it reached the sum of E_0 and E_{max}, which is the least number of days needed to achieve success and set to 1 day (**Figure 3.1F**). From this E_{max} model, a clofazimine $Cavg_{0\text{-}24H}$ of 227 ng/mL was needed to reduce the time to success by 50% of the maximum reduction possible and a $Cavg_{0\text{-}24H}$ of 2,040 ng/mL was needed to reduce the time by 90%. This time-to-event approach result further supports a conclusion that clofazimine treatment facilitated *Cryptosporidium* oocyst clearance. However, it should be noted that this data analysis approach has its limitations. Because 1 mouse was excluded from the analysis, as it never reached 90% reduction during the study, the EC_{50} and EC_{90} calculated were conservative estimates, meaning that they were lower than the values had that mouse been followed until success was achieved. Sensitivity analysis (not shown) was performed to ensure that the exclusion of one mouse did not significantly change the EC_{50} and EC_{90} or impact our conclusion. Furthermore, as the estimates were conservative, they should not compromise the validity of our analysis. While this model is not perfect, it is adequate and effective supporting evidence.

In addition to the mouse studies, an established calf model of cryptosporidiosis was used to further investigate the in vivo efficacy of clofazimine. Unlike mice, the calf model exhibits

clinical symptoms of cryptosporidiosis which allowed us to explore whether clofazimine treatment was associated with both microbiological and clinical outcomes. Daily oocyst count profiles of the control and the treatment groups suggested that calves in the clofazimine treatment group had a lower infection burden for the duration of the study (**Figure 3.2B**). While fecal volume did not differ much between the two groups (**Figure 3.2C**), fecal consistency score tended to be lower for the treatment group, suggesting that the treated calves produced more solid stool and had lower diarrhea severity (**Figure 3.2D**). The urine volume was generally greater and the clinical evaluation score lower for the treatment calves, indicating that treated calves were less dehydrated and had better overall health than the control calves (**Figure 3.2E** and **F**). However, most PD measurements, except for fecal consistency score, were not collected the day of clofazimine treatment initiation but instead starting 1 day after treatment initiation. Thus, baseline pretreatment values were missing for these endpoints, and the rate of reduction in oocyst counts and percentage reduction compared to baseline values could not be calculated in a manner analogous to the mouse efficacy study. Instead, an AUC was calculated for each outcome measure using all available data. The assumption for comparing the outcome AUCs between the treatment and control groups was that these two groups were not inherently different at baseline in disease severity and parasite burden. Although there is no definitive evidence to eliminate all doubt around this assumption without baseline measurements, these calves were infected with the same number of purified disinfected *C. parvum* oocysts at the same age and treated in the same fashion for the duration of the study. There is no reason to believe that the two groups would be different from each other at baseline. Furthermore, fecal consistency scores, the only PD outcome that was collected at treatment initiation, were very similar between the treatment and the control groups on day 2 post infection. This supports the notion that the treatment and control calves were similar in disease

severity prior to clofazimine treatment and that differences observed between the groups after clofazimine dosing were most likely due to the drug treatment.

Using calf clofazimine pharmacokinetic data collected in tandem with efficacy data, relationships between clofazimine concentrations and microbiological and clinical outcomes were evaluated. While increasing clofazimine average concentrations were generally associated with improved microbiological and clinical outcomes, statistical significance was not achieved for all of the relationships examined (**Table 3.2**).[161] When the clinical outcomes by treatment groups were compared using boxplots, the clofazimine treatment group had better overall health as well as more diarrhea symptom alleviation compared to the control group, although the differences were not statistically significant when Bonferroni correction was applied (**Figure 3.3C**). Overall, results from the calf study suggested that clofazimine treatment at 30 mg/kg PO BID might have had some effect in reducing oocyst burden and improving clinical outcomes, but its effect was at best marginal and did not produce consistent statistical significance. However, this lack of significance is likely attributable to a number of reasons including suboptimal clofazimine exposure, limited range in clofazimine exposure due to testing only one dose regimen, and limited number of calves included in this study. Using a model predicted EC_{90} of 2,770 ng/mL from the E_{max} oocyst reduction rate model generated with mouse data, it was calculated that the observed clofazimine $Cavg_{0\text{-}24H}$ 500 ng/mL and $Cavg_{96\text{-}108H}$ 1,330 ng/mL in calves were only 17.6% and 46.8% of the estimated EC_{90}, respectively (**Table 3.3**). It is likely that doses higher than 30 mg/kg would be needed to produce more pronounced and consistent treatment effects. In addition, more calves would have increased the power of the study, given the variability encountered. The lack of consistently significant treatment effects in the calf study does not prove that there was no clofazimine treatment effect. Instead, it might have been the product of suboptimal clofazimine

exposure and the study being underpowered due to feasibility concerns inherent in using an outbred population of animals.

When clinical trial data of clofazimine pharmacokinetics in HIV-infected adults with cryptosporidiosis were characterized, clofazimine concentrations were clearly lower than those associated with efficacy in the preclinical disease models. When the clofazimine efficacy and pharmacokinetic data observed in the clinical trial were reported previously[158], there were no data available at the time to determine whether clofazimine concentrations observed in the trial were analogous to those associated with efficacy in preclinical animal models.[158] Furthermore, given that the dosing regimen for the Phase 2a trial was beyond the recommended dosage for mycobacterial therapy, there was limited clinical data to support clofazimine plasma levels expected in healthy individuals with the dosing regimen and no data to support plasma concentrations expected in patients with diarrhea. With the preclinical data presented here, it is now abundantly clear that clofazimine levels in the Phase 2a trial were well below those associated with efficacy in preclinical models (**Figure 3.4A, Table 3.3**). Thus, it is not surprising that the oocyst shedding profiles were very similar between the treatment and control group participants (**Figure 3.4B**). When the rate of reduction in oocyst shedding was calculated for the clinical data, just as how it was done for the mouse efficacy study, there was no trend between the rates of reduction and average clofazimine concentration on day 1 of treatment (**Figure 3.4C**). Furthermore, linear regression models and a time-to-event approach did not identify any significant associations between microbiological responses and average clofazimine concentrations on days 1 or 5 of treatment (**Table 3.4**). A Kaplan-Meier curve was used to compare the number of days taken post clofazimine treatment initiation to achieve 90% oocyst reduction

between the treatment and the control groups (**Figure 3.4E**), and clofazimine treatment did not affect the probability of achieving 90% oocyst reduction.

Although this complete lack of clinical efficacy may appear to be conflicting with the promising preclinical in vivo model results, it is explainable once observed clofazimine exposure levels in the trial are compared to the clofazimine concentrations associated with efficacy in preclinical models (**Table 3.3**). The observed clofazimine $Cavg_{0\text{-}24H}$ and $Cavg_{96\text{-}108H}$ in the Phase 2a trial participants were more than 80% below the estimated EC_{90}. Therefore, it is likely that the clofazimine doses administered in the clinical trial, although greater than the highest approved doses to treat leprosy, were too low to treat cryptosporidiosis. The model prediction and actual observation comparisons in humans were made using the rate of oocyst reduction E_{max} model (**Equation 3.1**) generated with mouse data, because this model rests on the least number of assumptions and does not involve an artificially defined dichotomous variable. Using the other two models as references would not change our conclusion, as the observed average clofazimine concentrations are still orders of magnitude below the model-predicted EC_{90}s. It should be noted that clofazimine has >99% plasma protein binding in mice and humans, and we did not consider the impact of plasma protein binding in our modeling approach.[165,166] Interestingly, the predicted unbound EC_{50}s for the three PK/PD models developed with mouse data were ~3 ng/mL, which is very similar to the clofazimine EC_{50} value of 7 ng/mL observed in an established in vitro HCT-8 coculture model of infection.[155]

Finally, it should be noted that the PK/PD relationships described in this manuscript are informed by plasma drug levels that may not represent therapeutic concentrations at the site of action (i.e., the gastrointestinal tract). Our previous studies have established that gastrointestinal therapeutic levels, not plasma levels, were associated with the efficacy of bumped kinase inhibitors

for treatment of *Cryptosporidium* infection in mice.[167] For clofazimine, metabolism and/or transport are not expected to impact therapeutic absorption from the gastrointestinal tract which would be modulated by clofazimine's solubility and permeability. Therefore, clofazimine observed in plasma would reflect compound that went into solution in the intestinal lumen and likely transited through the gastrointestinal epithelium by a transcellular pathway. Transcellular transit is important given the localization of *Cryptosporidium* spp. to intracellular but extracytosolic parasitophorous vacuoles located beneath the apical plasma membrane of infected intestinal epithelial cells as this localization suggests that therapeutic exposure within intestinal epithelial cells is essential for therapeutic efficacy.[168–171]

Moving forward, the results described here demonstrate clofazimine's failure to treat cryptosporidiosis in a Phase 2a trial was most likely due to the concentrations observed in the study participants being too low for treatment of cryptosporidiosis. The dosage of clofazimine administered in the Phase 2a trial was the maximum given for leprosy in clinical practice, and an ~70-fold higher dose would be required to achieve an average clofazimine concentration value equal to the EC_{90} determined in mice.[171] This substantive dose increase has at least two concerns, specifically patient safety and uncertainty that higher doses will result in sufficient clofazimine concentrations. First, such a large dose increase raises safety concerns, because we could not find evidence that such high doses have been evaluated in humans. Second, clofazimine has very poor solubility, and it should not be assumed that increasing the dose of Lamprene, a gelatin capsule with a microcrystalline clofazimine suspension in an oil-wax base, will generate therapeutic levels in humans associated with efficacy against infection in preclinical in vivo models. To address challenges in improving clofazimine absorption for treatment of cryptosporidiosis, clofazimine nanoparticle powder formulations have been developed, but it is unclear whether these novel

formulations will generate clofazimine concentrations required for efficacy in humans.[172] In conclusion, unless alternative, safe clofazimine formulations with improved oral absorption are developed, it is unlikely that clofazimine will provide a remedy for the large number of cryptosporidiosis patients currently without a viable treatment option.

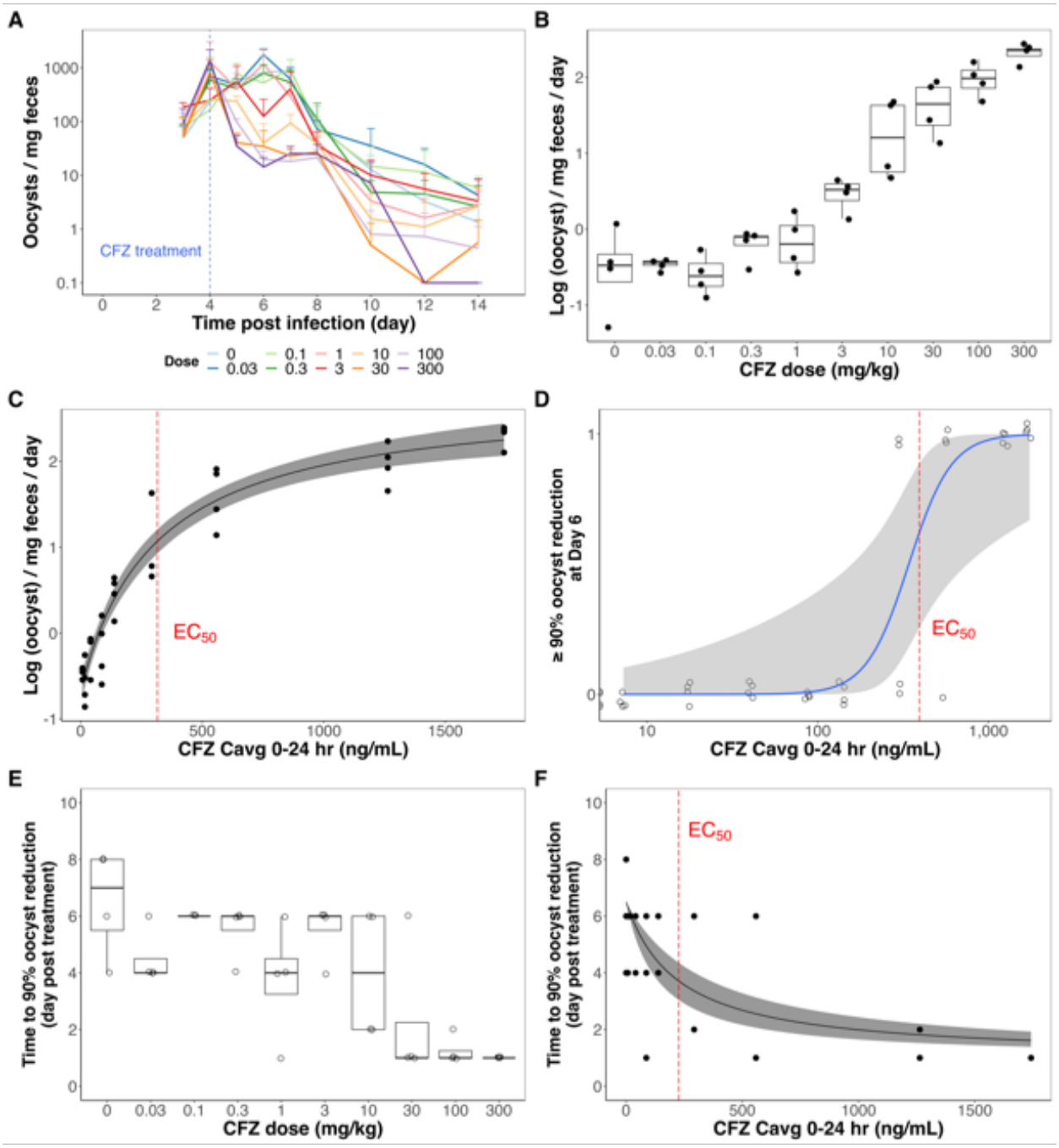

Figure 3.1. Clofazimine in vivo efficacy in mouse model of *Cryptosporidium* infection.

(A) Mean oocyst shedding profile for each clofazimine treatment group plotted over time. A single clofazimine oral dose of varying amounts was administered 4 days after oral inoculation with *C. parvum*. Each dose group contained four mice, and the fecal oocyst concentration for each mouse was quantified by flow cytometry. (B) Rate of reduction in log-transformed fecal

oocyst concentration from day 4 to day 6 post-infection, summarized by dose group. The tops and bottoms of the boxes are the 25th and 75th percentiles, respectively, and the center line is the median. The whiskers indicate the range of data distribution that are within 1.5-fold of the interquartile range (IQR). Points that lay out of the reach of the whiskers are outliers by the 1.5 IQR rule. (C) A simple Emax model (black solid line) with 90% confidence interval (grey shaded area) was fitted to describe the relationship between average clofazimine concentration over the 24 h post dosing ($Cavg_{0\text{-}24H}$) and the rate of oocyst reduction, with the model predicted EC_{50} marked by the red dash line. A dichotomous approach was also taken with an event ("1") being defined as having less than 10% of baseline oocyst load on day 6 post infection. (D) Logistic regression model (black solid line) with 90% confidence interval (grey shaded area), with the model predicted EC_{50} indicated by the red dash line. (E and F) Last, a time-to-event approach was employed. The number of days each mouse took to reach a 90% reduction in oocyst compared to the baseline oocyst concentration is summarized by dose group (E) or compared to $Cavg_{0\text{-}24H}$ (F). The boxplots in panel E were generated in the same fashion as those in panel B**.** A simple Emax model (black solid line) with 90% confidence interval (grey shaded area) was built to describe the correlation between the number of days and clofazimine $Cavg_{0\text{-}24H}$ (F). Red dash line represents EC_{50}.

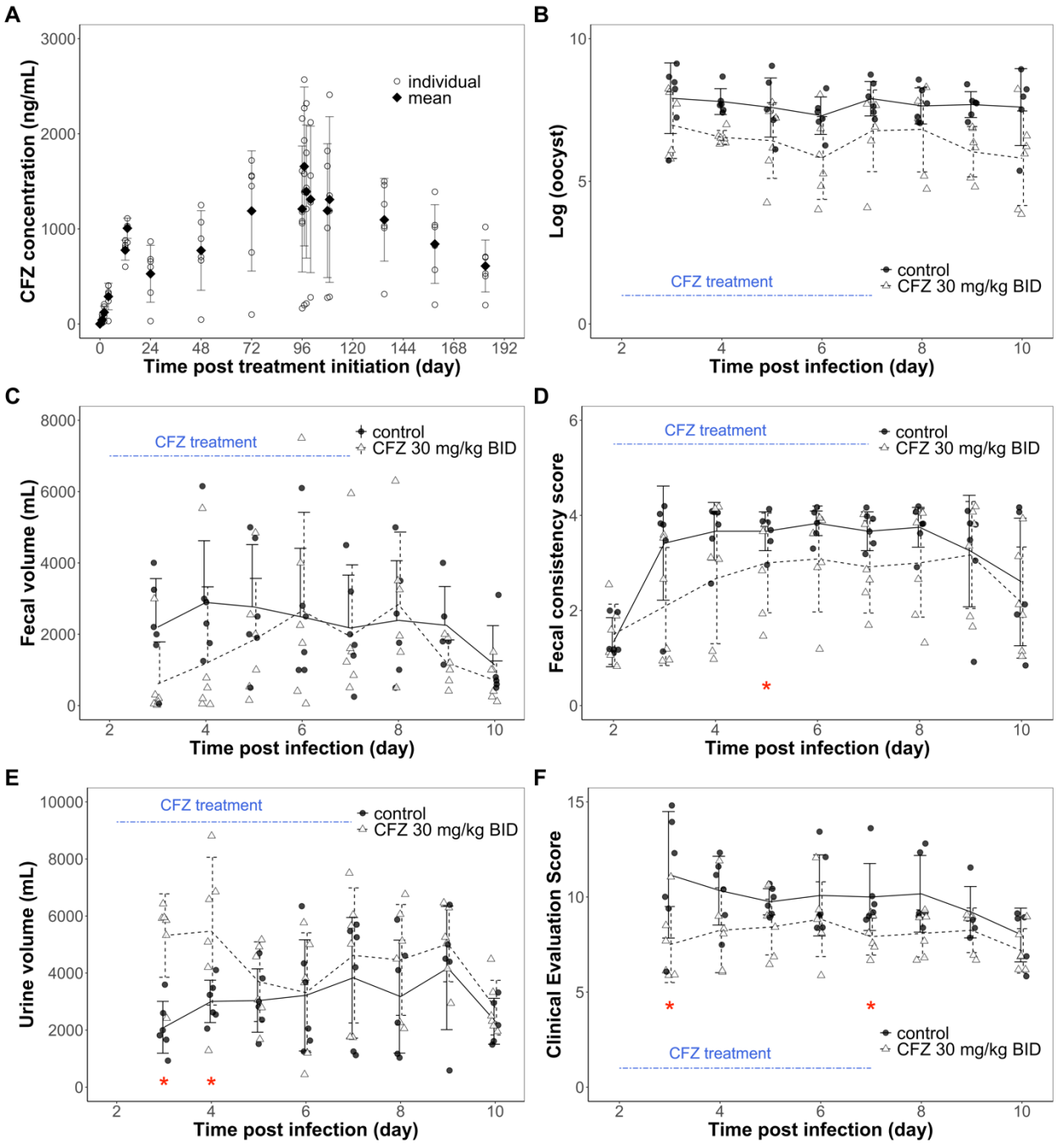

Figure 3.2. Clofazimine pharmacokinetics and pharmacodynamics in calf model of cryptosporidiosis.

Clofazimine was administered to calves with a dosing regimen of 30 mg/kg PO twice daily over 5 days for a total of 10 doses. (A) Up to 15 blood samples were collected from each calf (n = 6) over time, and mean and individual clofazimine concentrations are plotted in panel. (B) Stool

samples were collected every 24 h starting on day 3 post-infection for clofazimine- and vehicle control-treated calves, and fecal oocyst counts were quantified by real-time PCR. Mean and individual oocyst counts are plotted over time. (C to F) Other pharmacodynamic outcomes, including fecal volume (C), fecal consistency score (D), urine volume (E), and clinical evaluation score (F) were recorded daily and are shown as individual values and means (standard deviations are indicated by error bars). A red asterisk (*) indicates days on which the treatment group and the control group differed significantly ($P \leq 0.05$) at the collection endpoint.

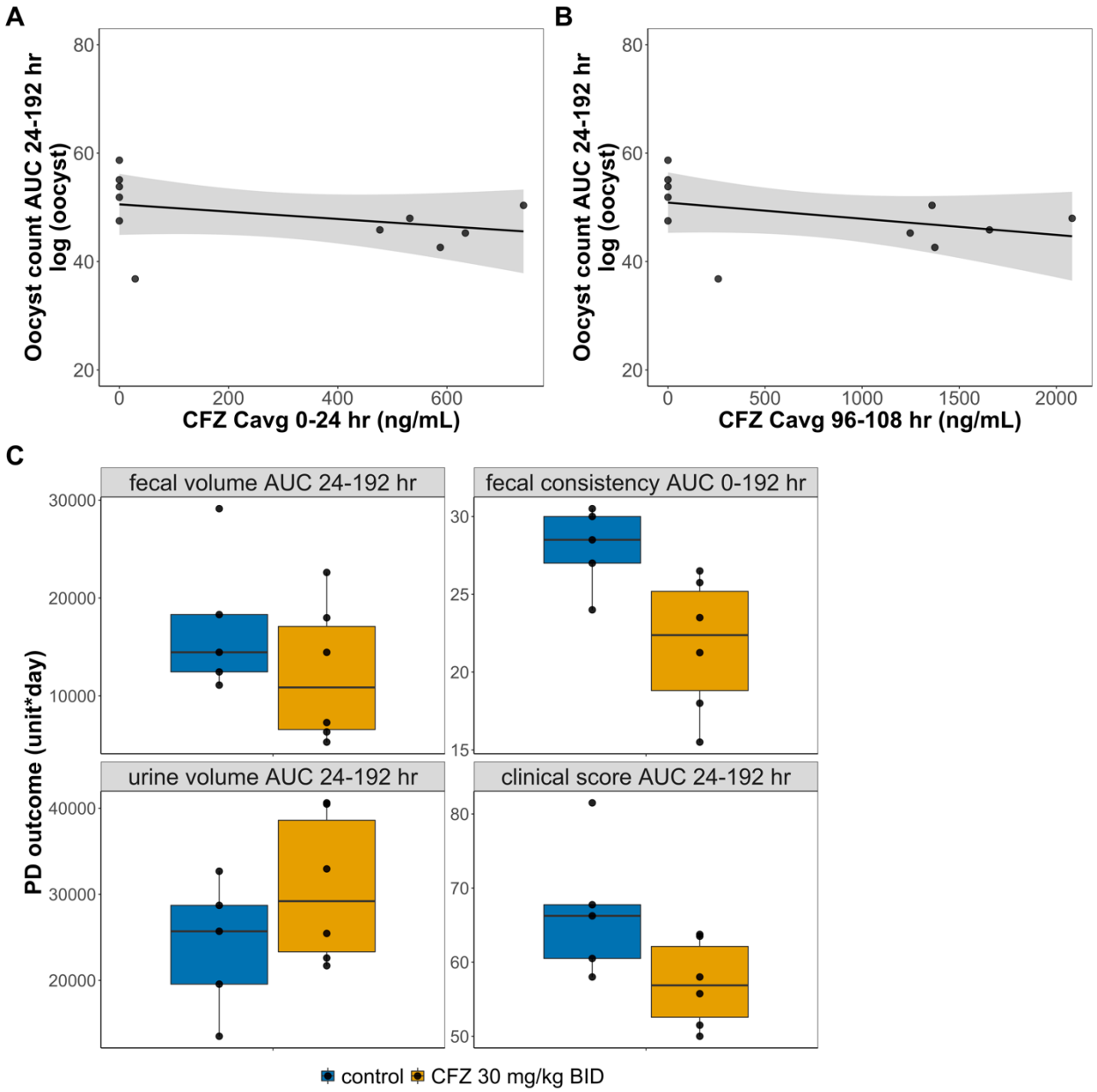

Figure 3.3. Relationship between clofazimine treatment and pharmacodynamic outcomes in calves.

The oocyst count area under the curve (AUC) for the duration of the study was calculated for each calf. The association between oocyst count $AUC_{24\text{-}192H}$ and average clofazimine concentrations, $Cavg_{0\text{-}24H}$ (A) and $Cavg_{96\text{-}108H}$ (B), were investigated using a simple linear regression model, and the results are summarized in **Table 3.**. Clinical outcome AUCs were also calculated for the duration of the study and compared between the treatment and the control groups (C). The differences between the groups were not statistically significant after Bonferroni

correction adjusting for multiple comparison. The top and bottom bars of the boxes represent the 25^{th} and 75^{th} percentiles, respectively, and the center lines mark the medians. The whiskers extend to the most extreme data point that is within 1.5 times the IQR away from the box. Points that fall beyond the end of the whiskers are outliers as defined by the 1.5 IQR rule.

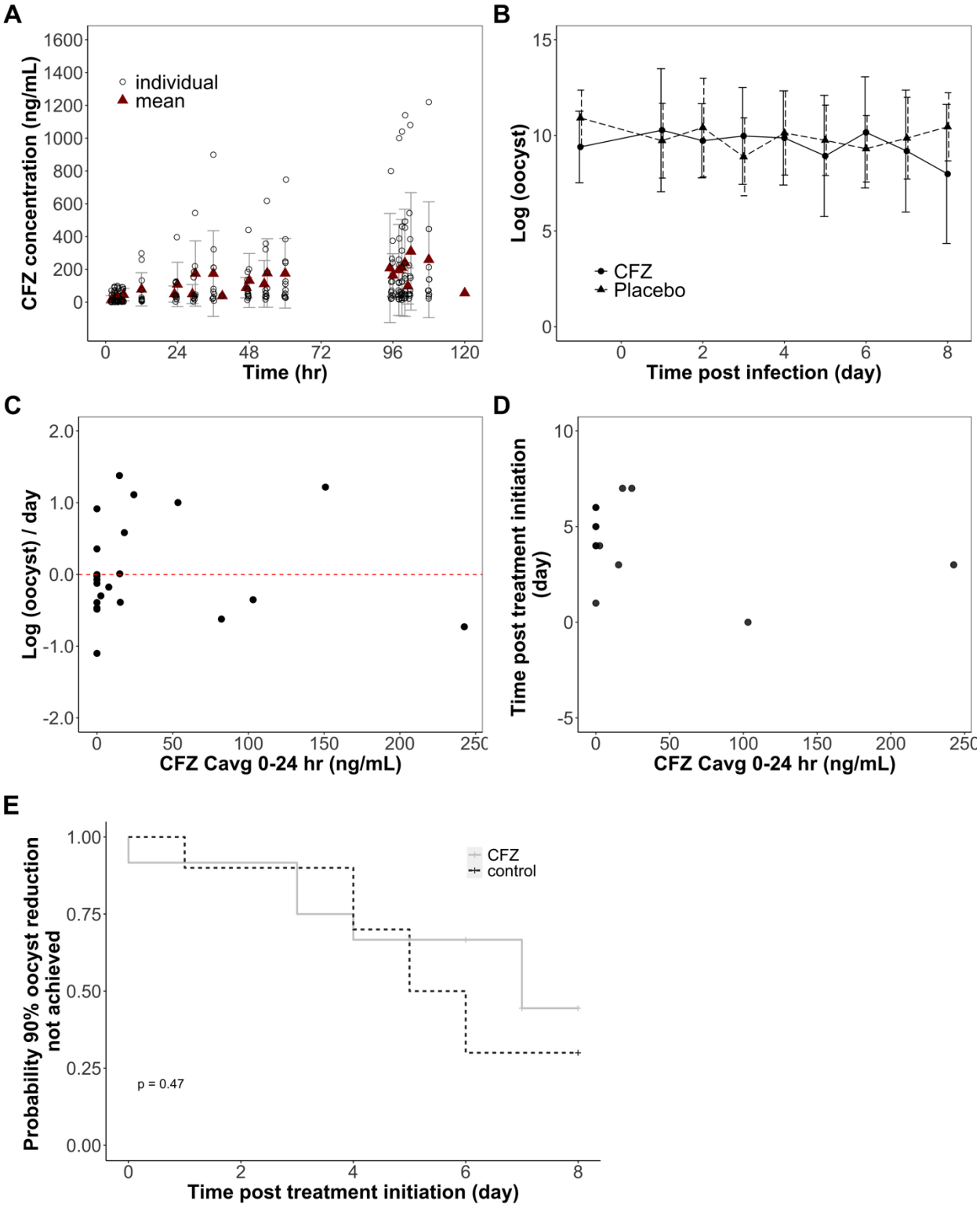
A
CFZ concentration (ng/mL)
individual
mean
Time (hr)
B
Log (oocyst)
CFZ
Placebo
Time post infection (day)
C
Log (oocyst) / day
CFZ Cavg 0-24 hr (ng/mL)
D
Time post treatment initiation (day)
CFZ Cavg 0-24 hr (ng/mL)
E
Probability 90% oocyst reduction not achieved
CFZ
control
p = 0.47
Time post treatment initiation (day)

Figure 3.4. Clofazimine pharmacokinetics and pharmacodynamics in Phase 2a clinical trial.

HIV-infected adults with cryptosporidiosis were administered clofazimine with a dosing regimen of 100 mg PO TID for participants who weighed ≥50 kg (n=2 participants) or 50 mg PO TID for participants who weighed <50 kg (n=10 participants) for a duration of 5 days. (A) Mean and individual clofazimine concentrations plotted over time. (B) Stool samples were collected and assessed three times a day, and oocyst shedding was quantified using qPCR. Mean daily oocyst shedding in the first stool was compared between clofazimine treatment group and the control group. (C) For each participant, the rate of reduction in daily oocyst shedding was calculated for the first 3 days of clofazimine treatment, with the result plotted against observed clofazimine $Cavg_{0\text{-}24H}$ to reveal a potential correlation between oocyst excretion rates and clofazimine concentrations. The dashed line marks no change in oocyst shedding rate. No correlation was clearly seen comparing the rate of reduction in oocyst shedding rates to clofazimine $Cavg_{0\text{-}24H}$. (D) A time-to-event approach was attempted, where the time to reach 90% oocyst reduction was compared to clofazimine $Cavg_{0\text{-}24H}$ and a significant correlation was not identified. (E) A Kaplan-Meier survival curve was used to compare the probability of achieving 90% reduction in oocyst count compared to the baseline count between clofazimine treatment group and the control group. A success was defined by having less than 10% of baseline oocyst count, and no significant difference was found, as shown by the log rank test ($P = 0.47$).

Table 3.1. Clofazimine pharmacokinetics in mice after a single, oral dose.

Dose (mg/kg)	**$t_{1/2}$** (h)	**C_{max}** (ng/mL)	**T_{max}** (hr)	**$AUC_{0\text{-}24H}$** (hr*ng/mL)	**$AUC_{0\text{-}240H}$** (hr*ng/mL)	**AUC_{INF}** (hr*ng/mL)	**CL/F** (mL/min/kg)
0.03	ND*	10	3	174	465	ND*	0.9
0.1	70	22	8	401	1,446	1,580	1.1
0.3	86	52	1	973	3,781	4,465	1.1
1	87	99	8	2,082	10,123	11,887	1.4
3	106	168	3	3,265	16,841	20,794	2.4
10	120	342	8	7,420	38,771	53,161	3.1
30	106	626	8	14,053	74,933	96,592	5.2
100	183	1,550	3	26,997	139,253	228,440	7.3
300	118	2,153	3	44,914	248,866	338,831	14.8

**ND, values were not provided because only two time points were available to calculate $t_{1/2}$ and AUC_{INF} for the 0.03 mg/kg dose group. $t_{1/2}$, half-life; C_{max}, maximum plasma concentration of drug; T_{max}, time to C_{max}; CL, clearance.*

Table 3.2. Calf study linear regression model estimates.

Outcome variable	Mean clofazimine concentration (ng/mL)	Estimate	*P*	R^2
Oocyst count $AUC_{24\text{-}192H}$	$Cavg_{0\text{-}24H}$	-0.00603	0.00570*	0.101
	$Cavg_{96\text{-}108H}$	-0.00267	0.243	0.134
Fecal volume $AUC_{24\text{-}192H}$	$Cavg_{0\text{-}24H}$	-8.072	0.292	0.122
	$Cavg_{96\text{-}108H}$	-4.60	0.103	0.268
Fecal consistency score $AUC_{0\text{-}192H}$	$Cavg_{0\text{-}24H}$	-0.00966	0.0359*	0.403
	$Cavg_{96\text{-}108H}$	-0.00481	0.00203*	0.671
Urine volume $AUC_{24\text{-}192H}$	$Cavg_{0\text{-}24H}$	10.80	0.224	0.160
	$Cavg_{96\text{-}108H}$	5.73	0.0798	0.302
Clinical evaluation score $AUC_{24\text{-}192H}$	$Cavg_{0\text{-}24H}$	-0.154	0.0762	0.308
	$Cavg_{96\text{-}108H}$	-0.00722	0.0228*	0.455

P values that reached statistical significance defined by an α value of ≤0.05 are marked with asterisks.

Table 3.3. Observed clofazimine concentrations in calf and human studies compared to estimated target exposure levels based on EC_{50}s and EC_{90}s established in mice.

Calf study						
	$Cavg_{0\text{-}24H}$			**$Cavg_{96\text{-}108H}$**		
	Mean (SD) (ng/mL)	Observed/EC_{50}	Observed/EC_{90}	Mean (SD) (ng/mL)	Observed/EC_{50}	Observed/EC_{90}
30 mg/kg BID, 5 days	500 (248)	1.58	0.176	1330 (605)	4.21	0.468
Phase 2a study (humans)						
	$Cavg_{0\text{-}24H}$			**$Cavg_{96\text{-}108H}$**		
	Mean (SD) (ng/mL)	Observed/EC_{50}	Observed/EC_{90}	Mean (SD) (ng/mL)	Observed/EC_{50}	Observed/EC_{90}
50 mg TID, 5 days	63.0 (79.4)	0.199	0.0222	233 (340)	0.737	0.0820
100 mg TID, 5 days	50.1 (45.3)	0.159	0.0176	182 (60.0)	0.576	0.0641

Table 3.4. Clinical trial linear regression model estimates.

Outcome variable	Clofazimine exposure (ng/mL)	Estimate	*P*	R^2
Time to >90% oocyst reduction	$Cavg_{0\text{-}24H}$	-0.0110	0.228	0.129
	$Cavg_{96\text{-}108H}$	-0.00227	0.278	0.106
Rate of reduction in daily oocyst counts	$Cavg_{0\text{-}24H}$	-0.00243	0.377	0.0715
	$Cavg_{96\text{-}108H}$	-0.000576	0.358	0.0773

Chapter 4. POPULATION PHARMACOKINETIC SIMULATION AND PHARMACODYNAMIC PREDICTION OF TEBIPENEM-PIVOXIL FOR TREATING CHILDREN WITH SHIGELLOSIS IN BANGLADESH

4.1 ABSTRACT

Background: Increasing antimicrobial resistance poses a serious challenge for the treatment of *Shigella* infections and there is an urgent need for alternative antibiotic treatments. A clinical trial was conducted to investigate the anti-*Shigella* efficacy of oral tebipenem-pivoxil, compared to intravenous ceftriaxone, in Bangladeshi children with shigellosis, aged from 24 to 59 months. Using demographic and pharmacokinetic (PK) data from this clinical trial, we performed population PK simulations that allowed trial outcome predictions and dosing regimen comparisons for the unique target population, establishing a workflow that can be adapted to other drugs and diseases to supply critical information for making dosing decisions.

Methods: Population PK simulations were conducted to predict tebipenem PK profiles for a virtual pediatric population following the proposed dosing regimen, using observed demographic characteristics of 2249 Bangladeshi children with suspected shigellosis. Subsequently, the model predictions estimated each virtual subject's fraction of time over the 3-day treatment period during which simulated free tebipenem plasma concentration was above the minimum inhibitory concentration (*f*T>MIC). Variability associated with the prevalence of different *Shigella* species in Bangladeshi children and the distribution of MICs for each *Shigella* species were incorporated. *Shigella* treatment effect was assumed for subjects that had *f*T>MIC for at least 40% of the 3-day treatment period (40% *f*T>MIC). Lastly, the probability of tebipenem-pivoxil being non-inferior to ceftriaxone, in a clinical trial containing 66 subjects in each arm, was

evaluated for two dosing regimens. Three levels of ceftriaxone resistance were simulated to examine how changing ceftriaxone resistance rate can impact the trial outcome.

Results: The probability of achieving 40% *f*T>MIC with 3 days of treatment was 86.4% for 4 mg/kg tebipenem-pivoxil three times daily (TID) dosing and 92.4% with 3 mg/kg tebipenem-pivoxil four times daily (QID) dosing. When administered at 4 mg/kg TID, the probability of tebipenem-pivoxil being non-inferior to ceftriaxone was 0.014, 0.262, and 0.708 when ceftriaxone resistance was at 0%, 10.25%, and 18.5%, respectively. When administered at 3 mg/kg QID, the probability of tebipenem-pivoxil being non-inferior to ceftriaxone was increased to 0.252, 0.822, and 0.980 when ceftriaxone resistance was at 0%, 10.25%, and 18.5%, respectively.

Conclusions: This study provides treatment efficacy and trial outcome predictions made specifically for the target population and highlights the complexity of factors involved in shaping the outcomes. Our findings, which suggest more frequent tebipenem-pivoxil dosing increases the chance of producing treatment effect, contribute valuable insights to inform dosing strategy selection.

4.2 INTRODUCTION

Shigellosis is a diarrheal disease caused by an infection with the gram-negative bacterium *Shigella*.[90] Common symptoms of shigellosis include bloody diarrhea, high fever, and abdominal pain.[91] Globally, *Shigella* infection is the second leading cause of diarrheal mortality among all age groups, predominantly impacting children under five years of age.[173,174] It has been estimated that *Shigella* was responsible for approximately 210,000 deaths among all ages and 64,000 deaths among children younger than 5 years, in 2016.[173] In Bangladesh, shigellosis is endemic and is a significant cause of morbidity and mortality.[174]

There are four species of *Shigella*: *S. flexneri, S. sonnei, S. dysenteriae,* and *S. boydii*. The distribution and prevalence of these species vary geographically, with *S. flexneri* being dominant in developing countries whereas *S. sonnei* being more prevalent in high-resource countries.[175] *S. dysenteriae* and *S. boydii* are relatively uncommon and have been declining.[176–180] However, the trend is everchanging due to global traveling, poorly regulated antimicrobial use, improving living conditions, and increasing availability of clean water in low-resource countries. In Bangladesh, *S. sonnei* prevalence has been growing over the recent years.[176,178,179,181]

Treatment of *Shigella* infections faces the challenge of a global rise in broad-spectrum antibiotic resistance.[90,91,176,180,182–187] Azithromycin is currently the first-line treatment for shigellosis in Bangladesh, with ceftriaxone being the second-line treatment in children. Use of oral ciprofloxacin, which is another World Health Organization (WHO)-recommended first-line treatment for shigellosis, is declining in Bangladesh due to rapidly rising drug resistance that reached over 70% by 2020.[176] Unfortunately, antimicrobial resistance to azithromycin and ceftriaxone are also on the rise. Nuzhat et al.'s study on shigellosis antimicrobial resistance in Bangladesh from 2001 to 2020 reported more than 50% azithromycin resistance in children less

than 5 years old in 2020.[176] While ceftriaxone resistance emerged more recently (after 2010), it has been steadily rising and reached over 10% by 2020.[176] Therefore, there is an urgent need for alternative antibiotic treatments for drug-resistant *Shigella* infections.

Tebipenem-pivoxil, an oral carbapenem, is a potential alternative treatment for shigellosis. As the prodrug form of tebipenem, tebipenem-pivoxil has improved absorption and bioavailability compared to the active form of the drug.[188,189] Tebipenem-pivoxil is licensed in Japan for treating otolaryngologic infections and respiratory infections in children.[190] The pharmacokinetic (PK) and safety profiles of tebipenem-pivoxil in Japanese children have already been studied.[191] Moreover, preclinical evidence has demonstrated the efficacy of tebipenem in clearing *Shigella* infection in animal models.[192] Therefore, a clinical trial was designed to evaluate the treatment effect of oral tebipenem-pivoxil, compared to intravenous (IV) ceftriaxone, on shigellosis in children between 24 and 59 months of age in Bangladesh.

In this study, we utilized screening data from the clinical trial (collected between May 2022 and September 2022) and tebipenem PK data from the pilot study to make population PK predictions reflecting the unique demographic characteristics of the target Bangladeshi pediatric population. Subsequently, the population PK predictions were used to predict treatment efficacy, after incorporating variability in minimum inhibitory concentration (MIC) distribution, differential *Shigella* spp. prevalence, increasing antimicrobial resistance, and random chance. This approach allowed the determination of the probability of target attainment (PTA) and prediction of the proposed non-inferiority clinical trial outcome. An alternative dosing strategy was also compared to the proposed dosing regimen.

4.3 METHODS

4.3.1 *Study Design*

A phase IIb randomized controlled trial, led by Dr. Sharika Nuzhat from the International Centre for Diarrhoeal Disease Research (Mohakhali, Dhaka, Bangladesh) was designed to evaluate the efficacy and safety of oral tebipenem-pivoxil for *Shigella* infections in a pediatric population that was unresponsive to first-line antibiotic therapy for their *Shigella* infections (Clinicaltrials.gov number: NCT05121974). Bangladeshi children who met the inclusion criteria, being between 24 and 59 months of age with suspected *Shigella* infection, were identified as potential subjects. Written informed consent was obtained from the guardian of each study subject before enrollment. The trial includes two parts: a pilot study and a main trial. Critical to this investigation, a pilot study of 30 patients was conducted to determine the PK, safety, and efficacy of oral tebipenem-pivoxil (n=15) at 4 mg/kg three times daily (TID) for 3 days, compared to oral azithromycin (n=15) at 10 mg/kg once daily (QD) for 3 days. The main trial (n=132) will compare key clinical, microbiologic, and safety outcomes of children randomized to receiving oral tebipenem-pivoxil (n=66) at 4 mg/kg TID or IV ceftriaxone (n=66) at 50 mg/kg QD for a total of 3 days. The primary aim of the main trial is to determine whether tebipenem-pivoxil is non-inferior to the WHO-recommended second-line therapy ceftriaxone, at a non-inferiority margin of 10%. Tebipenem PK data collected from the pilot study were used to validate the population PK model used in this chapter (**Section 4.3.4**), to make predictions about the main trial outcome (**Sections 4.3.5 and 4.3.6**).

4.3.2 *Pharmacokinetic Sampling and Analysis*

In the pilot study, pharmacokinetic blood samples were collected as follows: on Day 1 and Day 3 of tebipenem dosing, shortly before the first dose; 30 min, 1 h, 4 h after the first dose; and 1-2 h after the second and the third doses. On Day 2 of tebipenem dosing, blood samples were taken shortly before the first dose and 1-2 h after the second and third doses.

Immediately following collection, blood samples were centrifuged, and plasma samples were stored at -80°C. Subsequently, tebipenem plasma concentrations were measured using liquid chromatography-tandem mass spectrometry by Q2 Solution (Ithaca, NY, USA). The lower limit of quantification (LLOQ) was 30 ng/mL.

4.3.3 *Virtual Population Generation*

First, we generated a virtual subject population to characterize the distribution patterns and relationships among important baseline variables including sex, age, weight, and height. To generate this virtual subject population, we used demographic data collected from May 2022 to September 2022, from 2249 Bangladeshi children between ages 24 and 59 months with suspected *Shigella* infections who were screened for the clinical trial of interest. Relationships between baseline variables were utilized to generate 500 virtual trial populations; each trial enrolled 66 virtual subjects to align with the intended sample size for the main trial, as outlined in the clinical study protocol (NCT05121974).[193]

Since the risk of *Shigella* infection may be associated with sex,[194] retaining the sex difference observed in the target population would contribute to building a more realistic virtual population. A higher proportion of the population in our screening dataset was male, and the same was observed in a separate study of 204 Bangladeshi pediatric shigellosis patients, with

59.5% and 59% being male, respectively.[194] Thus, the sex of the virtual subjects was randomly determined with the probability of being assigned male equaling 0.6.[194]

To reproduce the age distribution of the target population for the virtual population, random samples with replacement (bootstrap samples) were drawn from the age data of the corresponding sex in the screening data set. The samples were drawn to account for potential differences in age distribution between the two sexes, in order to capture the full range of variability and provide an accurate representation of the target population.

Linear regression analysis was performed to evaluate the relationships between age and height for male and female subjects in the screening data set independently. All assumptions (linearity, homoscedasticity, independence, and normality) for using linear regression were met. Errors for the relationship between age and height were captured with an additive error model. Box Cox transformation was first performed on weight for male and female subjects separately. Subsequently, the relationship between transformed weight and height was estimated through linear regression analysis. Residual errors were estimated using an additive error model.

Next, using the linear relationship estimated (**Equation 4.1**) and incorporating random errors (**Equation 4.2**), the height of virtual subjects was simulated based on their age.

$$tvHeight_i = \theta_0 + \theta_1 \times Age_i$$

Equation 4.1

$$Height_i = tvHeight_i + \varepsilon_i$$

Equation 4.2

In the equations above, subscript *i* represents the virtual subject of interest. θ_0 is the intercept of the equation and θ_1 the slope. θ_0 and θ_1 were estimated separately for male and female subjects to account for potential sex differences. $tvHeight_i$ is the predicted typical value of height

(without error) for subject *i*, based on the age of subject *i* denoted by Age_i. $Height_i$ is the final height generated for individual *i*, after incorporating an error term ε_i that was randomly drawn from a normal distribution (0, σ).

Similarly, using the linear relationship (**Equation 4.3**) between Box Cox transformed weight and height and incorporating random errors with an additive error model (**Equation 4.4**), weight was generated separately for male and female virtual subjects.

$$transformed\ tvWeight_i = \theta_0 + \theta_1 \times Height_i$$

Equation 4.3

$$transformed\ Weight_i = transformed\ tvWeight_i + \ \varepsilon_i$$

Equation 4.4

Where subscript *i* represents the virtual subject of interest. θ_0 is the intercept of the equation and θ_1 the slope. θ_0 and θ_1 were estimated separately for males and females.

$Transformed\ tvWeight_i$ is the predicted typical weight with Box Cox transformation for subject *i*, based on the height of subject *i*, as denoted by $Height_i$. $Transformed\ Weight_i$ is the Box Cox transformed weight generated for subject *i*, after incorporating an error term ε_i that was randomly drawn from a normal distribution (0, σ). $Weight_i$, the untransformed weight for each virtual subject, was computed as the inverse of the Box Cox transformed weight (**Equation 4.5**).

$$Weight_i = (transformed\ Weight_i \times \lambda + 1)^{\frac{1}{\lambda}}$$

Equation 4.5

λ, the exponent for Box Cox transformation, is the optimal value that minimizes the standard deviation of the transformed data and improves the normality of the data. λ was different for male and female subjects.

Lastly, existing studies suggest limited interindividual variability in weight-normalized creatine clearance (CrCl) in children aged from 24 to 59 months.[195] Moreover, there is no evidence to date to suggest altered renal function in association with shigellosis. Since CrCl was not collected in the screening dataset, random sampling from a normal distribution of CrCl literature values reported for children was performed.[191]

4.3.4 *Population Pharmacokinetics Simulation*

Sato et al. have previously published a population PK model of tebipenem in pediatric patients with otolaryngological infection or pneumonia, using plasma tebipenem concentrations from five clinical studies with 217 patients aged 0.5 to 16 years.[191] Using Sato et al.'s population PK model with corrections for suspected errors (**Appendix A**), we validated published model performance with our available tebipenem PK data from 15 patients receiving tebipenem in the pilot study (**Figure 4.1**). More specifically, Sato et al.'s population PK model structure and corrected estimates were used, along with actual dosing and demographic information (age in years, weight in kg, and CrCl in L/hr/kg) for the 15 subjects in the pilot study, to simulate the expected tebipenem PK profile for each subject (**Equation 4.6**, **Equation 4.7**). Average fold error (AFE) and absolute average fold error (AAFE) were computed to assess the bias and precision of the predictions, respectively. The AFE is 1.25 and AAFE is 2.00, both within the conventional acceptance threshold of 2-fold.[196,197] This demonstrates that Sato et al.'s model effectively predicted the PK profiles of our PK study patients. An AFE of 1.25 suggests very slight bias towards model overprediction and AAFE of 2.00 suggests acceptable precision. Therefore, Sato et al.'s model was used for our subsequent simulations in a virtual target population after its predictive performance had been validated.

$$\frac{CL}{F} = 0.7707 \times (0.363 + 0.104 \times \frac{1000}{60} \times CrCl)$$

Equation 4.6

$$\frac{V}{F} = 0.7707 \times (1.18 \times Age^{-0.132})$$

Equation 4.7

The "mrgsolve" package in R was used to simulate PK profiles for 500 virtual trials each containing 66 virtual subjects, as described in the previous section. Sato et al.'s corrected model estimates (**Equation 4.6**, **Equation 4.7**) were adopted. Age, weight, and CrCl data for the virtual population were used to make individual virtual subject's predictions. For the main trial simulation, tebipenem-pivoxil doses were weight-based, determined as each subject's enrollment weight multiplied by 4 mg/kg and rounded up to the nearest multiples of 5. Dosing administration was every 8 hours and a total of 9 doses were simulated, as specified by the clinical study protocol. For alternative dosing strategy evaluation, tebipenem population PK profiles were simulated for 3 mg/kg four times daily (QID) dosing, for a total of 12 doses (**Section 4.3.7**).

4.3.5 *Probability of Target Attainment Analysis*

The simulated tebipenem PK profiles for 500 trials of 66 subjects each, as described in the previous section, were used to determine the probability of target attainment for the full trial, with a predetermined sample size of 66 subjects for the tebipenem arm. Carbapenems have concentration-independent bactericidal activity, and an unbound serum level above the MIC for at least 40% of the dosing interval is generally associated with maximal treatment effect.[198] Hence, the fraction of time over the 72-hour dosing period during which simulated free

tebipenem plasma concentration was above MIC (*f*T>MIC) was estimated for each virtual subject. Next, the percentage of pediatric subjects that achieved the target PK/PD endpoint of 40% *f*T>MIC (free tebipenem plasma concentration was above MIC for at least 40% of the 72-hour dosing period) was calculated for each virtual trial and compared to a target of 90%. Lastly, whether at least 90% of the subjects in each virtual trial achieved the target endpoint 40% *f*T>MIC was compiled for all 500 virtual trials. The PTA was calculated assuming a binomial distribution.

The simulated tebipenem PK levels were not compared to a uniform MIC, but rather a distribution of MIC values that realistically resemble what is expected in the target population. A distribution of MIC values was used because several factors may impact the MIC of tebipenem against *Shigella* infection. First, the prevalence of the different *Shigella* species needs to be considered for the target population. Based on available information on the percentage of different *Shigella* species in children under 5 in urban and rural hospitals in Bangladesh, *S. boydii* and *S. dysenteriae* were rare.[176] 0% of *Shigella* isolates collected at the rural site were *S. boydii* or *S. dysenteriae* in 2020. At the urban site, *S. boydii* made up about 10% of the tested isolates whereas *S. dysenteriae* accounted for 0% in 2020. Moreover, *S. dysenteriae* and *S. boydii* had been declining in prevalence in Bangladesh from 2001 to 2020. Therefore, *S. boydii* and *S. dysenteriae* were not included in the PTA analysis. Between the two remaining species, *S. flexneri* and *S. sonnei*, an average of 53% of isolates collected from the rural and urban hospitals in 2020 were *S. flexneri* and 47% were *S. sonnei*.[176] To capture variability in tebipenem MICs associated with the popularity of different *Shigella* species in the target population, *S. flexneri* or *S. sonnei* were randomly assigned to each virtual subject such that the probability of being assigned *S. flexneri* was 53% and *S. sonnei 47%.*

Next, MIC values also vary within the same species. A 2022 study reported MIC values for *S. flexneri* and *S. sonnei* isolates from Vietnam.[192] Based on this study, MIC values for *S. flexneri* were 0.016, 0.032, and 0.063 μg/mL at a probability of 12.5%, 75.0%, and 12.5%, respectively. MIC values for *S. sonnei* were 0.016, 0.032, 0.063, and 0.127 μg/mL at a probability of 1.35%, 66.2%, 21.6% and 10.8%, respectively. Consequently, these MIC values and their associated probabilities were utilized in the PTA analysis such that each virtual subject was randomly assigned to a MIC value at the probability level appropriate for their assigned *Shigella* species.

4.3.6 *Non-Inferiority Trial Simulation Comparing Tebipenem and Ceftriaxone Efficacy*

Since the aim for the main clinical trial is to compare oral tebipenem-pivoxil (n=66) and IV ceftriaxone (n=66) for the treatment of shigellosis, the risk difference of tebipenem and ceftriaxone was estimated and compared to a prespecified non-inferiority margin of 10%, following the study protocol.[193] Based on a previous IM ceftriaxone trial in Israeli children with invasive diarrhea, conducted in 1996-97, the clinical and microbiologic success rate for ceftriaxone was assumed to be 97% in the absence of ceftriaxone resistance.[199] Therefore, for Scenario 1 of non-inferiority trial prediction, efficacy outcomes for the active control ceftriaxone arm were randomly generated for 500 trials, assuming no ceftriaxone resistance and a binomial distribution with p=0.97. These simulated ceftriaxone trial outcomes were matched with the 500 simulated tebipenem trials. The risk difference of clinical failure was computed as the risk of failure in the tebipenem arm of a trial – risk of failure in the ceftriaxone arm of the same trial. Positive risk difference suggests that tebipenem treatment is less effective than ceftriaxone treatment and vice versa. 95% confidence intervals were constructed such that the upper tail would be compared with the 10% non-inferiority margin at a 2.5% one-sided alpha level. The

probability that the tebipenem treatment group is non-inferior to the ceftriaxone control group was estimated.

Rising antimicrobial resistance poses a significant threat to shigellosis treatment. Evidence suggests that there was a statistically significant increase in ceftriaxone resistance among children under 5 years of age in Bangladesh from 2001 to 2020.[176] Therefore, potential resistance to ceftriaxone was taken into consideration in an additional two sets of virtual trial outcome comparisons.

The average ceftriaxone resistance based on data collected from rural and urban hospitals in Bangladesh from 2016 to 2020 was estimated to be 10.25%.[176] For Scenario 2, assuming a ceftriaxone resistance rate of 10.25% and a 97% treatment success rate in the remaining non-resistant population, treatment outcomes were randomly generated for the ceftriaxone arm for another 500 trials following a binomial distribution with $p = 0.97 \times (1 - 0.1025) = 0.871$. The efficacy outcomes for ceftriaxone treatment were compared with simulated tebipenem trial outcomes and risk differences were computed in the same fashion as described previously.

Next, since antimicrobial resistance has been continuously rising for the past decades for various antibiotics, likely, ceftriaxone resistance will also be greater than the 10.25% reported in 2016-2020 by the time the current clinical trial is conducted. Therefore, projected ceftriaxone resistance was estimated using the average ceftriaxone resistance in under-5-year-old children in Bangladesh from 2011-2015 and 2016-2020, assuming a zero-order trend.[176] The projected ceftriaxone resistance was 18.5%. Hence, the non-inferiority trial outcome prediction for Scenario 3 involved treatment outcomes randomly generated for the ceftriaxone arm following a binomial distribution with p = 0.97 * (1-0.185) = 0.791. Subsequently, risk differences were computed comparing the ceftriaxone and tebipenem arms of the virtual trials.

4.3.7 *Alternative Dosing Strategy Evaluation*

Tebipenem PK was simulated for QID dosing to explore whether this alternative dosing strategy would improve efficacy outcomes with more frequent dosing while maintaining the same total daily dose. Population PK simulations were generated for the same 33,000 virtual subjects (500 trials of 66 subjects per trial) with 3 mg/kg tebipenem-pixovil dosing, rounded up to the nearest multiples of 5, administered QID for a total of 12 doses over 3 days. *Shigella* species and MIC value assignment to each virtual subject were unchanged. PTA analysis and non-inferiority trial outcome prediction methods were consistent with the description provided in **Sections 4.3.5** and **4.3.6**.

4.3.8 *Statistical Analysis*

Statistical analyses, population PK simulations, and plotting were all carried out using R version 4.3.0 (2023-04-21). Non-compartmental analysis was conducted using Phoenix WinNonlin version 8.3 (Certara, Princeton, NJ).

4.4 RESULTS

4.4.1 *Virtual Target Population*

A virtual population of 66 pediatric patients per trial, based on the target enrollment for the tebipenem treatment arm of the main trial, was simulated for 500 trials (a total of 33,000 virtual subjects) and compared with the observed data in the screening data set (**Table 4.1, Figure 4.2**). As shown, the virtual population not only reproduced the trend in the observed data but also accurately captured the variability in the target population. This suggests that our approach to constructing a virtual population that highly resembles the target population was successful and supports the use of the virtual population demographic parameters for making subsequent PK

predictions. The characterized relationships between demographic variables used to construct the virtual population are summarized in **Table 4.2**.

To illustrate how the target population differs from a typical pediatric population, the weight-for-age curves for males and females aged between 2 and 5 years were compared between our virtual population and the WHO data (**Figure 4.3**).[200] As shown, Bangladeshi children weigh less compared to the average children of the same age, as reported by the WHO. This may be associated with the high prevalence of undernutrition in under-5-year-old children in Bangladesh.[201] Therefore, to capture the unique characteristics of the target population to make accurate population PK predictions, it was necessary to construct a virtual target population instead of adopting a generic pediatric population for subsequent PK modeling and simulation exercises.

4.4.2 *Probability of Target Attainment for 4 mg/kg TID Dosing*

A summary of tebipenem PK parameters for the virtual target population containing 500 trials of 66 subjects each, following oral administration of 4 mg/kg tebipenem-pivoxil TID for three days, is presented in **Table 4.3**. The population PK simulation incorporated not only variability due to differences in important demographic variables among the virtual subjects but also random interindividual variability of unspecified sources, as reported by Sato et al..[191]

Using the simulated tebipenem PK profiles and individually assigned MIC values, the *f*T>MIC was estimated for each virtual subject and compared to a target threshold of 40%. The median probability of achieving the target PK/PD parameter of 40% *f*T>MIC was 86.4% (95% CI: 77.3% - 93.9%), based on the outcomes of 500 virtual trials (**Figure 4.4A**). This implies that there is an approximately 86.4% chance that a Bangladeshi child aged between 24 and 59 months with *Shigella* infection would receive maximal treatment effect after receiving 4 mg/kg

tebipenem-pivoxil TID for three days. The PTA, the probability at which at least 90% of the subjects in a virtual trial with a sample size of 66 would achieve the target endpoint of 40% *f*T>MIC, was 14.4% (95% CI: 11.6% - 17.7%). Therefore, it is unlikely that over 90% of the subjects receiving tebipenem in the actual main trial will achieve 40% *f*T>MIC. However, it is important to note that the probability of 40% *f*T>MIC, which was 86.4%, is very close to the 90% target, such that a slight increase in *f*T>MIC may result in a remarkable increase in PTA.

4.4.3 *Non-Inferiority Trial Comparing Tebipenem and Ceftriaxone Efficacy*

Through simulating 500 virtual trials and comparing the proportion of treatment success for tebipenem-pivoxil (n=66) and ceftriaxone (n=66), the probability for tebipenem-pivoxil treatment to be non-inferior to ceftriaxone treatment was calculated at a prespecified non-inferiority margin of 10%. The results and 95% confidence intervals are summarized in **Table 4.4** and illustrated in **Figure 4.5**.

Assuming no ceftriaxone resistance and a ceftriaxone treatment success rate of 97%, based on a trial evaluating IM ceftriaxone efficacy in Israeli children that took place from 1996 to 1997,[199] the probability for tebipenem treatment at the proposed dosing regimen to be non-inferior to ceftriaxone was 1.40% (95% CI: 0.680% - 2.86%) (**Figure 4.5**).

However, since antimicrobial resistance is both geographically- and time-dependent, potential resistance to ceftriaxone in Bangladesh at the time the proposed full trial is to be completed (by 2025) must be taken into account. Importantly, ceftriaxone resistance has started to rise significantly among Bangladeshi children since around 2010.[176] Hence, the 97% treatment success rate associated with IM ceftriaxone against shigellosis, observed from 1996 to 1997, is likely obsolete. Consequently, two additional scenarios were proposed, for which the probability of tebipenem achieving non-inferiority compared with ceftriaxone was estimated. If 10.25% of

the study population is resistant to ceftriaxone, consistent with the mean reported resistance for Bangladeshi children under 5 for the years of 2016 to 2020,[176] then there is a 26.2% (95% CI: 22.5% - 30.2%) chance for tebipenem to be non-inferior to ceftriaxone in a clinical trial with 66 subjects in each treatment arm (**Figure 4.5**). If ceftriaxone resistance keeps rising following a zero-order trend from the period of 2011 to 2015 and that of 2016 to 2020 to reach 18.5% in the study population,[176] then the probability of tebipenem-pivoxil being non-inferior to ceftriaxone would be 70.8% (95% CI: 66.7% - 74.6%) (**Figure 4.5**).

4.4.4 *Alternative Dosing Strategy Evaluation*

When tebipenem PK was simulated for 3 mg/kg tebipenem-pivoxil QID dosing in the same virtual population, the median probability of achieving the target PK/PD parameter 40% *f*T>MIC was 92.4% (95% CI: 86.4% - 98.5%). The PTA, as defined by the probability at which at least 90% of the subjects in a virtual trial achieved 40% *f*T>MIC, was 77.2% (95% CI: 73.3% - 80.7%) (**Figure 4.4B**).

By comparing the proportion of treatment success for virtual subjects receiving tebipenem-pivoxil (n=66) at 3 mg/kg QID and ceftriaxone (n=66), the probability for QID tebipenem-pivoxil treatment to be non-inferior to ceftriaxone treatment was calculated at a prespecified non-inferiority margin of 10%. Three levels of ceftriaxone resistance (no resistance, 10.25% resistance, and 18.5% resistance) were considered for efficacy simulation. The virtual non-inferiority trial results and 95% confidence intervals are summarized (**Table 4.5; Figure 4.5)**.

Although the median probability of achieving 40% *f*T>MIC did not differ much between TID (86.4%) and QID (92.4%) tebipenem-pivoxil dosing, the PTA drastically increased from 14.4% to 77.2%. The non-inferiority trial outcomes were also improved with QID dosing,

particularly if ceftriaxone resistance was assumed to be 10.25%, at which the probability of tebipenem-pivoxil treatment achieving non-inferiority improved from 0.262, under TID dosing, to 0.822, under QID dosing.

4.5 DISCUSSION

Understanding and properly characterizing sources of variability is key to making accurate population PK predictions that can inform clinical decisions and shape study designs. In this chapter, a clinical study screening data set of 2249 children aged between 24 and 59 months and with suspected shigellosis was utilized to support the simulation of virtual trials consisting of subjects that closely resemble the target population, which is unique due to its high prevalence of malnutrition and underweight.[201–204] Demographic variables such as age and weight directly impact tebipenem PK predictions. Therefore, by reproducing the distribution of these variables for the virtual population, our study was empowered to make tebipenem PK predictions specifically tailored to the target Bangladeshi pediatric population, which has not been accomplished previously.

In addition to variability in tebipenem PK associated with varying demographic characteristics, other factors can also contribute to variability in treatment outcomes. For instance, antimicrobial resistance can vary both geographically and temporally. Its emergence poses a significant public health threat and is a reason why alternative treatment options, such as tebipenem, are being explored for *Shigella* infection. It is crucial to know the prevalence of drug resistance in the target population to make predictions about the efficacy of a drug. In this study, we made trial outcome predictions for three different scenarios with different ceftriaxone resistance levels. The findings illustrate that trial outcomes can be drastically changed, from a

0.014 probability of tebipenem being non-inferior to ceftriaxone to a 0.708 probability of tebipenem being non-inferior to ceftriaxone when ceftriaxone resistance rate increases from 0 to 18.5% while tebipenem-pivoxil dosing regimen remains unchanged at 4 mg/kg TID. This highlights the importance of monitoring the changing patterns of antimicrobial resistance because this knowledge can greatly impact the accuracy and certainty of drug efficacy and clinical trial outcome predictions.

However, emerging drug resistance can be resource-intensive to monitor and challenging to predict, because changes in resistance prevalence do not follow a consistent trend. Therefore, despite our best efforts, it is difficult to predict ceftriaxone resistance in our target population at the time of the main trial. It may even change from the time of trial initiation to the time of trial completion. Although we evaluated three scenarios to account for possible trial outcomes associated with different ceftriaxone resistance rates, it is possible that when the main trial is conducted, ceftriaxone resistance is outside of the range we evaluated, resulting in trial outcomes deviating from our predictions. Furthermore, as ceftriaxone and tebipenem are both β-lactam antibiotics and share common mechanisms of action, some ceftriaxone-resistant Shigella strains may have cross-resistance to tebipenem.[205] To address this uncertainty, one approach is to collect *Shigella* isolates from the target Bangladeshi population to test for resistance and measure the MIC.

There is variability in tebipenem MIC values associated with different *Shigella* species. Accordingly, to capture the distribution of MIC values in our virtual population, *Shigella* spp. prevalence data for Bangladeshi children along with MIC values reported for *Shigella* isolates from Vietnam were used in the simulation.[192] Although it is not expected for tebipenem MIC values against *Shigella* spp. to differ markedly between Vietnam and Bangladesh, using MIC

values for *Shigella* isolates collected in Bangladesh would improve the accuracy and boost the confidence of the simulations. Therefore, once available, MIC information for Bangladesh *Shigella* isolates should be used to replace the currently employed literature values.

Finally, our analyses comparing tebipenem-pivoxil TID and QID dosing regimens with the same total daily dose show that dosing more frequently may improve the chance of trial success. Out of the three scenarios examined, this impact is most prominent when the ceftriaxone resistance rate is modeled at 10.25%. In this scenario, the probability of tebipenem achieving non-inferiority, compared to ceftriaxone, improved from 0.262 with TID dosing to 0.822 with QID dosing. The PTA also increased from 14.4% to 77.2%, with TID and QID dosing, respectively. This is because the proportion of subjects achieving 40% *f*T>MIC comes very close to the 90% threshold, with a median of 86.4% associated with TID dosing and 92.4% associated with QID dosing. Therefore, changing the dosing regimen, while boosting the median probability of achieving 40% *f*T>MIC by only 6%, can result in most virtual trials surpassing the 90% threshold and an approximately 63% increase in the PTA. Similarly, the outcome of the full clinical trial depends on both tebipenem and ceftriaxone response rates because it compares the two. Since the probability of 40% *f*T>MIC for tebipenem is close to 90%, the expected ceftriaxone response rate, which also fluctuates around 90% depending on the resistance rate, has a profound impact on the chance of trial success. Changing the tebipenem dosing strategy from TID to QID dosing can improve the chance of trial success while keeping the total dose unchanged because increasing dosing frequency reduces the fluctuation in tebipenem plasma concentrations and helps maintain plasma levels above the MIC. This effect is most pronounced when tebipenem and ceftriaxone response rates are in proximity to each other.

A QID dosing regimen may create practical challenges for patients and clinic personnel, and feasibility needs to be weighed against the potential treatment benefits, as suggested by this study. Higher non-adherence is associated more frequent dosing, increasing the risk of treatment failure.[206–208] Non-adherence was not built into our simulations because the study subjects in the clinical trial of interest will be hospitalized and tebipenem-pivoxil will be administered by clinic personnel, minimizing the risk of non-adherence. However, when tebipenem-pivoxil is self-administered outside of the trial of interest, non-adherence may be markedly higher for QID dosing compared to TID dosing. Thus, QID dosing may not produce as much additional treatment benefit as shown by our analyses, which assumed zero non-adherence. While providing critical PK information for efficacy predictions, our study findings should be considered with other influential factors for treatment outcomes to make the best dosing decision.

In conclusion, our study applied the available population demographic, *Shigella* spp. prevalence, *Shigella* MIC distribution, and ceftriaxone resistance data to simulate tebipenem PK and make trial outcome predictions specific to the target population. The workflow can be adapted to make similar predictions for other antimicrobials and in different disease areas. Moreover, our results demonstrate that a plethora of factors can influence trial outcomes and highlight the importance of having reliable estimates of these factors for making accurate and precise predictions. Lastly, this study's clinical trial outcome predictions contribute valuable information that should be considered along with clinical feasibility to inform study design and dosing strategy decisions.

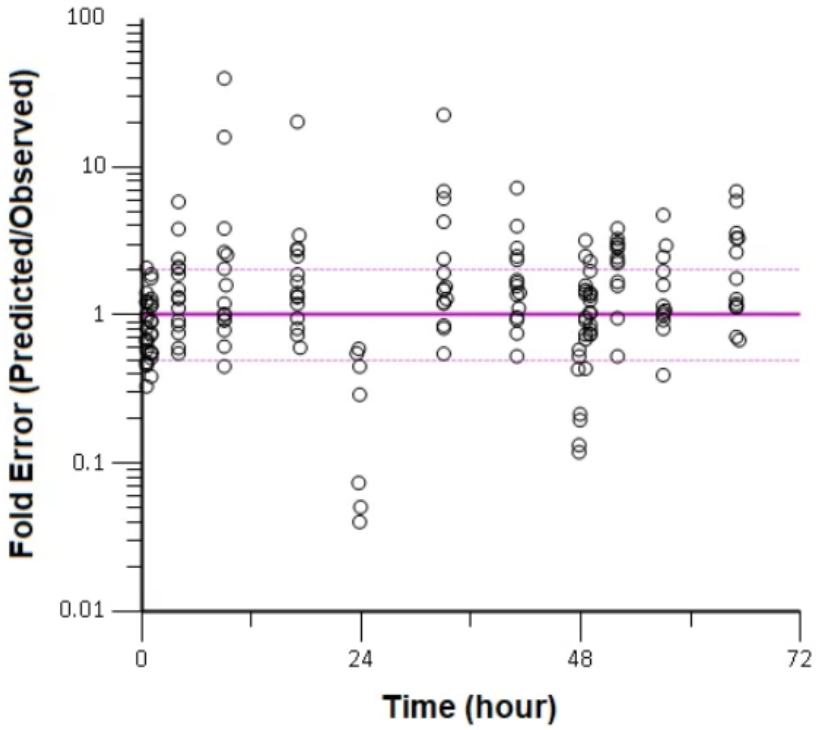

Figure 4.1. Fold error comparing individual predictions made using Sato et al.'s tebipenem population PK model[191] and the observed data.

Fold errors were calculated as the ratio of model-predicted tebipenem concentrations over the observed tebipenem concentrations at each respective time point. The observed data were collected from subjects receiving tebipenem-pivoxil in the pilot study (n=15). Dotted lines mark 2-fold difference between the predicted and observed concentrations.

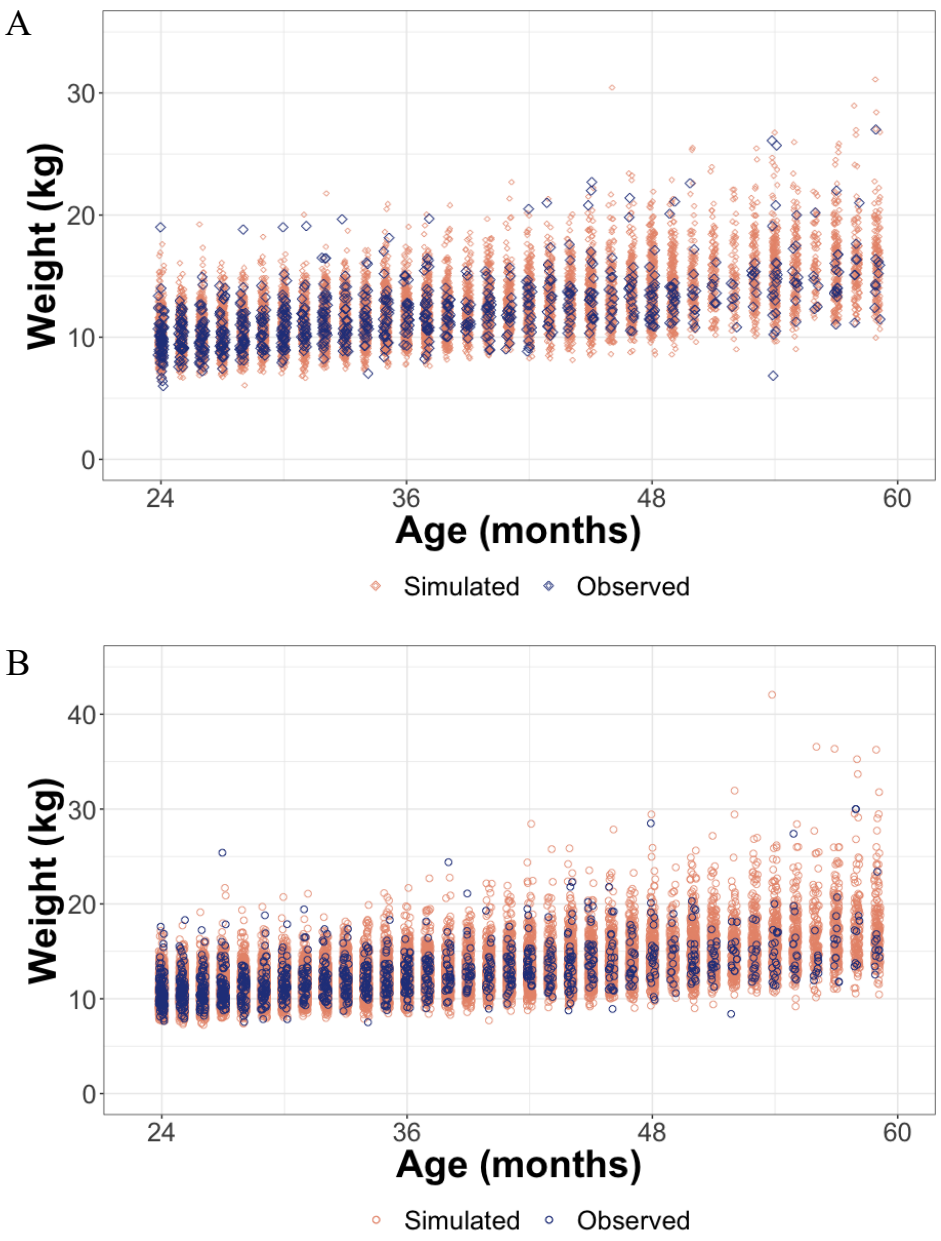

Figure 4.2. Weight versus age for (A) female and (B) male individuals between ages 24 and 59 months.

Orange circles represent virtual subjects and dark blue circles represent observed data from the screening data set.

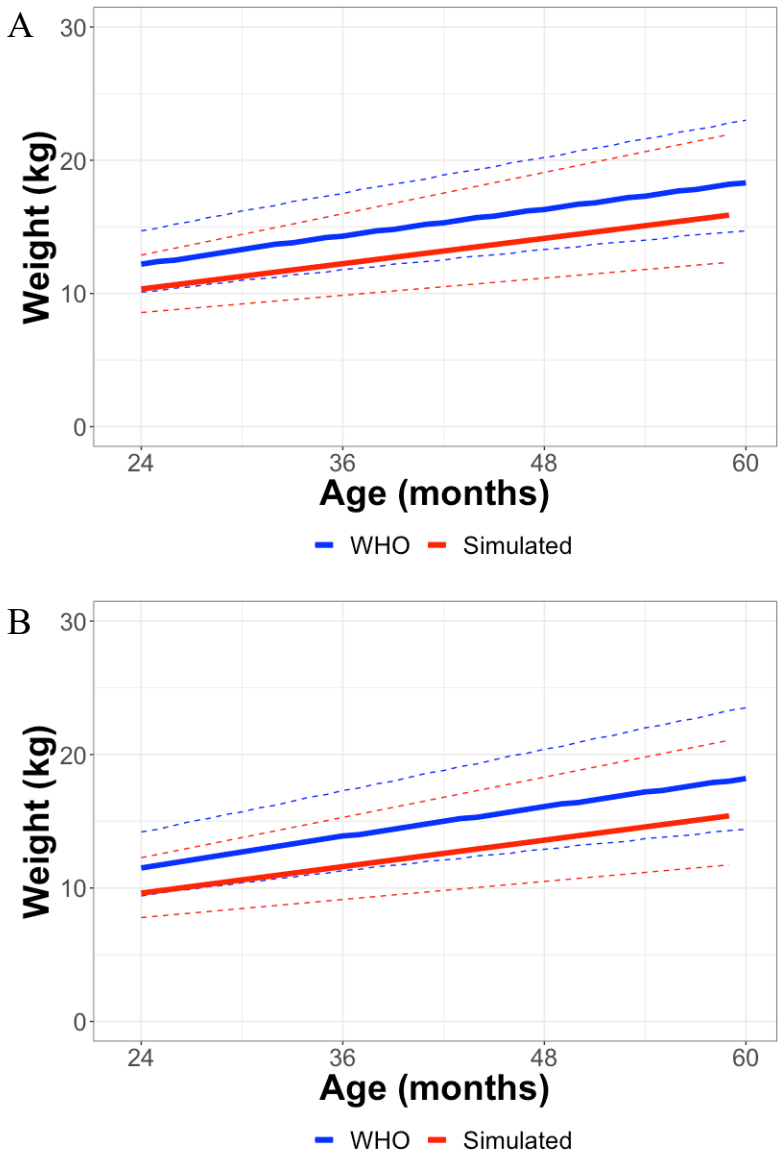

Figure 4.3. Comparison of the virtual target population and the WHO standards. Weight-for-age curves were plotted for (A) males and (B) females for the ages of two to five years. Solid lines represent the median based on the WHO standards (blue) or the simulated target population (red). Dashed lines represent the 5th and 95th percentiles of the WHO data (blue) or the simulated target population (red).

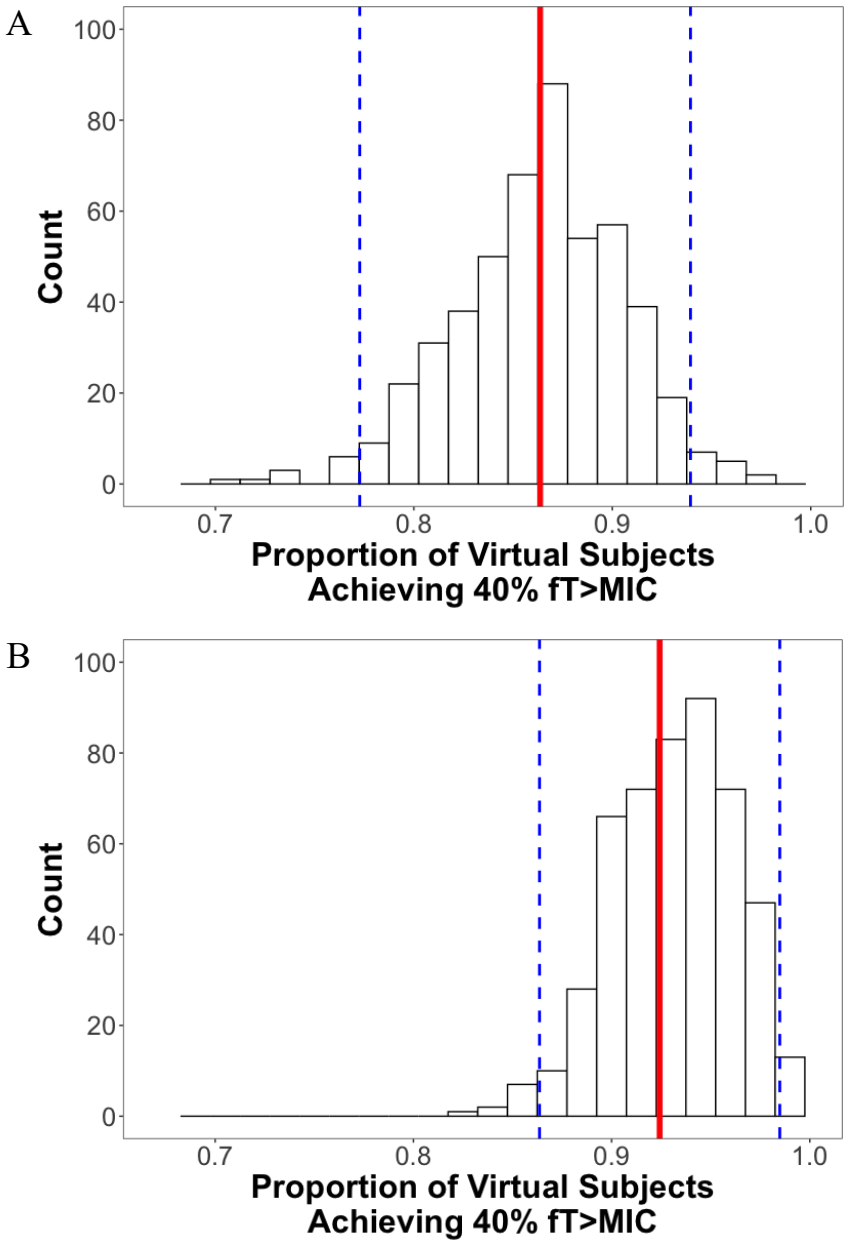

Figure 4.4. Proportion of subjects in a virtual trial achieving the target PK/PD metric of 40% *f*T>MIC.

The target PK/PD metric is defined as the unbound tebipenem plasma concentration being above the minimum inhibitory concentration for at least 40% of the 3-day treatment. Tebipenem-pivoxil doses used for simulation were (A) 4 mg/kg TID and (B) 3 mg/kg QID. A total of 500 virtual trials each containing 66 subjects were simulated for each dosing regimen. The red solid

line represents the median proportion of virtual subjects successfully meeting the target endpoint of 40% *f*T>MIC with each dosing regimen. Blue dashed lines mark the 95% confidence interval.

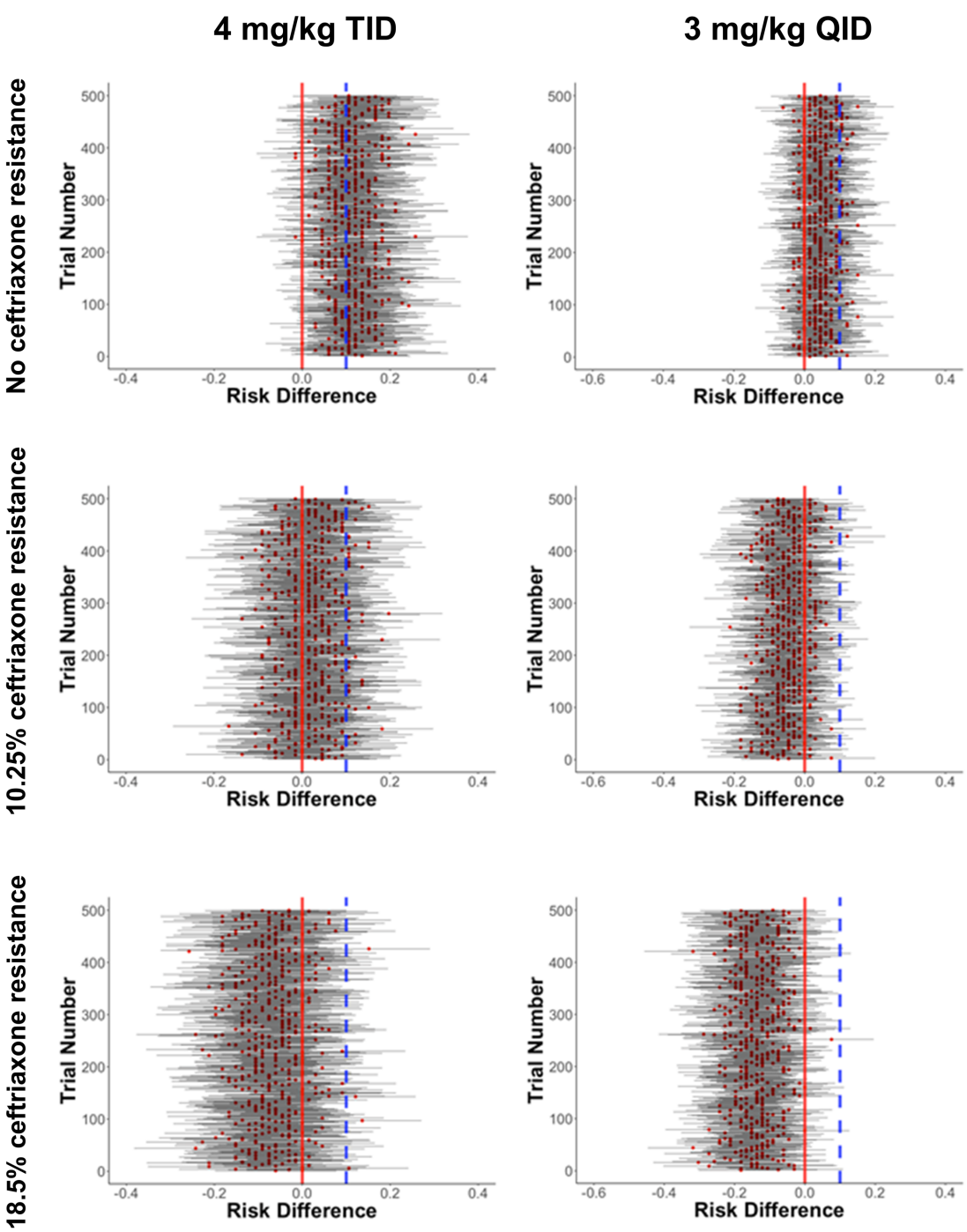

Figure 4.5. Risk difference between oral tebipenem-pivoxil treatment and IV ceftriaxone treatment.

The risk difference of clinical failure was computed as the risk of failure in the tebipenem arm – the risk of failure in the ceftriaxone arm. Results from 500 virtual trials each containing 66

subjects receiving oral tebipenem-pivoxil and 66 subjects receiving IV ceftriaxone are shown. Two tebipenem-pivoxil dosing regimens were simulated: 4 mg/kg TID and 3 mg/kg QID. Three ceftriaxone resistance levels were evaluated: no resistance, 10.25% resistance, and 18.5% resistance. Solid red circles represent risk difference estimates. Grey lines mark the 95% confidence intervals around the risk differences. Blue dashed lines represent the 10% non-inferiority margin.

Table 4.1. Comparison of demographic variables between the screening data set (n=2249) and the virtual population (n=33,000).

		Screening			Virtual Population		
		Mean	SD	Median	Mean	SD	Median
Age (m)	Female	36.27	9.66	34.0	36.35	9.65	34.0
	Male	35.58	9.38	34.0	35.60	9.37	34.0
Height (cm)	Female	91.68	7.68	91.3	91.71	7.70	91.04
	Male	92.66	7.33	92.0	92.66	7.35	92.09
Weight (kg)	Female	11.89	2.64	11.47	11.90	2.62	11.40
	Male	12.42	2.58	12.02	12.44	2.58	11.94
Sex	Female	910 (40.5%)			13111 (39.7%)		
	Male	1339 (59.5%)			19889 (60.3%)		
Total		2249			33000		

Table 4.2. Linear regression model parameters of demographic variables in the screening data set of pediatric patients.

Dependent Variable	**Explanatory Variable**	**Sex**	**Intercept**	**Regression Coefficient**	**p-value**	R-square
Height (cm)	Age (month)	Female	68.8	0.632	< 2.2e-16	0.629
		Male	70.7	0.616	< 2.2e-16	0.621
Transformed Weight	Height (cm)	Female	0.833	0.00564	< 2.2e-16	0.663
		Male	0.805	0.00231	< 2.2e-16	0.649

Table 4.3. Summary tebipenem PK parameters for the virtual target population containing 500 trials of 66 subjects each, following oral administration of 4 mg/kg tebipenem-pivoxil TID for three days.

	Mean	SD	Median
C_{max} (μg/mL)	3.46	2.34	2.80
$AUC_{0\text{-}72H}$ (μg*hr/mL)	52.98	19.37	50.44

Abbreviation: $AUC_{0\text{-}72H}$, area under the tebipenem concentration-time curve from 0 to 72 h post first dose; C_{max}, maximum plasma concentration of drug; SD, standard deviation.

Table 4.4. Probability for tebipenem-pivoxil treatment administered at 4 mg/kg TID to be non-inferior to IV ceftriaxone treatment, based on a non-inferiority margin of 10%.

Ceftriaxone Response Rate	Probability of Non-Inferiority	95% CI
97% (no resistance)	0.014	0.00680, 0.0286
87.1% (10.25% resistance)	0.262	0.225, 0.302
79.1% (18.5% resistance)	0.708	0.667, 0.746

Table 4.5. Probability for tebipenem-pivoxil treatment administered at 3 mg/kg QID to be non-inferior to ceftriaxone treatment, based on a non-inferiority margin of 10%.

Ceftriaxone Response Rate	Probability of Non-Inferiority	95% CI
97% (no resistance)	0.252	0.216, 0.292
87.1% (10.25% resistance)	0.822	0.786, 0.853
79.1% (18.5% resistance)	0.980	0.964, 0.989

Chapter 5. CONCLUSIONS

It is well-recognized that diarrhea can impact oral drug pharmacokinetics (PK) by altering physiological parameters critical to oral drug absorption, potentially accountable for suboptimal drug exposure and treatment failure in patients with diarrhea.[119] However, to the best of our knowledge, aside from speculations and observational findings, no one had quantitatively described the effect of diarrhea on oral drug absorption prior to our work presented in this dissertation. This knowledge gap creates several opportunities to impact the treatment of patients with diarrhea and the field of PK. First, it is difficult to evaluate or predict whether diarrhea symptoms would result in clinically significant consequences and whether dose adjustments must be made to achieve treatment efficacy. Secondly, without knowing the magnitude of the impact of diarrhea on oral drug PK, dose adjustment decisions would have to be made empirically and likely involve drug level and/or response monitoring, if feasible. Furthermore, characteristics of the patient population, such as age and body weight distribution, may be associated with varying degrees of diarrhea impact on oral drug PK. The unique pathophysiology of different types of diarrhea may also contribute to variability in the diarrhea impact. Lastly, because diarrheal diseases disproportionally impact populations living in low- and middle-income countries, who also heavily depend on oral treatments due to limitations in resources, the lack of understanding of how diarrhea impacts oral drug PK would likely have the most profound impact on the very populations that are already burdened with various other public health challenges. Hence, if unaddressed, the knowledge gap may perpetuate inequality in healthcare.

5.1 Estimation of Cryptosporidiosis-Associated Diarrhea Impact on Oral Clofazimine Bioavailability

The development and qualification of our population PK model of clofazimine demonstrated that relative oral bioavailability can be incorporated into a population PK model to evaluate the impact of various potential covariates on bioavailability. Importantly, the unique matched design employed by the clinical trial in HIV-infected adults with or without cryptosporidiosis and diarrhea, as described in Chapter 2, allowed the identification of a diarrhea-associated effect on clofazimine bioavailability among other causes.[79,84,127] The clofazimine population PK model we developed accurately captured the variability in observed clofazimine PK, describing the typical trend and the expected range of PK values for subjects with different diarrhea severity. Moreover, we quantified the effect of diarrhea on oral drug bioavailability by modeling the observed data. Our findings that mild and severe diarrhea during the study was associated with an over 6- and 22-fold reduction in clofazimine bioavailability effectively highlight the importance of studying diarrhea-associated effects on oral drug PK. With the level of reduction in oral clofazimine bioavailability we discovered, we demonstrated that diarrhea-associated effects on oral drug PK may be clinically significant and future research in this neglected area is warranted.

As a Biopharmaceutics Classification System (BCS) class II drug, clofazimine has high membrane permeability but is practically insoluble in water (water solubility = 0.225×10 mg/L; log P = 7.66).[209] Its bioavailability is solubility rate-limited. Hence, it is possible that physiological changes associated with diarrhea, such as a reduction in total gastrointestinal (GI) transit time, led to incomplete dissolution, causing a reduction in clofazimine bioavailability. Moreover, clofazimine is weakly basic and may be subject to reduced solubility associated with

elevated GI pH, another physiological change common to diarrheal diseases. Mechanistic modeling techniques, such as physiologically-based pharmacokinetic (PBPK) modeling, can be studied in the future to predict and compare the impact of these aforementioned diarrhea-induced physiological changes on clofazimine absorption. Furthermore, we hope that our findings presented in Chapter 2 will inspire future research into the effects of diarrhea on BCS class II drugs. This drug category, represented by clofazimine, may be particularly susceptible to PK changes when diarrhea is present.

5.2 Determination of the Reason Behind the Clofazimine Phase 2a Clinical Study Failure

Although we had demonstrated that oral clofazimine PK can be significantly influenced by diarrhea, we could not attribute the failure of the phase 2a trial on clofazimine treatment effect against cryptosporidiosis in HIV-infect adults[79] to diarrhea alone without additional studies. Using clofazimine PK and *Cryptosporidium* infection burden data collected from a dose-ranging mouse study, we built an E_{max} model that allowed us to predict a clofazimine concentration of 2,770 ng/mL, which we set as the efficacy target. Thereafter, comparisons between the observed clofazimine levels from the clinical trial and the predicted efficacy target showed that the observed levels were over 10-fold below levels associated with cryptosporidiosis treatment efficacy. Hence, we concluded that subtherapeutic clofazimine concentrations for cryptosporidiosis therapy were likely the cause of the trial failure. The prescribed doses of the trial were insufficient to produce any anti-*Cryptosporidium* treatment effect, even without the impact of diarrhea on bioavailability.

5.3 Prediction of Tebipenem PK and Treatment Effects in Bangladeshi Pediatric Patients with Shigellosis

Since the effect of diarrhea on oral drug PK is likely drug- and disease-specific, we studied a different diarrheal disease, shigellosis, and a different oral drug, tebipenem-pivoxil, in Chapter 4. By comparing PK predictions made using an existing tebipenem population PK model, which was built with data from Japanese pediatric patients without diarrheal diseases, we showed that the existing model could adequately capture tebipenem PK in our target Bangladeshi pediatric population with shigellosis. Interestingly, unlike clofazimine, tebipenem PK is not sensitive to diarrhea. This is likely because tebipenem bioavailability in our trial of interest was not limited by solubility. Tebipenem-pivoxil was given to pediatric patients as fine granules dissolved in distilled water, while clofazimine was administered to study participants in soft gelatin capsules. Consequently, tebipenem absorption would not be significantly affected by physiological changes that impact the dissolution process. Next, population PK simulations were performed using demographic characteristics unique to the target Bangladeshi pediatric population. By randomly generating distributions of tebipenem minimum inhibitory concentrations for different *Shigella* species and simulating three ceftriaxone resistance levels, we were able to make outcome predictions for an ongoing clinical trial with rising antimicrobial resistance taken into consideration. Additionally, we extended this modeling approach to compare how varying the tebipenem dosing frequency might affect trial success. With the work presented in Chapter 4, we set up a workflow that can be applied to making PK, efficacy, and dose predictions for other diseases and drugs.

5.4 CONCLUSION

In conclusion, this thesis dissertation shows that population PK and PK/PD modeling approaches can be used to estimate the impact of diarrhea on oral drug PK and predict the efficacy outcomes associated with different antimicrobial dosing regimens. The modeling approaches can offer valuable insights to guide dose selection/adjustment and clinical decisions, benefiting a significant number of individuals affected by diarrhea and its complications. Furthermore, the models presented in this dissertation are highly versatile. Unique characteristics of future target populations can be incorporated into our model framework to enhance the prediction accuracy. Antimicrobial resistance, which is dynamic and has geographic dependence, can be updated with the most up-to-date data to improve model predictive power and keep the results current. Finally, although the drugs studied in this dissertation are antimicrobials, our modeling approaches can be applied to other therapeutic classes, making them broadly applicable.

BIBLIOGRAPHY

1. Vinarov Z, Abdallah M, Agundez JAG, et al. Impact of gastrointestinal tract variability on oral drug absorption and pharmacokinetics: An UNGAP review. *European Journal of Pharmaceutical Sciences*. 2021;162:105812. doi:10.1016/j.ejps.2021.105812
2. Kostewicz ES, Aarons L, Bergstrand M, et al. PBPK models for the prediction of in vivo performance of oral dosage forms. *European Journal of Pharmaceutical Sciences*. 2014;57:300-321. doi:10.1016/j.ejps.2013.09.008
3. Jamei M, Turner D, Yang J, et al. Population-Based Mechanistic Prediction of Oral Drug Absorption. *AAPS J*. 2009;11(2):225-237. doi:10.1208/s12248-009-9099-y
4. Effinger A, O'Driscoll CM, McAllister M, Fotaki N. Impact of gastrointestinal disease states on oral drug absorption – implications for formulation design – a PEARRL review. *Journal of Pharmacy and Pharmacology*. 2019;71(4):674-698. doi:10.1111/jphp.12928
5. Abuhelwa AY, Williams DB, Upton RN, Foster DJR. Food, gastrointestinal pH, and models of oral drug absorption. *European Journal of Pharmaceutics and Biopharmaceutics*. 2017;112:234-248. doi:10.1016/j.ejpb.2016.11.034
6. Dattani S, Spooner F, Ritchie H, Roser M. Diarrheal Diseases. https://ourworldindata.org/diarrheal-diseases#:~:text=In%202019%20around%201.5%20million,than%20all%20violent%20deaths%20combined.&text=Around%20half%20a%20million%20of,result%20of%20public%20health%20interventions.
7. Troeger CE, Khalil IA, Blacker BF, et al. Quantifying risks and interventions that have affected the burden of diarrhoea among children younger than 5 years: an analysis of the Global Burden of Disease Study 2017. *Lancet Infect Dis*. 2020;20(1):37-59. doi:10.1016/S1473-3099(19)30401-3
8. Troeger C, Blacker BF, Khalil IA, et al. Estimates of the global, regional, and national morbidity, mortality, and aetiologies of diarrhoea in 195 countries: a systematic analysis for the Global Burden of Disease Study 2016. *Lancet Infect Dis*. 2018;18(11):1211-1228. doi:10.1016/S1473-3099(18)30362-1
9. Sweetser S. Evaluating the Patient With Diarrhea: A Case-Based Approach. *Mayo Clin Proc*. 2012;87(6):596-602. doi:10.1016/j.mayocp.2012.02.015
10. Whyte LA, Jenkins HR. Pathophysiology of diarrhoea. *Paediatr Child Health*. 2012;22(10):443-447. doi:10.1016/j.paed.2012.05.006
11. Saeid Seyedian S, Nokhostin F, Dargahi Malamir M. A review of the diagnosis, prevention, and treatment methods of inflammatory bowel disease. *J Med Life*. 2019;12(2):113-122. doi:10.25122/jml-2018-0075
12. Brunner E. Reaktionsgeschwindigkeit in heterogenen Systemen. *Zeitschrift für Physikalische Chemie*. 1904;47U(1):56-102. doi:10.1515/zpch-1904-4705
13. Nernst W. Theorie der Reaktionsgeschwindigkeit in heterogenen Systemen. *Zeitschrift für Physikalische Chemie*. 1904;47U(1):52-55. doi:10.1515/zpch-1904-4704
14. Wang J, Flanagan DR. General solution for diffusion-controlled dissolution of spherical particles. 1. Theory. *J Pharm Sci*. 1999;88(7):731-738. doi:10.1021/js980236p
15. Johnson KC. Dissolution and Absorption Modeling: Model Expansion to Simulate the Effects of Precipitation, Water Absorption, Longitudinally Changing Intestinal

Permeability, and Controlled Release on Drug Absorption. *Drug Dev Ind Pharm*. 2003;29(8):833-842. doi:10.1081/DDC-120024179
16. Dahlgren D, Roos C, Sjögren E, Lennernäs H. Direct In Vivo Human Intestinal Permeability (Peff) Determined with Different Clinical Perfusion and Intubation Methods. *J Pharm Sci*. 2015;104(9):2702-2726. doi:10.1002/jps.24258
17. Youhanna S, Lauschke VM. The Past, Present and Future of Intestinal In Vitro Cell Systems for Drug Absorption Studies. *J Pharm Sci*. 2021;110(1):50-65. doi:10.1016/j.xphs.2020.07.001
18. Arnold SLM, Isoherranen N. Role of Pharmacokinetics and Pharmacokinetic Modeling in Drug Development. In: *Comprehensive Pharmacology*. Elsevier; 2022:743-768. doi:10.1016/B978-0-12-820472-6.00066-9
19. Manallack DT. The pK(a) Distribution of Drugs: Application to Drug Discovery. *Perspect Medicin Chem*. 2007;1:25-38.
20. Charifson PS, Walters WP. Acidic and Basic Drugs in Medicinal Chemistry: A Perspective. *J Med Chem*. 2014;57(23):9701-9717. doi:10.1021/jm501000a
21. Gaohua L, Miao X, Dou L. Crosstalk of physiological pH and chemical pKa under the umbrella of physiologically based pharmacokinetic modeling of drug absorption, distribution, metabolism, excretion, and toxicity. *Expert Opin Drug Metab Toxicol*. 2021;17(9):1103-1124. doi:10.1080/17425255.2021.1951223
22. Brouwers J, Brewster ME, Augustijns P. Supersaturating Drug Delivery Systems: The Answer to Solubility-Limited Oral Bioavailability? *J Pharm Sci*. 2009;98(8):2549-2572. doi:10.1002/jps.21650
23. Press, Hauptmann, Hauptmann, et al. Gastrointestinal pH profiles in patients with inflammatory bowel disease. *Aliment Pharmacol Ther*. 1998;12(7):673-678. doi:10.1046/j.1365-2036.1998.00358.x
24. A. van Herwaarden MSAJ, M. 24-h Recording of Intragastric pH: Technical Aspects and Clinical Relevance. *Scand J Gastroenterol*. 1999;34(230):9-16. doi:10.1080/003655299750025219
25. Abuhelwa AY, Foster DJR, Upton RN. A Quantitative Review and Meta-Models of the Variability and Factors Affecting Oral Drug Absorption—Part I: Gastrointestinal pH. *AAPS J*. 2016;18(5):1309-1321. doi:10.1208/s12248-016-9952-8
26. Fadda HM, Hellström PM, Webb DL. Intra- and inter-subject variability in gastric pH following a low-fat, low-calorie meal. *Int J Pharm*. 2022;625:122069. doi:10.1016/j.ijpharm.2022.122069
27. Kletzl H, Giraudon M, Ducray PS, Abt M, Hamilton M, Lum BL. Effect of gastric pH on erlotinib pharmacokinetics in healthy individuals. *Anticancer Drugs*. 2015;26(5):565-572. doi:10.1097/CAD.0000000000000212
28. Srinivas N. Antacid Use and Reduced Bioavailability of Oral Drugs. *Arzneimittelforschung*. 2011;59(07):327-334. doi:10.1055/s-0031-1296404
29. Lohitnavy M, Lohitnavy O, Thangkeattiyanon O, Srichai W. Reduced oral itraconazole bioavailability by antacid suspension. *J Clin Pharm Ther*. 2005;30(3):201-206. doi:10.1111/j.1365-2710.2005.00632.x
30. Kelly P, Shawa T, Mwanamakondo S, et al. Gastric and intestinal barrier impairment in tropical enteropathy and HIV: limited impact of micronutrient supplementation during a randomised controlled trial. *BMC Gastroenterol*. 2010;10:72. doi:10.1186/1471-230X-10-72

31. Geraghty J, Thumbs A, Kankwatira A, et al. Helicobacter pylori, HIV and Gastric Hypochlorhydria in the Malawian Population. *PLoS One*. 2015;10(8):e0132043. doi:10.1371/journal.pone.0132043
32. Camilleri M. Bile Acid Diarrhea: Prevalence, Pathogenesis, and Therapy. *Gut Liver*. 2015;9(3). doi:10.5009/gnl14397
33. Farrugia A, Arasaradnam R. Bile acid diarrhoea: pathophysiology, diagnosis and management. *Frontline Gastroenterol*. 2021;12(6):500-507. doi:10.1136/flgastro-2020-101436
34. Walters JRF, Pattni SS. Managing bile acid diarrhoea. *Therap Adv Gastroenterol*. 2010;3(6):349-357. doi:10.1177/1756283X10377126
35. Karlstrom L, Cassuto J, Jodal M, Lundgren O. Involvement of the Enteric Nervous System in the Intestinal Secretion Induced by Sodium Deoxycholate and Sodium Ricinoleate. *Scand J Gastroenterol*. 1986;21(3):331-340. doi:10.3109/00365528609003083
36. Kidd M, Modlin IM, Gustafsson BI, Drozdov I, Hauso O, Pfragner R. Luminal regulation of normal and neoplastic human EC cell serotonin release is mediated by bile salts, amines, tastants, and olfactants. *American Journal of Physiology-Gastrointestinal and Liver Physiology*. 2008;295(2):G260-G272. doi:10.1152/ajpgi.00056.2008
37. Bajor A, Gillberg PG, Abrahamsson H. Bile acids: short and long term effects in the intestine. *Scand J Gastroenterol*. 2010;45(6):645-664. doi:10.3109/00365521003702734
38. Yan W, Sundaram U. Chronic Diarrhea, Malabsorption, Villous Blunting, and Microscopy Colitis due to Common Variable Immunodeficiency Syndrome. *American Journal of Gastroenterology*. 2013;108:S287. doi:10.14309/00000434-201310001-00960
39. Uzzan M, Ko HM, Mehandru S, Cunningham-Rundles C. Gastrointestinal Disorders Associated with Common Variable Immune Deficiency (CVID) and Chronic Granulomatous Disease (CGD). *Curr Gastroenterol Rep*. 2016;18(4):17. doi:10.1007/s11894-016-0491-3
40. Sakai E, Higurashi T, Ohkubo H, et al. Investigation of Small Bowel Abnormalities in HIV-Infected Patients Using Capsule Endoscopy. *Gastroenterol Res Pract*. 2017;2017:1-7. doi:10.1155/2017/1932647
41. Batman PA, Kotler DP, Kapembwa MS, et al. HIV enteropathy: crypt stem and transit cell hyperproliferation induces villous atrophy in HIV/Microsporidia-infected jejunal mucosa. *AIDS*. 2007;21(4):433-439. doi:10.1097/QAD.0b013e3280142ee8
42. Vyhlidal CA, Chapron BD, Ahmed A, Singh V, Casini R, Shakhnovich V. Effect of Crohn's Disease on Villous Length and CYP3A4 Expression in the Pediatric Small Intestine. *Clin Transl Sci*. 2021;14(2):729-736. doi:10.1111/cts.12938
43. Schulzke JD, Bentzel CJ, Schulzke I, Riecken EO, Fromm M. Epithelial Tight Junction Structure in the Jejunum of Children with Acute and Treated Celiac Sprue. *Pediatr Res*. 1998;43(4):435-441. doi:10.1203/00006450-199804000-00001
44. Schumann M, Günzel D, Buergel N, et al. Cell polarity-determining proteins Par-3 and PP-1 are involved in epithelial tight junction defects in coeliac disease. *Gut*. 2012;61(2):220-228. doi:10.1136/gutjnl-2011-300123
45. Schulzke JD, Schulzke I, Fromm M, Riecken EO. Epithelial barrier and ion transport in coeliac sprue: electrical measurements on intestinal aspiration biopsy specimens. *Gut*. 1995;37(6):777-782. doi:10.1136/gut.37.6.777

46. Vanuytsel T, Tack J, Farre R. The Role of Intestinal Permeability in Gastrointestinal Disorders and Current Methods of Evaluation. *Front Nutr*. 2021;8. doi:10.3389/fnut.2021.717925
47. Davis SS, Hardy JG, Fara JW. Transit of pharmaceutical dosage forms through the small intestine. *Gut*. 1986;27(8):886-892. doi:10.1136/gut.27.8.886
48. Grybäck P, Hermansson G, Lyrenäs E, Beckman KW, Jacobsson H, Hellström PM. Nationwide standardisation and evaluation of scintigraphic gastric emptying: reference values and comparisons between subgroups in a multicentre trial. *Eur J Nucl Med Mol Imaging*. 2000;27(6):647-655. doi:10.1007/s002590050558
49. Gajendran M, Loganathan P, Jimenez G, et al. A comprehensive review and update on ulcerative colitis,. *Disease-a-Month*. 2019;65(12):100851. doi:10.1016/j.disamonth.2019.02.004
50. Haase AM, Gregersen T, Christensen LA, et al. Regional gastrointestinal transit times in severe ulcerative colitis. *Neurogastroenterology & Motility*. 2016;28(2):217-224. doi:10.1111/nmo.12713
51. Nugent SG, Rampton DS, Kumar D, Yazaki E, Evans DF. Gut pH and transit time in ulcerative colitis appear sufficient for complete dissolution of pH-dependent 5-ASA-containing capsules. *Digestive and Liver Disease*. 2000;32:A45. doi:10.1016/S1590-8658(00)80222-4
52. Rao SSC, Read NW. Gastrointestinal Motility in Patients with Ulcerative Colitis. *Scand J Gastroenterol*. 1990;25(sup172):22-28. doi:10.3109/00365529009091905
53. Rana S V., Sharma S, Malik A, et al. Small Intestinal Bacterial Overgrowth and Orocecal Transit Time in Patients of Inflammatory Bowel Disease. *Dig Dis Sci*. 2013;58(9):2594-2598. doi:10.1007/s10620-013-2694-x
54. Fischer M, Siva S, Wo JM, Fadda HM. Assessment of Small Intestinal Transit Times in Ulcerative Colitis and Crohn's Disease Patients with Different Disease Activity Using Video Capsule Endoscopy. *AAPS PharmSciTech*. 2017;18(2):404-409. doi:10.1208/s12249-016-0521-3
55. Hardy J, Davis S, Khosla R, Robertson C. Gastrointestinal transit of small tablets in patients with ulcerative colitis. *Int J Pharm*. 1988;48(1-3):79-82. doi:10.1016/0378-5173(88)90249-9
56. Fireman Z, Kopelman Y, Friedman S, et al. Age and Indication for Referral to Capsule Endoscopy Significantly Affect Small Bowel Transit Times: The Given Database. *Dig Dis Sci*. 2007;52(10):2884-2887. doi:10.1007/s10620-007-9789-1
57. Sharpstone D, Neild P, Crane R, et al. Small intestinal transit, absorption, and permeability in patients with AIDS with and without diarrhoea. *Gut*. 1999;45(1):70-76. doi:10.1136/gut.45.1.70
58. Densupsoontorn N, Issaragraiseel P, Thamonsiri N, Wongarn R, Jirapinyo P. Whole gastrointestinal transit time is associated with clinical severity and nutritional status of HIV-infected children. *J Med Assoc Thai*. 2009;92(7):914-919.
59. Johansson ME V., Sjövall H, Hansson GC. The gastrointestinal mucus system in health and disease. *Nat Rev Gastroenterol Hepatol*. 2013;10(6):352-361. doi:10.1038/nrgastro.2013.35
60. Love AH. Water and sodium absorption by the intestine in cholera. *Gut*. 1969;10(1):63-67. doi:10.1136/gut.10.1.63

61. Lee JS, Silverberg JW. Effect of Cholera Toxin on Fluid Absorption and Villus Lymph Pressure in Dog Jejunal Mucosa. *Gastroenterology*. 1972;62(5):993-1000. doi:10.1016/S0016-5085(72)80116-1
62. Englund G, Jacobson A, Rorsman F, Artursson P, Kindmark A, Rönnblom A. Efflux transporters in ulcerative colitis. *Inflamm Bowel Dis*. 2007;13(3):291-297. doi:10.1002/ibd.20030
63. Blokzijl H, Borght S Vander, Bok LIH, et al. Decreased P-glycoprotein (P-gp/MDR1) expression in inflamed human intestinal epithelium is independent of PXR protein levels. *Inflamm Bowel Dis*. 2007;13(6):710-720. doi:10.1002/ibd.20088
64. Wilson A, Tirona RG, Kim RB. CYP3A4 Activity is Markedly Lower in Patients with Crohn's Disease. *Inflamm Bowel Dis*. 2017;23(5):804-813. doi:10.1097/MIB.0000000000001062
65. Wilson A, Urquhart BL, Ponich T, et al. Crohn's Disease Is Associated with Decreased CYP3A4 and P-Glycoprotein Protein Expression. *Mol Pharm*. 2019;16(9):4059-4064. doi:10.1021/acs.molpharmaceut.9b00459
66. Alrubia S, Al-Majdoub ZM, Achour B, Rostami-Hodjegan A, Barber J. Quantitative Assessment of the Impact of Crohn's Disease on Protein Abundance of Human Intestinal Drug-Metabolising Enzymes and Transporters. *J Pharm Sci*. 2022;111(10):2917-2929. doi:10.1016/j.xphs.2022.07.012
67. Plewka D, Plewka A, Szczepanik T, et al. Expression of selected cytochrome P450 isoforms and of cooperating enzymes in colorectal tissues in selected pathological conditions. *Pathol Res Pract*. 2014;210(4):242-249. doi:10.1016/j.prp.2013.12.010
68. Morón B, Verma AK, Das P, et al. CYP3A4-Catalyzed Simvastatin Metabolism as a Non-Invasive Marker of Small Intestinal Health in Celiac Disease. *American Journal of Gastroenterology*. 2013;108(8):1344-1351. doi:10.1038/ajg.2013.151
69. Brantley RK, Williams KR, Silva TMJ, et al. AIDS-associated diarrhea and wasting in northeast Brazil is associated with subtherapeutic plasma levels of antiretroviral medications and with both bovine and human subtypes of Cryptosporidium parvum. *Brazilian Journal of Infectious Diseases*. 2003;7(1). doi:10.1590/S1413-86702003000100003
70. Bushen OY, Davenport JA, Lima AB, et al. Diarrhea and Reduced Levels of Antiretroviral Drugs: Improvement with Glutamine or Alanyl-Glutamine in a Randomized Controlled Trial in Northeast Brazil. *Clinical Infectious Diseases*. 2004;38(12):1764-1770. doi:10.1086/421394
71. Macnab KA, Gill MJ, Sutherland LR, De Boer Visser N, Church D. Erratic zidovudine bioavailability in HIV seropositive patients. *J Antimicrob Chemother*. 1993;31(3):421-428. doi:10.1093/jac/31.3.421
72. Zorza G, Beaugerie L, Taburet AM, Le Quintrec Y, Singlas E. Absorption of zidovudine in patients with diarrhoea. *Eur J Clin Pharmacol*. 1993;44(5):501-503. doi:10.1007/BF00315553
73. Macnab KA, Gill MJ, Sutherland LR, Brant R. Zidovudine absorption and small intestinal function in HIV seropositive patients. *Journal of Antimicrobial Chemotherapy*. 1996;37(4):825-829. doi:10.1093/jac/37.4.825
74. Knox TA, Spiegelman D, Skinner SC, Gorbach S. Diarrhea and Abnormalities of Gastrointestinal Function in A Cohort of Men and Women With Hiv Infection. *American*

Journal of Gastroenterology. 2000;95(12):3482-3489. doi:10.1111/j.1572-0241.2000.03365.x
75. MacArthur RD, DuPont HL. Etiology and pharmacologic management of noninfectious diarrhea in HIV-infected individuals in the highly active antiretroviral therapy era. *Clin Infect Dis*. 2012;55(6):860-867. doi:10.1093/cid/cis544
76. Moreira Júnior ED, Silva N, Brites C, et al. Characteristics of the acquired immunodeficiency syndrome in Brazil. *Am J Trop Med Hyg*. 1993;48(5):687-692. doi:10.4269/ajtmh.1993.48.687
77. Colebunders R, Francis H, Mann JM, et al. Persistent diarrhea, strongly associated with HIV infection in Kinshasa, Zaire. *Am J Gastroenterol*. 1987;82(9):859-864.
78. Kumar A, Kochhar S, Ings R, et al. Pharmacokinetics and tolerability of iOWH032, an inhibitor of the cystic fibrosis transmembrane conductance regulator (CFTR) chloride channel, in normal volunteers and cholera patients. *www.path.org*. Published online April 2014.
79. Iroh Tam P, Arnold SLM, Barrett LK, et al. Clofazimine for Treatment of Cryptosporidiosis in Human Immunodeficiency Virus Infected Adults: An Experimental Medicine, Randomized, Double-blind, Placebo-controlled Phase 2a Trial. *Clinical Infectious Diseases*. 2021;73(2):183-191. doi:10.1093/cid/ciaa421
80. Dillingham RA, Lima AA, Guerrant RL. Cryptosporidiosis: epidemiology and impact. *Microbes Infect*. 2002;4(10):1059-1066. doi:10.1016/S1286-4579(02)01630-1
81. Checkley W, Epstein LD, Gilman RH, Black RE, Cabrera L, Sterling CR. Effects of Cryptosporidium parvum Infection in Peruvian Children: Growth Faltering and Subsequent Catch-up Growth. *Am J Epidemiol*. 1998;148(5):497-506. doi:10.1093/oxfordjournals.aje.a009675
82. Abubakar I, Aliyu SH, Arumugam C, Usman NK, Hunter PR. Treatment of cryptosporidiosis in immunocompromised individuals: systematic review and meta-analysis. *Br J Clin Pharmacol*. 2007;63(4):387-393. doi:10.1111/j.1365-2125.2007.02873.x
83. Mould D, Upton R. Basic Concepts in Population Modeling, Simulation, and Model-Based Drug Development—Part 2: Introduction to Pharmacokinetic Modeling Methods. *CPT Pharmacometrics Syst Pharmacol*. 2013;2(4):1-14. doi:10.1038/psp.2013.14
84. Zhang CX, Conrad TM, Hermann D, et al. Clofazimine pharmacokinetics in HIV-infected adults with diarrhea: Implications of diarrheal disease on absorption of orally administered therapeutics. *CPT Pharmacometrics Syst Pharmacol*. Published online January 2, 2024. doi:10.1002/psp4.13092
85. Derendorf H, Meibohm B. Modeling of Pharmacokinetic/Pharmacodynamic (PK/PD) Relationships: Concepts and Perspectives. *Pharm Res*. 1999;16(2):176-185. doi:10.1023/A:1011907920641
86. Upton R, Mould D. Basic Concepts in Population Modeling, Simulation, and Model-Based Drug Development: Part 3—Introduction to Pharmacodynamic Modeling Methods. *CPT Pharmacometrics Syst Pharmacol*. 2014;3(1):1-16. doi:10.1038/psp.2013.71
87. Meibohm B, Derendorf H. Basic concepts of pharmacokinetic/pharmacodynamic (PK/PD) modelling. *Int J Clin Pharmacol Ther*. 1997;35(10):401-413.
88. Rajman I. PK/PD modelling and simulations: utility in drug development. *Drug Discov Today*. 2008;13(7-8):341-346. doi:10.1016/j.drudis.2008.01.003

89. Zhang CX, Love MS, McNamara CW, et al. Pharmacokinetics and Pharmacodynamics of Clofazimine for Treatment of Cryptosporidiosis. *Antimicrob Agents Chemother*. 2022;66(1). doi:10.1128/AAC.01560-21
90. Ranjbar R, Farahani A. Shigella: Antibiotic-Resistance Mechanisms And New Horizons For Treatment. *Infect Drug Resist*. 2019;Volume 12:3137-3167. doi:10.2147/IDR.S219755
91. Puzari M, Sharma M, Chetia P. Emergence of antibiotic resistant Shigella species: A matter of concern. *J Infect Public Health*. 2018;11(4):451-454. doi:10.1016/j.jiph.2017.09.025
92. Fallingborg J, Christensen LA, Jacobsen BA, Rasmussen SN. Very low intraluminal colonic pH in patients with active ulcerative colitis. *Dig Dis Sci*. 1993;38(11):1989-1993. doi:10.1007/BF01297074
93. Ewe K, Schwartz S, Petersen S, Press AG. Inflammation does not decrease intraluminal pH in chronic inflammatory bowel disease. *Dig Dis Sci*. 1999;44(7):1434-1439. doi:10.1023/A:1026664105112
94. Resnick RH, Royal H, Marshall W, Barron R, Werth T. Intestinal permeability in gastrointestinal disorders. *Dig Dis Sci*. 1990;35(2):205-211. doi:10.1007/BF01536764
95. Caviglia GP, Dughera F, Ribaldone DG, et al. Serum zonulin in patients with inflammatory bowel disease: a pilot study. *Minerva Med*. 2019;110(2). doi:10.23736/S0026-4806.18.05787-7
96. Fallingborg J, Pedersen P, Jacobsen BA. Small Intestinal Transit Time and Intraluminal pH in Ileocecal Resected Patients with Crohn's Disease. *Dig Dis Sci*. 1998;43(4):702-705. doi:10.1023/A:1018893409596
97. Jenkins RT, Ramage JK, Jones DB, Collins SM, Goodacre RL, Hunt RH. Small bowel and colonic permeability to 51Cr-EDTA in patients with active inflammatory bowel disease. *Clin Invest Med*. 1988;11(2):151-155.
98. Wyatt J, Oberhuber G, Pongratz S, et al. Increased gastric and intestinal permeability in patients with Crohn's disease. *Am J Gastroenterol*. 1997;92(10):1891-1896.
99. Holt S, Heading RC, Clements JA, Tothill P, Prescott LF. Acetaminophen absorption and metabolism in celiac disease and Crohn's disease. *Clin Pharmacol Ther*. 1981;30(2):232-238. doi:10.1038/clpt.1981.153
100. Tursi A, Brandimarte G, Giorgetti G, Nasi G. Assessment of orocaecal transit time in different localization of Crohn's disease and its possible influence on clinical response to therapy. *Eur J Gastroenterol Hepatol*. 2003;15(1):69-74. doi:10.1097/00042737-200301000-00012
101. Castiglione F, Del Vecchio Blanco G, Rispo A, et al. Orocecal Transit Time and Bacterial Overgrowth in Patients with Crohn's Disease. *J Clin Gastroenterol*. 2000;31(1):63-66. doi:10.1097/00004836-200007000-00015
102. Edsbäcker S, Bengtsson B, Larsson P, et al. A pharmacoscintigraphic evaluation of oral budesonide given as controlled-release (Entocort) capsules. *Aliment Pharmacol Ther*. 2003;17(4):525-536. doi:10.1046/j.1365-2036.2003.01426.x
103. Niv E, Fishman S, Kachman H, Arnon R, Dotan I. Sequential capsule endoscopy of the small bowel for follow-up of patients with known Crohn's disease. *J Crohns Colitis*. 2014;8(12):1616-1623. doi:10.1016/j.crohns.2014.03.003

104. Nóbrega ACM, Ferreira BRS, Oliveira GJ, et al. Dyspeptic symptoms and delayed gastric emptying of solids in patients with inactive Crohn's disease. *BMC Gastroenterol*. 2012;12(1):175. doi:10.1186/1471-230X-12-175
105. Kitis G, Lucas ML, Bishop H, et al. Altered Jejunal Surface pH in Coeliac Disease: Its Effect on Propranolol and Folic Acid Absorption. *Clin Sci*. 1982;63(4):373-380. doi:10.1042/cs0630373
106. Lebwohl B, Murray JA, Rubio-Tapia A, Green PHR, Ludvigsson JF. Predictors of persistent villous atrophy in coeliac disease: a population-based study. *Aliment Pharmacol Ther*. 2014;39(5):488-495. doi:10.1111/apt.12621
107. Urgesi R, Cianci R, Bizzotto A, Costamagna G, Riccioni ME. Evaluation of gastric and small bowel transit times in coeliac disease with the small bowel PillCam®: a single centre study in a non gluten-free diet adult Italian population with coeliac disease. *Eur Rev Med Pharmacol Sci*. 2013;17(9):1167-1173.
108. Chiarioni G, Bassotti G, Germani U, et al. Gluten-free diet normalizes mouth-to-cecum transit of a caloric meal in adult patients with celiac disease. *Dig Dis Sci*. 1997;42(10):2100-2105. doi:10.1023/a:1018878703699
109. Dunmire CN, Chac D, Chowdhury F, et al. Vibrio cholerae Isolation from Frozen Vomitus and Stool Samples. *J Clin Microbiol*. 2022;60(10). doi:10.1128/jcm.01084-22
110. Magnusson KE, KihlstrÃ¶m E, Sundqvist T. Effect of cholera toxin on rat intestinal permeability assessed with fluorescent dextran 3000. *FEMS Microbiol Lett*. 1985;29(1-2):15-18. doi:10.1111/j.1574-6968.1985.tb00827.x
111. Molla A, Molla AM, Sarker SA, Khatun M. Whole-Gut Transit Time and Its Relationship to Absorption of Macronutrients during Diarrhoea and after Recovery. *Scand J Gastroenterol*. 1983;18(4):537-543. doi:10.3109/00365528309181634
112. Lippi D, Gotuzzo E, Caini S. Cholera. *Microbiol Spectr*. 2016;4(4). doi:10.1128/microbiolspec.PoH-0012-2015
113. Sack DA, Sack RB, Nair GB, Siddique A. Cholera. *The Lancet*. 2004;363(9404):223-233. doi:10.1016/S0140-6736(03)15328-7
114. Welage LS, Carver PL, Revankar S, Pierson C, Kauffman CA. Alterations in Gastric Acidity in Patients Infected with Human Immunodeficiency Virus. *Clinical Infectious Diseases*. 1995;21(6):1431-1438. doi:10.1093/clinids/21.6.1431
115. Conlon CP, Pinching AJ, Perera CU, Moody A, Luo NP, Lucas SB. HIV-related enteropathy in Zambia: a clinical, microbiological, and histological study. *Am J Trop Med Hyg*. 1990;42(1):83-88. doi:10.4269/ajtmh.1990.42.83
116. Murphy B, Taylor C, Crane R, Okong P, Bjarnason I. Comparison of intestinal function in human immunodeficiency virus-seropositive patients in Kampala and London. *Scand J Gastroenterol*. 1999;34(5):491-495. doi:10.1080/003655299750026227
117. Konturek JW, Fischer H, Van Der Voort IR, Domschke W. Disturbed Gastric Motor Activity in Patients with Human Immunodeficiency Virus Infection. *Scand J Gastroenterol*. 1997;32(3):221-225. doi:10.3109/00365529709000198
118. Effinger A, O'Driscoll CM, McAllister M, Fotaki N. Impact of gastrointestinal disease states on oral drug absorption – implications for formulation design – a PEARRL review. *Journal of Pharmacy and Pharmacology*. 2019;71(4):674-698. doi:10.1111/jphp.12928
119. Zhang CX, Arnold SLM. Potential and Challenges in Application of Physiologically Based Pharmacokinetic Modeling in Predicting Diarrheal Disease Impact on Oral Drug

Pharmacokinetics. *Drug Metabolism and Disposition*. Published online September 15, 2023:DMD-MR-2022-000964. doi:10.1124/dmd.122.000964
120. Chigutsa E, Kambhampati SRP, Karen Sykes A, Posada MM, Walt J, Turner PK. Development and Application of a Mechanistic Population Modeling Approach to Describe Abemaciclib Pharmacokinetics. *CPT Pharmacometrics Syst Pharmacol*. 2020;9(9):523-533. doi:10.1002/psp4.12544
121. Leitch GJ, He Q. Cryptosporidiosis-an overview. *J Biomed Res*. 2012;25(1):1-16. doi:10.1016/S1674-8301(11)60001-8
122. Gerace E, Lo Presti VDM, Biondo C. Cryptosporidium Infection: Epidemiology, Pathogenesis, and Differential Diagnosis. *Eur J Microbiol Immunol (Bp)*. 2019;9(4):119-123. doi:10.1556/1886.2019.00019
123. Hunter PR, Nichols G. Epidemiology and clinical features of Cryptosporidium infection in immunocompromised patients. *Clin Microbiol Rev*. 2002;15(1):145-154. doi:10.1128/CMR.15.1.145-154.2002
124. Khalil IA, Troeger C, Rao PC, et al. Morbidity, mortality, and long-term consequences associated with diarrhoea from Cryptosporidium infection in children younger than 5 years: a meta-analyses study. *Lancet Glob Health*. 2018;6(7):e758-e768. doi:10.1016/S2214-109X(18)30283-3
125. Love MS, Beasley FC, Jumani RS, et al. A high-throughput phenotypic screen identifies clofazimine as a potential treatment for cryptosporidiosis. *PLoS Negl Trop Dis*. 2017;11(2):e0005373. doi:10.1371/journal.pntd.0005373
126. Esmat M, Abdel-Aal AA, Shalaby MA, et al. Efficacy of clofazimine and nitazoxanide combination in treating intestinal cryptosporidiosis and enhancing intestinal cellular regeneration in immunocompromised mice. *Food Waterborne Parasitol*. 2022;27:e00161. doi:10.1016/j.fawpar.2022.e00161
127. Nachipo P, Hermann D, Quinnan G, Gordon MA, Van Voorhis WC, Iroh Tam PY. Evaluating the safety, tolerability, pharmacokinetics and efficacy of clofazimine in cryptosporidiosis (CRYPTOFAZ): study protocol for a randomized controlled trial. *Trials*. 2018;19(1):456. doi:10.1186/s13063-018-2846-6
128. Swanson R V., Adamson J, Moodley C, et al. Pharmacokinetics and Pharmacodynamics of Clofazimine in a Mouse Model of Tuberculosis. *Antimicrob Agents Chemother*. 2015;59(6):3042-3051. doi:10.1128/AAC.00260-15
129. Schaad-Lanyi Z, Dieterle W, Dubois JP, Theobald W, Vischer W. Pharmacokinetics of clofazimine in healthy volunteers. *Int J Lepr Other Mycobact Dis*. 1987;55(1):9-15.
130. Holdiness MR. Clinical pharmacokinetics of clofazimine. A review. *Clin Pharmacokinet*. 1989;16(2):74-85. doi:10.2165/00003088-198916020-00002
131. Abdelwahab MT, Wasserman S, Brust JCM, et al. Clofazimine pharmacokinetics in patients with TB: dosing implications. *Journal of Antimicrobial Chemotherapy*. 2020;75(11):3269-3277. doi:10.1093/jac/dkaa310
132. Nix DE, Adam RD, Auclair B, Krueger TS, Godo PG, Peloquin CA. Pharmacokinetics and relative bioavailability of clofazimine in relation to food, orange juice and antacid. *Tuberculosis*. 2004;84(6):365-373. doi:10.1016/j.tube.2004.04.001
133. Faraj A, Svensson RJ, Diacon AH, Simonsson USH. Drug Effect of Clofazimine on Persisters Explains an Unexpected Increase in Bacterial Load in Patients. *Antimicrob Agents Chemother*. 2020;64(5). doi:10.1128/AAC.01905-19

134. Lee JS, Silverberg JW. Effect of Cholera Toxin on Fluid Absorption and Villus Lymph Pressure in Dog Jejunal Mucosa. *Gastroenterology*. 1972;62(5):993-1000. doi:10.1016/S0016-5085(72)80116-1
135. Amadi B, Kelly P, Mwiya M, et al. Intestinal and Systemic Infection, HIV, and Mortality in Zambian Children With Persistent Diarrhea and Malnutrition. *J Pediatr Gastroenterol Nutr*. 2001;32(5):550-554. doi:10.1097/00005176-200105000-00011
136. Mor SM, Tzipori S. Cryptosporidiosis in Children in Sub-Saharan Africa: A Lingering Challenge. *Clinical Infectious Diseases*. 2008;47(7):915-921. doi:10.1086/591539
137. Khalil IA, Troeger C, Rao PC, et al. Morbidity, mortality, and long-term consequences associated with diarrhoea from Cryptosporidium infection in children younger than 5 years: a meta-analyses study. *Lancet Glob Health*. 2018;6(7):e758-e768. doi:10.1016/S2214-109X(18)30283-3
138. Lima AA, Guerrant DI, Patrick PD, Schorling JB, Moore SR, Guerrant RL. Association of early childhood diarrhea and cryptosporidiosis with impaired physical fitness and cognitive function four-seven years later in a poor urban community in northeast Brazil. *Am J Trop Med Hyg*. 1999;61(5):707-713. doi:10.4269/ajtmh.1999.61.707
139. Mølbak K, Andersen M, Aaby P, et al. Cryptosporidium infection in infancy as a cause of malnutrition: a community study from Guinea-Bissau, west Africa. *Am J Clin Nutr*. 1997;65(1):149-152. doi:10.1093/ajcn/65.1.149
140. Checkley W, Epstein LD, Gilman RH, Black RE, Cabrera L, Sterling CR. Effects of Cryptosporidium parvum Infection in Peruvian Children: Growth Faltering and Subsequent Catch-up Growth. *Am J Epidemiol*. 1998;148(5):497-506. doi:10.1093/oxfordjournals.aje.a009675
141. Checkley W, Gilman RH, Epstein LD, et al. Asymptomatic and Symptomatic Cryptosporidiosis: Their Acute Effect on Weight Gain in Peruvian Children. *Am J Epidemiol*. 1997;145(2):156-163. doi:10.1093/oxfordjournals.aje.a009086
142. Liu J, Platts-Mills JA, Juma J, et al. Use of quantitative molecular diagnostic methods to identify causes of diarrhoea in children: a reanalysis of the GEMS case-control study. *Lancet*. 2016;388(10051):1291-1301. doi:10.1016/S0140-6736(16)31529-X
143. Khalil IA, Troeger C, Blacker BF, et al. Morbidity and mortality due to shigella and enterotoxigenic Escherichia coli diarrhoea: the Global Burden of Disease Study 1990–2016. *Lancet Infect Dis*. 2018;18(11):1229-1240. doi:10.1016/S1473-3099(18)30475-4
144. Adeyemo FE, Singh G, Reddy P, Bux F, Stenström TA. Efficiency of chlorine and UV in the inactivation of Cryptosporidium and Giardia in wastewater. *PLoS One*. 2019;14(5):e0216040. doi:10.1371/journal.pone.0216040
145. Carpenter C, Fayer R, Trout J, Beach MJ. Chlorine Disinfection of Recreational Water for Cryptosporidium parvum. *Emerg Infect Dis*. 1999;5(4):579-584. doi:10.3201/eid0504.990425
146. Peeters JE, Mazás EA, Masschelein WJ, Villacorta Martiez de Maturana I, Debacker E. Effect of disinfection of drinking water with ozone or chlorine dioxide on survival of Cryptosporidium parvum oocysts. *Appl Environ Microbiol*. 1989;55(6):1519-1522. doi:10.1128/aem.55.6.1519-1522.1989
147. Pumipuntu N, Piratae S. Cryptosporidiosis: A zoonotic disease concern. *Vet World*. 2018;11(5):681-686. doi:10.14202/vetworld.2018.681-686

148. Hlavsa MC, Cikesh BL, Roberts VA, et al. Outbreaks Associated with Treated Recreational Water — United States, 2000–2014. *MMWR Morb Mortal Wkly Rep*. 2018;67(19):547-551. doi:10.15585/mmwr.mm6719a3
149. Painter JE, Gargano JW, Yoder JS, Collier SA, Hlavsa MC. Evolving epidemiology of reported cryptosporidiosis cases in the United States, 1995–2012. *Epidemiol Infect*. 2016;144(8):1792-1802. doi:10.1017/S0950268815003131
150. Rossignol J, Kabil SM, El–Gohary Y, Younis AM. Effect of Nitazoxanide in Diarrhea and Enteritis Caused by Cryptosporidium Species. *Clinical Gastroenterology and Hepatology*. 2006;4(3):320-324. doi:10.1016/j.cgh.2005.12.020
151. Amadi B, Mwiya M, Musuku J, et al. Effect of nitazoxanide on morbidity and mortality in Zambian children with cryptosporidiosis: a randomised controlled trial. *The Lancet*. 2002;360(9343):1375-1380. doi:10.1016/S0140-6736(02)11401-2
152. Amadi B, Mwiya M, Sianongo S, et al. High dose prolonged treatment with nitazoxanide is not effective for cryptosporidiosis in HIV positive Zambian children: a randomised controlled trial. *BMC Infect Dis*. 2009;9(1):195. doi:10.1186/1471-2334-9-195
153. Love MS, McNamara CW. Phenotypic screening techniques for Cryptosporidium drug discovery. *Expert Opin Drug Discov*. 2021;16(1):59-74. doi:10.1080/17460441.2020.1812577
154. Pushpakom S, Iorio F, Eyers PA, et al. Drug repurposing: progress, challenges and recommendations. *Nat Rev Drug Discov*. 2019;18(1):41-58. doi:10.1038/nrd.2018.168
155. Love MS, Beasley FC, Jumani RS, et al. A high-throughput phenotypic screen identifies clofazimine as a potential treatment for cryptosporidiosis. *PLoS Negl Trop Dis*. 2017;11(2):e0005373. doi:10.1371/journal.pntd.0005373
156. Arbiser JL, Moschella SL. Clofazimine: A review of its medical uses and mechanisms of action. *J Am Acad Dermatol*. 1995;32(2):241-247. doi:10.1016/0190-9622(95)90134-5
157. Cholo MC, Steel HC, Fourie PB, Germishuizen WA, Anderson R. Clofazimine: current status and future prospects. *Journal of Antimicrobial Chemotherapy*. 2012;67(2):290-298. doi:10.1093/jac/dkr444
158. Iroh Tam P, Arnold SLM, Barrett LK, et al. Clofazimine for Treatment of Cryptosporidiosis in Human Immunodeficiency Virus Infected Adults: An Experimental Medicine, Randomized, Double-blind, Placebo-controlled Phase 2a Trial. *Clinical Infectious Diseases*. 2021;73(2):183-191. doi:10.1093/cid/ciaa421
159. National Research Council. Guide for the care and use of laboratory animals, 8th ed. Published online 2011.
160. Federation of Animal Science Societies. Guide for the care and use of agricultural animals in research and teaching, 3rd ed. *Federation of Animal Science Societies, Champaign, IL*. Published online 2020.
161. Schaefer DA, Betzer DP, Smith KD, et al. Novel Bumped Kinase Inhibitors Are Safe and Effective Therapeutics in the Calf Clinical Model for Cryptosporidiosis. *Journal of Infectious Diseases*. 2016;214(12):1856-1864. doi:10.1093/infdis/jiw488
162. Imboden M, Schaefer DA, Bremel RD, Homan EJ, Riggs MW. Antibody fusions reduce onset of experimental Cryptosporidium parvum infection in calves. *Vet Parasitol*. 2012;188(1-2):41-47. doi:10.1016/j.vetpar.2012.02.014
163. Gomes M, Ribeiro I, Warsame M, Karunajeewa H, Petzold M. Rectal artemisinins for malaria: a review of efficacy and safety from individual patient data in clinical studies. *BMC Infect Dis*. 2008;8(1):39. doi:10.1186/1471-2334-8-39

164. Bendel D, Rulisa S, Ansah P, Sirima S. Efficacy of a Novel Sublingual Spray Formulation of Artemether in African Children with Plasmodium falciparum Malaria. *Antimicrob Agents Chemother*. 2015;59(11):6930-6938. doi:10.1128/AAC.00243-15
165. Irwin SM, Gruppo V, Brooks E, et al. Limited Activity of Clofazimine as a Single Drug in a Mouse Model of Tuberculosis Exhibiting Caseous Necrotic Granulomas. *Antimicrob Agents Chemother*. 2014;58(7):4026-4034. doi:10.1128/AAC.02565-14
166. Everitt D. Clofazimine in clinical trials for tuberculosis: resurrecting clofazimine. TB alliance, Global Alliance for TB drug development. http:// www.resisttb.org/wp-content/uploads/2013/08/Global-Alliance-Clinical- Work-with-Clofazimine.pdf.
167. Arnold SLM, Choi R, Hulverson MA, et al. Necessity of Bumped Kinase Inhibitor Gastrointestinal Exposure in Treating Cryptosporidium Infection. *J Infect Dis*. 2017;216(1):55-63. doi:10.1093/infdis/jix247
168. Tzipori S, Griffiths J. Natural History and Biology of Cryptosporidium parvum. *Adv Parasitol*. 1998;40:5-36. doi:10.1016/S0065-308X(08)60116-5
169. Huang BQ, Chen XM, LaRusso NF. Cryptosporidium parvum attachment to and internalization by human biliary epithelia in vitro: a morphologic study. *Journal of Parasitology*. 2004;90(2):212-221. doi:10.1645/GE-3204
170. Arnold SLM, Choi R, Hulverson MA, et al. P-Glycoprotein–Mediated Efflux Reduces the In Vivo Efficacy of a Therapeutic Targeting the Gastrointestinal Parasite Cryptosporidium. *J Infect Dis*. 2019;220(7):1188-1198. doi:10.1093/infdis/jiz269
171. Yawalkar SJ, Vischer W. Lamprene (Clofazimine) in Leprosy. *Lepr Rev*. 1979;50(2). doi:10.5935/0305-7518.19790020
172. Zhang Y, Feng J, McManus SA, et al. Design and Solidification of Fast-Releasing Clofazimine Nanoparticles for Treatment of Cryptosporidiosis. *Mol Pharm*. 2017;14(10):3480-3488. doi:10.1021/acs.molpharmaceut.7b00521
173. Khalil IA, Troeger C, Blacker BF, et al. Morbidity and mortality due to shigella and enterotoxigenic Escherichia coli diarrhoea: the Global Burden of Disease Study 1990–2016. *Lancet Infect Dis*. 2018;18(11):1229-1240. doi:10.1016/S1473-3099(18)30475-4
174. Troeger C, Forouzanfar M, Rao PC, et al. Estimates of global, regional, and national morbidity, mortality, and aetiologies of diarrhoeal diseases: a systematic analysis for the Global Burden of Disease Study 2015. *Lancet Infect Dis*. 2017;17(9):909-948. doi:10.1016/S1473-3099(17)30276-1
175. Thompson CN, Duy PT, Baker S. The Rising Dominance of Shigella sonnei: An Intercontinental Shift in the Etiology of Bacillary Dysentery. *PLoS Negl Trop Dis*. 2015;9(6):e0003708. doi:10.1371/journal.pntd.0003708
176. Nuzhat S, Das R, Das S, et al. Antimicrobial resistance in shigellosis: A surveillance study among urban and rural children over 20 years in Bangladesh. *PLoS One*. 2022;17(11):e0277574. doi:10.1371/journal.pone.0277574
177. Livio S, Strockbine NA, Panchalingam S, et al. Shigella Isolates From the Global Enteric Multicenter Study Inform Vaccine Development. *Clinical Infectious Diseases*. 2014;59(7):933-941. doi:10.1093/cid/ciu468
178. Muzembo BA, Kitahara K, Mitra D, et al. Shigellosis in Southeast Asia: A systematic review and meta-analysis. *Travel Med Infect Dis*. 2023;52:102554. doi:10.1016/j.tmaid.2023.102554

179. Ud-Din AIMS, Wahid SUH, Latif HA, et al. Changing Trends in the Prevalence of Shigella Species: Emergence of Multi-Drug Resistant Shigella sonnei Biotype g in Bangladesh. *PLoS One*. 2013;8(12):e82601. doi:10.1371/journal.pone.0082601
180. Salleh MZ, Nik Zuraina NMN, Hajissa K, Ilias MI, Banga Singh KK, Deris ZZ. Prevalence of Multidrug-Resistant and Extended-Spectrum Beta-Lactamase-Producing Shigella Species in Asia: A Systematic Review and Meta-Analysis. *Antibiotics*. 2022;11(11):1653. doi:10.3390/antibiotics11111653
181. Das SK, Ahmed S, Ferdous F, et al. Changing Emergence of Shigella Sero-Groups in Bangladesh: Observation from Four Different Diarrheal Disease Hospitals. *PLoS One*. 2013;8(4):e62029. doi:10.1371/journal.pone.0062029
182. Rahman M, Shoma S, Rashid H, et al. Increasing spectrum in antimicrobial resistance of Shigella isolates in Bangladesh: resistance to azithromycin and ceftriaxone and decreased susceptibility to ciprofloxacin. *J Health Popul Nutr*. 2007;25(2):158-167.
183. Muthuirulandi Sethuvel DP, Devanga Ragupathi NK, Anandan S, Veeraraghavan B. Update on: Shigella new serogroups/serotypes and their antimicrobial resistance. *Lett Appl Microbiol*. 2017;64(1):8-18. doi:10.1111/lam.12690
184. Srinivasa H, Baijayanti M, Raksha Y. Magnitude of drug resistant Shigellosis: a report from Bangalore. *Indian J Med Microbiol*. 2009;27(4):358-360. doi:10.4103/0255-0857.55460
185. Ahmed S, Chowdhury MIH, Sultana S, Alam SS, Marzan M, Islam MA. Prevalence of Antibiotic-Resistant Shigella spp. in Bangladesh: A Systematic Review and Meta-Analysis of 44,519 Samples. *Antibiotics*. 2023;12(5):817. doi:10.3390/antibiotics12050817
186. Chung The H, Baker S. Out of Asia: the independent rise and global spread of fluoroquinolone-resistant Shigella. *Microb Genom*. 2018;4(4). doi:10.1099/mgen.0.000171
187. Tariq A, Haque A, Ali A, et al. Molecular profiling of antimicrobial resistance and integron association of multidrug-resistant clinical isolates of Shigella species from Faisalabad, Pakistan. *Can J Microbiol*. 2012;58(9):1047-1054. doi:10.1139/w2012-085
188. Mangum BR, Pogue JM, Barber KE. Tebipenem and Sulopenem: Dynamic Duo or Double Trouble? *Curr Infect Dis Rep*. Published online February 10, 2024. doi:10.1007/s11908-024-00831-1
189. Mahalingam A. Tebipenem: A Novel Oral Carbapenem. *Pediatr Infect Dis*. 2020;2(1):25-28. doi:10.5005/jp-journals-10081-1237
190. McEntee L, Johnson A, Farrington N, et al. Pharmacodynamics of Tebipenem: New Options for Oral Treatment of Multidrug-Resistant Gram-Negative Infections. *Antimicrob Agents Chemother*. 2019;63(8). doi:10.1128/AAC.00603-19
191. Sato N, Kijima K, Koresawa T, et al. Population Pharmacokinetics of Tebipenem Pivoxil (ME1211), a Novel Oral Carbapenem Antibiotic, in Pediatric Patients with Otolaryngological Infection or Pneumonia. *Drug Metab Pharmacokinet*. 2008;23(6):434-446. doi:10.2133/dmpk.23.434
192. Fernández Álvaro E, Voong Vinh P, de Cozar C, et al. The repurposing of Tebipenem pivoxil as alternative therapy for severe gastrointestinal infections caused by extensively drug-resistant Shigella spp. *Elife*. 2022;11. doi:10.7554/eLife.69798
193. International Centre for Diarrhoeal Disease Research B. Tebepenem Trial in Children with Shigellosis. https://classic.clinicaltrials.gov/ct2/show/NCT05121974.

194. Zakir Hossain AKM, Zahid Hasan Md, Mina SA, Sultana N, Chowdhury AMMA. Occurrence of shigellosis in pediatric diarrheal patients in Chattogram, Bangladesh: A molecular based approach. *PLoS One*. 2023;18(6):e0275353. doi:10.1371/journal.pone.0275353
195. Chuang GT, Tsai IJ, Tsau YK. Serum Creatinine Reference Limits in Pediatric Population—A Single Center Electronic Health Record-Based Database in Taiwan. *Front Pediatr*. 2021;9. doi:10.3389/fped.2021.793446
196. Guimarães M, Vertzoni M, Fotaki N. Performance Evaluation of Montelukast Pediatric Formulations: Part II — a PBPK Modelling Approach. *AAPS J*. 2022;24(1):27. doi:10.1208/s12248-021-00662-1
197. Van der Veken M, Brouwers J, Ozbey AC, et al. Investigating Tacrolimus Disposition in Paediatric Patients with a Physiologically Based Pharmacokinetic Model Incorporating CYP3A4 Ontogeny, Mechanistic Absorption and Red Blood Cell Binding. *Pharmaceutics*. 2023;15(9):2231. doi:10.3390/pharmaceutics15092231
198. Craig WA. State-of-the-Art Clinical Article: Pharmacokinetic/Pharmacodynamic Parameters: Rationale for Antibacterial Dosing of Mice and Men. *Clinical Infectious Diseases*. 1998;26(1):1-10. doi:10.1086/516284
199. LEIBOVITZ E, JANCO J, PIGLANSKY L, et al. Oral ciprofloxacin vs. intramuscular ceftriaxone as empiric treatment of acute invasive diarrhea in children. *Pediatr Infect Dis J*. 2000;19(11):1060-1067. doi:10.1097/00006454-200011000-00006
200. World Health Organization. Weight-for-age Child Growth Standards. https://www.who.int/tools/child-growth-standards/standards/weight-for-age.
201. Chowdhury MRK, Rahman MS, Billah B, Rashid M, Almroth M, Kader M. Prevalence and factors associated with severe undernutrition among under-5 children in Bangladesh, Pakistan, and Nepal: a comparative study using multilevel analysis. *Sci Rep*. 2023;13(1):10183. doi:10.1038/s41598-023-36048-w
202. Ahmed T, Ireen S, Ahmed AS, et al. Nutrition of Children and Women in Bangladesh: Trends and Directions for the Future. *J Health Popul Nutr*. 2012;30(1). doi:10.3329/jhpn.v30i1.11268
203. Rahman MT, Jahangir Alam M, Ahmed N, Roy DC, Sultana P. Trend of risk and correlates of under-five child undernutrition in Bangladesh: an analysis based on Bangladesh Demographic and Health Survey data, 2007–2017/2018. *BMJ Open*. 2023;13(6):e070480. doi:10.1136/bmjopen-2022-070480
204. Das S, Baffour B, Richardson A. Prevalence of child undernutrition measures and their spatio-demographic inequalities in Bangladesh: an application of multilevel Bayesian modelling. *BMC Public Health*. 2022;22(1):1008. doi:10.1186/s12889-022-13170-4
205. Hines KM, Shen T, Ashford NK, et al. Occurrence of cross-resistance and β-lactam seesaw effect in glycopeptide-, lipopeptide- and lipoglycopeptide-resistant MRSA correlates with membrane phosphatidylglycerol levels. *Journal of Antimicrobial Chemotherapy*. 2020;75(5):1182-1186. doi:10.1093/jac/dkz562
206. Mann M, Eliasson O, Patel K, ZuWallack RL. A Comparison of the Effects of bid and qid Dosing on Compliance with Inhaled Flunisolide. *Chest*. 1992;101(2):496-499. doi:10.1378/chest.101.2.496
207. Sadosky A, Kunal Srivastava, Anamika Arora, Aditi Kataria, Cappelleri, Andrew M Peterson. Impact of reducing dosing frequency on adherence to oral therapies: a literature

review and meta-analysis. *Patient Prefer Adherence*. Published online May 2013:419. doi:10.2147/PPA.S44646
208. Dezii CM, Kawabata H, Tran M. Effects of once-daily and twice-daily dosing on adherence with prescribed glipizide oral therapy for type 2 diabetes. *South Med J*. 2002;95(1):68-71.
209. Zhang Y, Feng J, McManus SA, et al. Design and Solidification of Fast-Releasing Clofazimine Nanoparticles for Treatment of Cryptosporidiosis. *Mol Pharm*. 2017;14(10):3480-3488. doi:10.1021/acs.molpharmaceut.7b00521

APPENDIX A

Sato et al.'s tebipenem (TBPM) popPK model[191] incorrectly used Ccr in mL/min/kg for computing apparent clearance (CL/F). To correct for this, a scaling factor was applied to the CL/F equation such that Sato model parameters would still be valid with Ccr in the correct unit (L/hr/kg):

$$\frac{CL}{F} = 0.363 + 0.104 \times \frac{1000}{60} \times Ccr$$

where 1000/60 is the scaling factor accounting for unit conversion of Ccr levels from mL/min/kg to L/hr/kg.

Moreover, Sato et al.'s tebipenem popPK model[191] appears to have used tebipenem-pivoxil (TBPM-PI) dose in their model for tebipenem. To correct the model for TBPM dosing, we used the molecular weight ratio of TBPM to TBPM-PI and scaled CL/F and V/F accordingly.

Tebipenem molecular weight: 383.5 g/ml (PubChem)

Tebipenem-pivoxil molecular weight; 497.63 g/mol (PubChem)

MW ratio $\frac{TBPM}{TBPM-PI} = \frac{383.5}{497.63} \approx 0.7707$

Let CL° be the clearance estimated when TBPM-PI dose was used, D° the TBPM-PI dose, CL' the clearance associated with TBPM dose, and D' the TBPM dose. Then,

$D' = D° \times MW\ ratio = 0.7707 \times D°$

By definition,

$$\frac{CL°}{F} = \frac{D°}{AUC}$$

$$\frac{CL'}{F} = \frac{D'}{AUC} = 0.7707 \times \frac{D°}{AUC}$$

Since AUC was estimated using observed TBPM data and does not change,

$$\frac{CL'}{F} = 0.7707 \times \frac{CL°}{F}$$

$\frac{CL°}{F} = 0.363 + 0.104 \times \frac{1000}{60} \times Ccr$ (See Point 1)

Therefore,

$$\frac{CL'}{F} = 0.7707 \times (0.363 + 0.104 \times \frac{1000}{60} \times Ccr)$$

Similarly, let V° be the volume estimated when TBPM-PI dose was used, D° the TBPM-PI dose, C_0 the TBPM concentration at time = 0 hr, V' the volume associated with TBPM dose, and D' the TBPM dose.

By definition,

$$\frac{V°}{F} = \frac{D°}{C_0}$$

$$\frac{V'}{F} = \frac{D'}{C_0} = 0.7707 \times \frac{D°}{C_0}$$

Since C_0 was based on observed TBPM data and does not change,

$$\frac{V'}{F} = 0.7707 \times \frac{V°}{F}$$

$\frac{V°}{F} = 1.18 \times Age^{-0.132}$ (Sato et al., 2008)

Therefore,

$$\frac{V'}{F} = 0.7707 \times (1.18 \times Age^{-0.132})$$

$$\frac{V'}{F} = 0.9094 \times Age^{-0.132}$$

VITA

Cindy Zhang was born in Yantai, Shandong, China, and raised in Vancouver, BC, Canada. She earned her Bachelor of Science in Human Biology and Immunology from the University of Toronto in Toronto, ON, Canada and Master of Science in Biostatistics from Columbia University in New York, NY, USA.